REPORT No. 8399

LASER COMMUNICATION SATELLITE EXPERIMENT (LCSE)

July 1, 1966

PERKIN-ELMER

PERKIN-ELMER

ELECTRO-OPTICAL DIVISION NORWALK, CONNECTICUT

ENGINEERING REPORT NO. 8399

LASER COMMUNICATION

SATELLITE EXPERIMENT

(LCSE)

DATE: JULY 1, 1966

PREPARED FOR: MARSHALL SPACE FLIGHT CENTER

NATIONAL AERONAUTICS AND SPACE ADMINISTRATION

HUNTSVILLE, ALABAMA

Herbert F. Wischnia, Senior Staff Engineer,
Space Optics Department

Approved:

R. Crane, Manager
Advanced Technology Development

CONTRIBUTORS

R. J. Arguello

J. D. Buckley

S. R. Habijanec

M. S. Lipsett

W. N. Peters

E. R. Schlesinger

M. L. Skolnick

Frontispiece

TABLE OF CONTENTS

LIST OF ILLUSTRATIONS

LIST OF ILLUSTRATIONS (Continued)

LIST OF ILLUSTRATIONS (Continued)

LIST OF TABLES

SECTION I

SUMMARY

Since the advent of the laser in 1960, numerous scientists and engineers concerned with the exploration of space have sought to apply the laser to space communication problems.* The practical realization of a coherent oscillator in the optical part of the electromagnetic spectrum has generated two separable breakthroughs in the art of space communication:

- The first is the high directivity or equivalent antenna gain due to the laser's spatial coherence.
- The second is that enormous bandwidths are achieveable in a communications system because of the laser's temporal coherence.

The major advantage offered by optical communications in the state of space communications art is the reduction of transmitter power due to the directivity of a laser communications antenna. This reduction of transmitter power permits high data rate communications at distances that are impractical with microwave systems. Deep space laser communication systems are superior to microwave systems in the number of bits per second transmitted per watt of power required from the spacecraft.

An optimum choice for laser communications through the earth's atmosphere in today's state of the art is a system based on quantum detection of the optical photons transmitting digitized information. An intensity detection system on the earth collecting photons transmitted by a spaceborne laser has been analyzed** and breadboarded*** for feasibility using today's laser technology.

The intensity detection technique avoids the wavefront distortion problems introduced by the atmosphere that exist in a coherent detection technique. Coherent detection of optical radiation, as in microwave systems, requires a constant phase relationship between the radiation incident at various points in the receiver aperture. It has been shown that, when a visible laser

*Cameron, A.G.W. (ed.) Interstellar Communication, New York: W.A. Benjamin, Inc. 1963; Article by R.N. Schwartz and C.H. Townes, pp. 223-231.

**Determination of Optical Technology Experiments for a Satellite, Perkin-Elmer, Contract NAS8-11408, NASA Report CR-252, July 1965.

***Laser/Optics Techniques, Perkin-Elmer Report No. 8387, Contract NAS8-20115, June 1966.

beam traverses an appreciable portion of the atmosphere, the phase coherence across the wavefront is soon lost. This wavefront degradation is a function of wavelength and severely limits any coherent communication link with visible light although it does not deteriorate intensity detection operations.

It is with this background that an optical communication experimental package is proposed within the framework of the Apollo Applications Program. All of the components necessary for such a system exist today and the technical impact of a space laser communication subsystem to future manned and unmanned payloads invite the space flight of such a system at the earliest time that NASA can make a synchronous orbit spacecraft available for engineering experiments necessary for development of space laser communication. Thus the principal function of the Laser Communication Satellite Experiment (LCSE) as illustrated in the frontispiece is to establish and maintain optical communications via a diffraction-limited laser beam utilizing techniques which are applicable to a deep space mission.

In addition, the LCSE equipment can provide valuable data for future missions involving man in space. Provisions have been made in the proposed design of the spaceborne Laser/Telescope to accommodate experiments that permit the astronaut to view the earth through the telescope. These earth-viewing experiments would establish the utility of a moderately large optical aid, the 16-inch telescope, to an astronaut orbiting a planet.

The proposed 16-inch diameter telescope is an instrument well suited to evaluate how successfully the astronaut can perform space tasks with a viewing optical system. The telescope has a fine guidance system and uses the Apollo Telescoping Mast (ATM)* to provide earth-viewing stability of 0.1 arc-second and 10 arc-seconds. In addition, the astronaut can observe the earth with a 2 arc-minute and a 1 degree field of view.

The experiment design approach described in this report is an outgrowth of theoretical study, laboratory work, and the laser system engineering which has been sponsored by the Marshall Space Flight Center and the Office of Advance Research and Technology for several years. This report applies the current developments in space laser communication technology. Fundamental engineering approaches that are illustrated in the report are laboratory techniques which have been demonstrated already in the Laser/Optics Techniques Project.

THE PROPOSED EXPERIMENT SYSTEM

The important characteristics of the proposed LCSE relate to the function of an optical communication system demonstration from space. The experiment can provide 10 million bit/second laser communications from a synchronous orbit Apollo Applications Program (AAP) space vehicle. The equipment as described would be suitable for both manned and unmanned missions of the future.

*See Footnote page 9 .

There are two design features of the proposed experiment that make it particularly compatible with the AAP concept:

- The Laser/Telescope is attached to the AAP spacecraft by means of a boom and gimbal arrangement similar to the approach used in Stratoscope II. That is, the pointing system has a coarse mode (spacecraft attitude control to 1/2 degree), fine pointing mode with command signals originating in the optical payload (gimbal pointing to 10 arc-seconds), and a very precise pointing mode using optical techniques (line-of-sight steering to 0.1 arc-second).

- The experiment package would be compatible with the AAP hardware (Saturn Booster, Command Module, Service Module, Lunar Excursion Module (LEM), etc.) and would utilize the existing electrical power systems, communication systems and LEM attitude control system. In addition, the boom and gimbal hardware needed for the experiment will be the Apollo Telescoping Mast (ATM) or equivalent mechanism.

Precision, simplicity, and high communication efficiency have been contrived by using four technical principles:

- On the spacecraft, common telescope optics are used for both the laser transmitter and guidance receiver channel. This approach eliminates major misalignment problems between the transmit and receive optical channels.

- The key tracking system in the experiment incorporates a two-axis, servo controlled optical element which directs the laser beam very precisely. The servo controlled optical element is a transfer lens which has a high dynamic response as well as extremely fine pointing precision. The servo transfer lens subsystem will compensate for angular disturbances about the line of sight due to equipment vibration of the spacecraft structure or man-induced motions.

- The helium-neon gas laser with an electro-optic modulator can provide 10^7 bits/second channel for the experiment. The modulation scheme is the efficient pulse code modulation using left and right circular polarization (PCM/PL).

- The necessary subsystems for the in-flight alignment of the transmit and receive channel are provided. In addition, optical auxiliaries of beam spoiling, focus control, point ahead, and station transfer are incorporated into the design approach.

The laser communication experiment concept, as developed in the Laser Communication Satellite Experiment is based on the single minded objective of the program: -- Conduct space optical communication experiments whose principles of operation are applicable to future deep space missions.

The essence of communicating via a diffraction-limited laser beam is precise pointing. The laser beam must be aimed ahead of the receiver so that the receiver aperture is within the central maximum of the far field pattern of the transmitter. To achieve this, the orbit position and the relative velocity of the spaceborne transmitter to the earth receiver must be known.

To accomplish 0.1 arc-second pointing of the space laser beam at the earth laser beacon (with the point ahead), the five key functions must be performed:

- Acquisition of the earth laser beacon by the spacecraft telescope (field of view of 1 degree).
- Acquisition of the sun by the sun tracker to provide a roll reference for the point ahead offset angle.
- Tracking of the earth laser beacon to a fraction of an arc-second.
- Transmission to the spacecraft (from earth) of the point ahead angle in the spacecraft coordinate system. This point ahead angle compensates for Bradley effect aberrations, due to the relative velocity between the spacecraft and the earth station telescope.
- Articulating the laser beam from the apparent LOS by the point ahead angle aboard the spacecraft.

Accomplishing these five functions in a simulated deep space environment, and conducting the related communication experiments such as station transfer, incoherent reception, and down-looking scintillation, are important to the overall mission of the LCSE.

To conduct the LCSE communications experiment (Table II, page 8), the precision of the roll reference need be only 2.25 degrees; while for deep space, the roll reference precision must be 0.056 degree. In order to conduct a 50 arc-second point ahead experiment with the LCSE, the roll reference precision must be 0.167 degree instead of the previously indicated 2.25

degrees. The station transfer experiment requires a roll reference precision of 0.5 degree. All of these roll reference requirements can be met since sun tracker hardware is capable of obtaining precision of 0.003 degrees. The roll reference specifications for the LCSE are summarized in Table IX (page 132) for the various point ahead experiments to be conducted.

Thus, it can be seen that the principal purpose of the proposed experiment is to collect engineering and scientific data to establish the technical feasibility of a deep space laser communication system. The optical, opto-mechanical and electro-optical ancillaries which are required to acquire and track a narrow laser beam are provided so that the proposed experiment will utilize techniques and procedures applicable to deep space optical communication links.

The proposed engineering experiments of laser communications from a synchronous orbit will verify the engineering solutions and hardware that are needed to establish and maintain the very narrow optical communication beam from the laser transmitter aboard the spacecraft to the receiver telescope on the earth surface. The width of the laser beam will be determined by the diffraction limit of the primary mirror antenna in a space telescope. The Laser/Telescope will establish a broadband laser communication telemetry link in a manner that will verify the practicality of the techniques and procedures for space telemetry. The low angular rates between a synchronous vehicle and an earth receiver telescope are ideal to simulate the angular rates between a deep-space-probe system and an earth station. The altitude is sufficient to insure that the laser beam will traverse the entire atmosphere surrounding the earth.

The astronaut will assist in the experimental procedures when necessary to insure that the experimental apparatus of the Laser/Telescope functions satisfactorily. The adjustment capability of the astronaut in an EVA mode when the vehicle is on station will enhance the overall reliability of the mission.

An additional objective of the proposed Laser Communication Satellite Experiment, is to collect engineering data on the utility of a space telescope to an astronaut. The 16-inch aperture, long-focal-length telescope is an instrument that will be used to assist the astronaut in observing the earth features. It is planned that the astronaut would have two viewing arrangements: one arrangement would provide a very stable line of sight at a long focal length; the second arrangement would provide a moderately stable line of sight at a somewhat shorter focal length. The astronaut will be able to evaluate the usefulness and assistance of the telescope in the identification and recognition of earth targets in the vicinity of the earth station. In addition, the astronaut has the option of pointing the optical instrument at targets other than the earth receiver with ordinary optical pointing and tracking precision.

The proposed Laser Communication Satellite Experiment requires a synchronous orbit type of manned vehicle in order to obtain the necessary data from the proposed communication and astronaut viewing experiments. Table I is a summary of key spacecraft requirements necessary to accomplish the experiments listed in Table II.

THE PRESENT STATE OF DEVELOPMENT IN THE FIELD OF SPACE LASER COMMUNICATIONS

The present state of development in the field of space laser communications is composed of published literature in component development, theoretical systems development, two simple space experiments in laser propagation from space vehicles and breadboards of subsystems for the proposed Laser Communication Satellite Experiment. The state of the art is such that every basic component needed to develop a deep space laser communication system exists today as a commercial item or laboratory device. The breadboard of the proposed experiment has been developed under contract to Marshall Space Flight Center by Perkin-Elmer Corporation (NAS8-20115). All of the components necessary to accomplish laser communications from a space vehicle are being assembled into a single Laser/Telescope assembly to evaluate complete functionality of the proposed experiments.

This breadboard consists of a 16-inch diameter Laser/Telescope in Wilton, Connecticut. The present breadboard apparatus has been used in ground experiments to develop the key components needed for the proposed space laser communicator experiment. The laser transmitter, fine guidance tracking equipment, beamsplitters, beam dividers, alignment and focus devices, beam isolators and a servo controlled transfer lens have all been assembled with the basic 16-inch telescope to demonstrate the principles needed for the proposed experiment. In addition, the auxiliary equipment needed for coarse guidance, self-alignment servos, modulators and beamsplitters (for astronaut viewing) will be available in the equipment shortly.

The technical approach for the Laser Communication Satellite Experiment represents the current state of the art in space optical communications and is based upon study sponsored by the Marshall Space Flight Center and the Office of Advance Research and Technology (OART) in Contracts NAS8-11408, NAS8-20255, and the laboratory-experimental work in Contract NAS8-20115.

TABLE I

KEY SPACECRAFT REQUIREMENTS SUMMARY

1. SYNCHRONOUS ORBIT FOR SIX MONTHS
   - Equatorial Crossing 110° W
   - 28.3° Inclination
2. LASER/TELESCOPE PAYLOAD CAPACITY
   - 30 Inch Diameter
   - 90 Inch Length
   - 100 Watts Power
   - 45,000 Watt Hours
   - 500 Pounds
3. ASTRONAUT PARTICIPATION DURING 14 DAYS OF MANNED FLIGHT
   - EVA - 3 Hours
   - Inside LEM - 19 Hours
4. ATTITUDE CONTROL
   - ±1/2 Degree Pitch, Yaw and Roll of AAP Vehicle
   - 0.1 Degree/Second Angular Stabilization
   - Cold Gas Jets for Attitude Control System when Laser Experiments are being conducted
5. ATM OR EQUIVALENT BOOM/GIMBALS FOR PITCH AND YAW
   - 10 Arc-Second Pointing in Response to LCSE Commands (Maximum error tolerable with present Laser/Telescope Concept is ±30 Arc-Second Peak)
6. 1.5 KBPS TELEMETRY FOR LCSE
7. LAUNCH MOUNTS FOR SOFT SUSPENSION DURING LAUNCH

TABLE II

SPACE EXPERIMENTS SUMMARY

1/10 Arc-Second Tracking	Necessary to Provide Megabit Communication
Acquisition	
Point Ahead	
Station Transfer	
Alignment and Focus	
Down-Looking Scintillation	Atmospheric Science Data
Tracking With Disturbances	Man/Telescope Applications
Earth Viewing	

SECTION II

THE LCSE EQUIPMENT

2.1 LCSE EQUIPMENT DESCRIPTION AND EXPERIMENT PROCEDURES

The equipment needed to conduct the Laser Communication Satellite Experiment consists of three major units aboard the spacecraft: The Laser/Telescope, the ATM* or equivalent mast and gimbals, and an experiments control console located in the LEM. Five different conceptual arrangements for conducting the experiments were considered during the course of this study:

- Basic AAP
- Autonomous Vehicle
- Pallet
- Autonomous Spacecraft Separable From Boom and Gimbals
- Integrated LEM

Each concept is illustrated and described in the following pages and the advantages and disadvantages associated with each concept are discussed. The experimental procedure would vary between concepts to some degree. However, the description of the experimental procedure which can be found in Section 2.2 is based on the Basic AAP Concept (Figure 1).

BASIC AAP CONCEPT (Figure 1)

This sketch shows the Laser/Telescope attached to the ATM with the astronaut looking at the earth. The telescope is about 7-1/2 feet long, 30 inches in diameter and weighs 500 pounds. Power required from the LEM is 85 watts. The second astronaut would be monitoring the experiment from a control station in the LEM while the Command Astronaut remains in the Command Module. The equipment would be used in the communication and earth viewing experiments for 8 days during the 14 day orbit. At the end of the 14th day of the flight,

*Although the Apollo Telescoping Mount (ATM) is referenced throughout this report, boom/gimbal structures specially suited to the LCSE Mission could be used instead. The actual selection of ATM or special boom/gimbals will depend upon cost, schedule, and performance considerations.

the CSM separates from LEM and de-orbits leaving the LEM with the attached Laser/Telescope on station. The LCSE would be shut down, no power on and the telescope cap closed, for 3 months. At the end of 3 months, the equipment would be activated for 3 days. Acquisition, track, and unmanned communication experiments would be conducted for 3 days. The equipment would then be shut down again for another 3 months when the unmanned communication experiments would be repeated. Although this 3 month off-cycle, 3 to 8 days on-cycle could be repeated until equipment malfunction, the LEM power sources would be depleted at the end of 6 months.

AUTONOMOUS VEHICLE CONCEPT (Figure 2)

This illustration shows a variation of the basic concept that utilizes a separate spacecraft section behind the Laser/Telescope for attitude control, microwave communications and power. In this arrangement, the LCSE has its solar collectors folded up to permit the equipment to be stored for launch inside the LEM descent structure. The EVA Astronaut is shown in two positions (the same astronaut at two different times). At the Laser/Telescope deployment station (the bottom of the LEM descent structure), the astronaut monitors and assists in separating the LCSE from the main Apollo equipments. The launch clamps in the descent structure are opened, then, the CSM and LEM units are moved away leaving the LCSE on station a short distance away from the main Apollo equipments. The solar collectors are unfolded and the LCSE proceeds through the acquisition and track operations of the earth laser beacon. The laser communication experiments are conducted as in the Basic AAP Concept of Figure 1; the earth viewing experiments are conducted with the EVA Astronaut connected to the Apollo equipments by means of a tether, or if possible, with the astronaut completely free from the Apollo. The LCSE Monitor Astronaut is sketched at his control station in the LEM.

PALLET CONCEPT (Figure 3)

This arrangement is quite similar to the Basic AAP Concept of Figure 1 with the exception that the equipment complex is shown attached to the Service Module rather than the LEM descent structure. The Experiments Monitor Station would now have to be located inside the Command Module rather than in the LEM Life Cell. The EVA Astronaut (not shown) could conduct the earth viewing experiments as previously described. At the conclusion of the 14 day mission, prior to de-orbiting, the Laser/Telescope is jettisoned or returned to its compartment in Sector 1 of the Service Module. Although no EVA Astronaut is shown in Figure 3, the astronaut earth-viewing operations could be conducted as illustrated in Figure 2.

AUTONOMOUS SPACECRAFT SEPARABLE FROM BOOM AND GIMBAL CONCEPT (Figure 4)

Figure 4 illustrates the Autonomous Vehicle Concept (Figure 2) with the exception that an extendable boom is supplied to assist in the

erection and deployment operations. Also, experiments related to the pointing and tracking errors (due to man disturbances) in the Apollo Command Module and LEM can be conducted. The gimbals shown are passive gimbals (no servo torquers). The spacecraft attitude control system is used to point the Laser/Telescope as a coarse guidance operation during the time that the unit is connected to the LEM as well as when the boom separates at the separation joint illustrated in Figure 4. The gimbals have simple locks to prevent rotation at random when the equipment is in the autonomous mode (and no longer connected to the LEM).

INTEGRATED LEM CONCEPT (Figure 5)

In this arrangement, the Laser/Telescope is located in the space normally used by the LEM descent engine. The Laser/Telescope is gimballed about its center of gravity with servo torquer motors which are used to position the instrument in response to commands from the programmer, the sun seeker, the coarse guidance electronics or the fine guidance electronics. The telescope and the gimbals are in a non-pressurized environment while the astronaut remains in the LEM Life Cell. The gimbals are attached to the LEM descent structure. The earth-viewing experiment by the astronaut can be accomplished in this configuration as well as the four other concepts, but the astronaut viewing port must be located close to the front of the telescope rather than the region behind the primary mirror as shown in the other concepts. This will mean relaying the fine stabilized optical image from the optical path behind the transfer lens. It is necessary to change this viewing arrangement to avoid astronaut interference with the gimbals. Therefore, for the earth-viewing operation, the astronaut can be visualized as looking into the telescope with his head just below the inner-most gimbal.

LASER COMMUNICATION SATELLITE EXPERIMENT

BASIC AAP CONCEPT

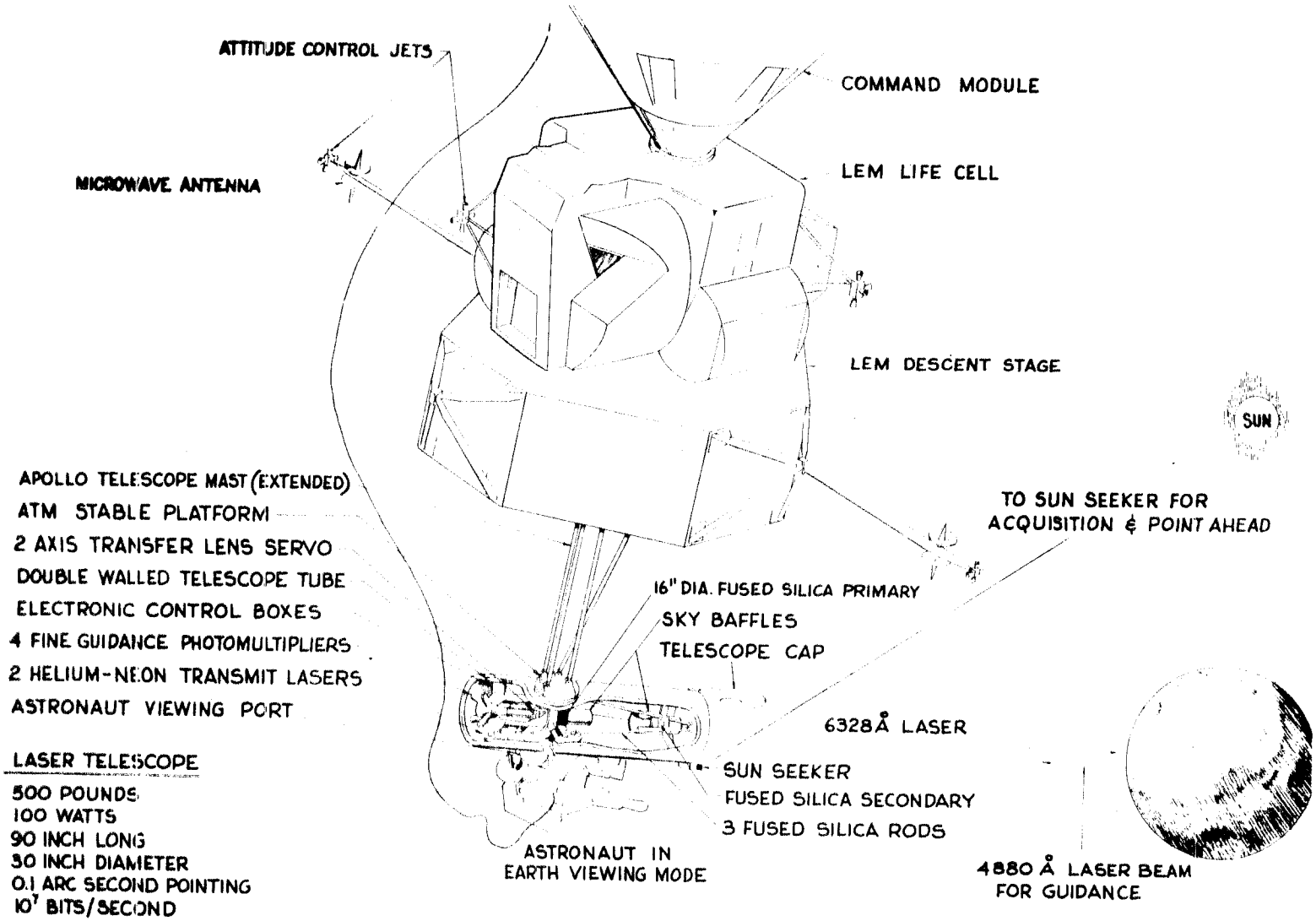

LASER TELESCOPE

500 POUNDS
100 WATTS
90 INCH LONG
30 INCH DIAMETER
0.1 ARC SECOND POINTING
10^7 BITS/SECOND
ERROR RATE PER BIT < .001
3 MILLIWATT HELIUM-NEON LASER
11 db SAFETY MARGIN (WITH 24" DIA. GROUND STATION)

Figure 1

Figure 1a. Detail

LASER COMMUNICATION SATELLITE EXPERIMENT

AUTONOMOUS VEHICLE CONCEPT

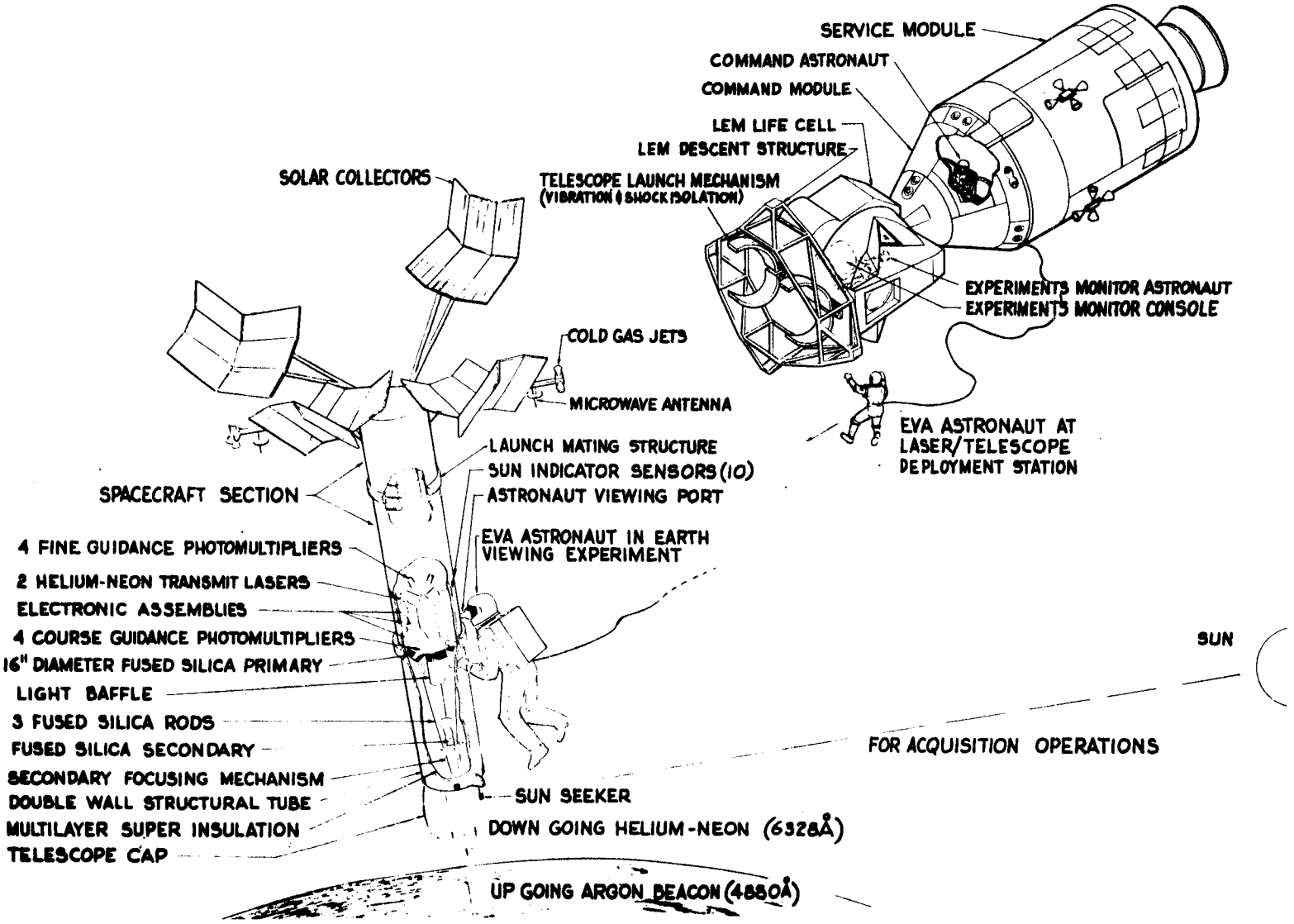

Figure 2

LASER COMMUNICATION SATELLITE EXPERIMENT

PALLET CONCEPT

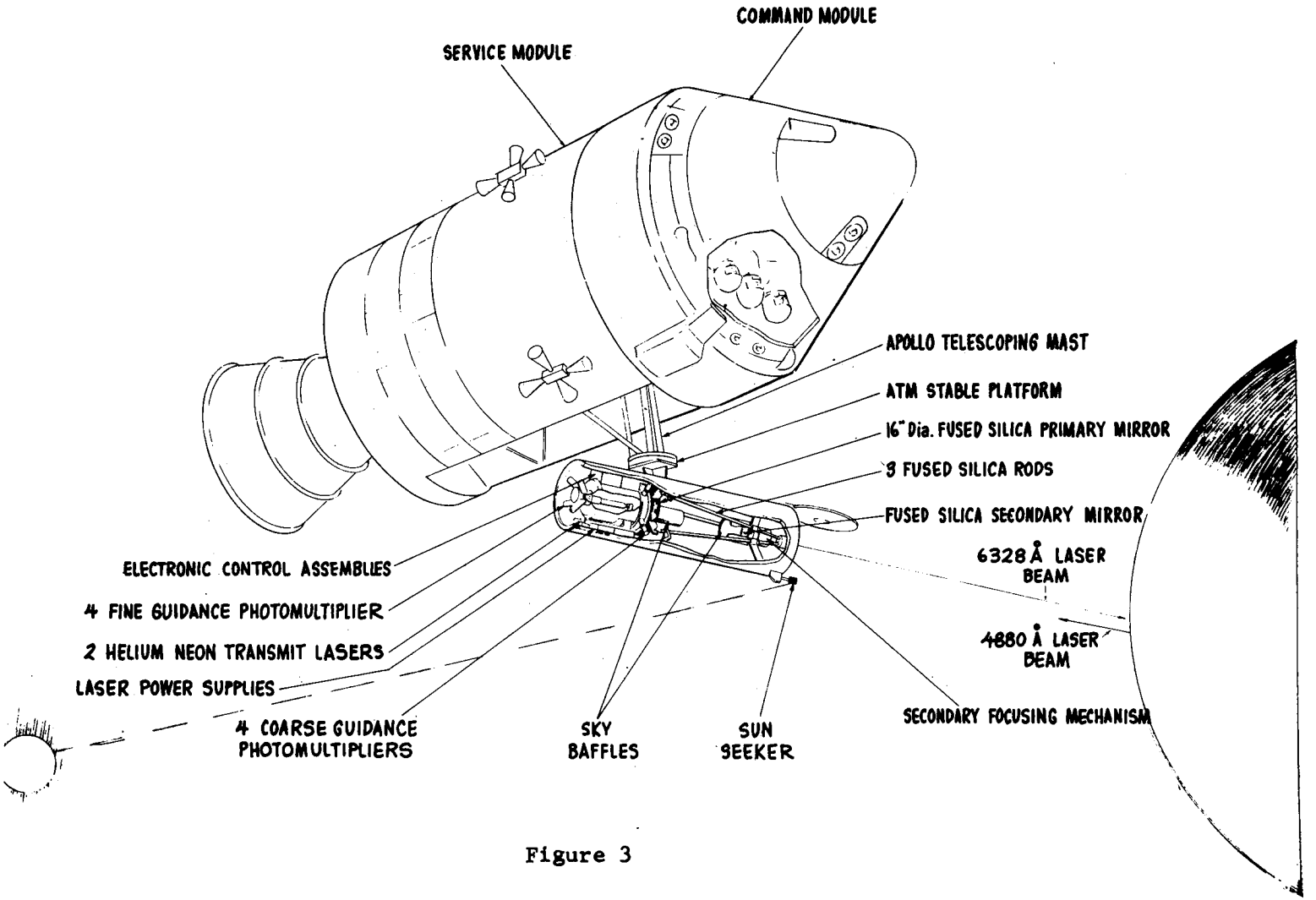

Figure 3

LASER COMMUNICATION SATELLITE EXPERIMENT

AUTONOMOUS SPACECRAFT SEPARABLE FROM BOOM AND GIMBAL CONCEPT

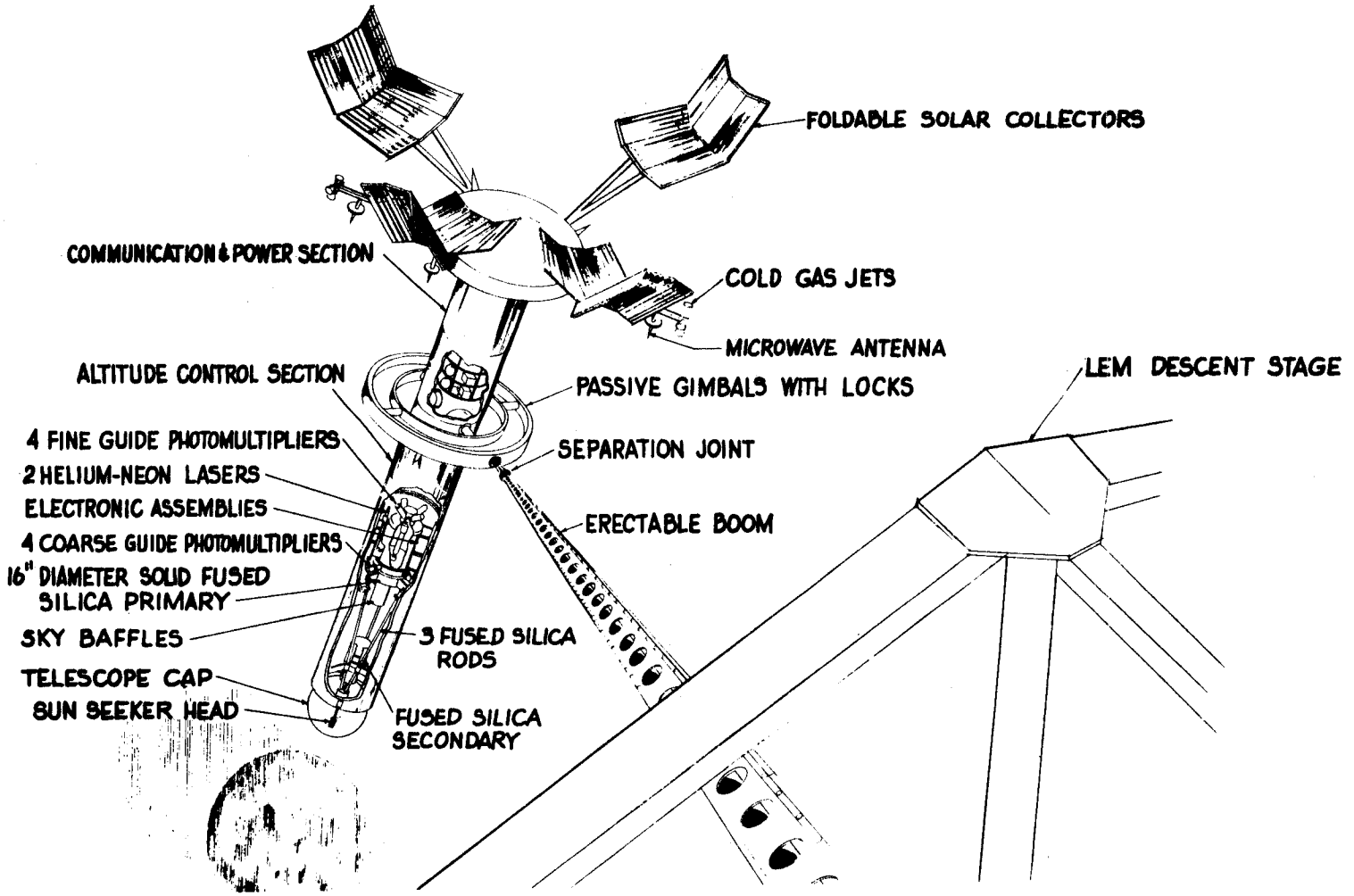

Figure 4

LASER COMMUNICATION SATELLITE EXPERIMENT

INTEGRATED LEM CONCEPT

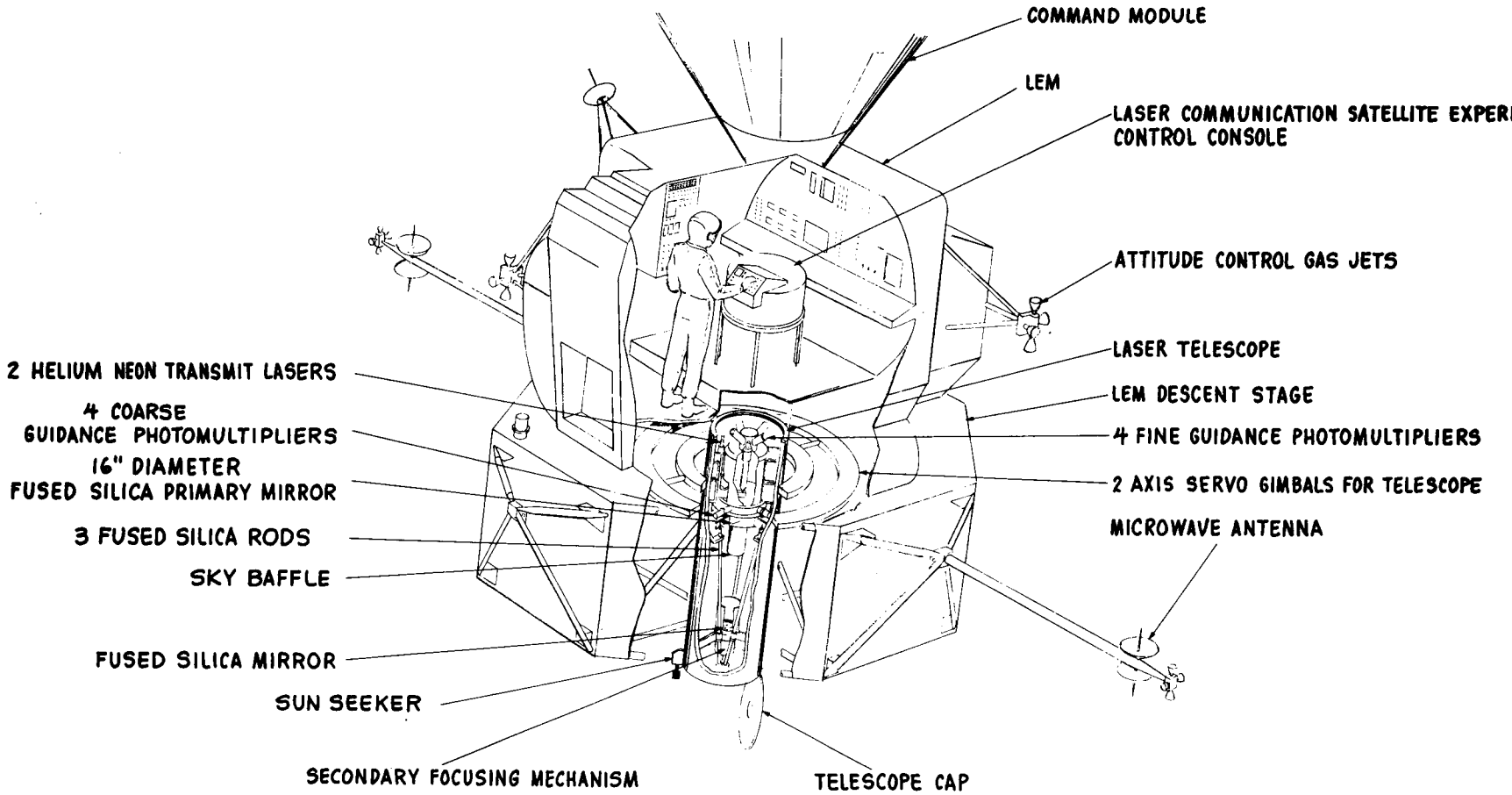

Figure 5

2.2 LCSE PROCEDURE

In order to conduct the proposed experiments (space laser communications and evaluation of active astronaut participation (Table II page 8)), the key steps in the experimental procedure are summarized in the following paragraphs. The sequential steps necessary to bring the AAP vehicle from the launch pad to the "on station" of Step 1 are typical of a Saturn V launch into synchronous orbit. These steps are tabulated in Table III on page 18 .

Step 1. SPACECRAFT ON STATION

The entire vehicle is placed in a synchronous orbit with a 28.3 degree inclination and the equatorial crossing point of the orbit is 110.6° W. The ground track of the vehicle will be figure "8" patterns in the vicinity of the ground station located in western United States. The equatorial crossing point of 110.6° W is the location of a stable node. The ground station location should be in the vicinity of the 110° W longitude, but since the operations will involve line-of-sight tracking, and the line of sight extends for some 4000 miles (10 degrees above the horizon), the location of the ground station and/or the location of the equatorial crossing are not critical. A plus/minus 1 degree longitude variation is quite acceptable for the match between the equatorial crossing and the location of the ground station. The spacecraft will need a Δv capability of less than 200 feet/second to remove the injection error.

Step 2. START OF EVA (Figure 4)

One astronaut leaves the spacecraft in an EVA mode and proceeds to the vicinity of the caged Laser/Telescope. One astronaut proceeds to the LEM Life Cell to monitor experiment operations. The third astronaut remains at his command station in the Command Module. The attitude control requirement for the spacecraft during this mode is not critical. The primary concern is to avoid entangling the astronaut life lines with the spacecraft structures.

Step 3. UNCAGE LASER/TELESCOPE FROM LAUNCH MOUNTS

The equipment uncaging operations should be conducted when the angular rates of the spacecraft are as low as practical (about 0.1 degree/second). Specific attitude orientation during this operation is not important.

Step 4. BOOM EXTENDED

The Apollo Telescoping Mount is extended so that the Laser/Telescope, which is attached to the stable platform at the end of the ATM, is free

TABLE III

SATURN V LAUNCH SEQUENCE INTO SYNCHRONOUS ORBIT

Event No.	Event	Apollo Activity
1	Saturn V/LCSE Liftoff	S-IC ignition and space vehicle liftoff. Space vehicle pitch over. S-IC engine cutoff; S-II ullage rocket ignition; S-IC separation.
2	Begin S-II Stage Thrusting	The S-II stage will propel the launch vehicle from an altitude 33.3 nm to an altitude of approx. 100 nm with a velocity of 22,200 fps.
3	Jettison LES and Interstage	After the Saturn V/LCSE has obtained an appropriate altitude, the launch escape system is jettisoned.
4	Begin S-IVB Stage Thrusting	The S-IVB/Instrumentation Unit and LCSE will be injected into a 100 nm parking orbit by the first burn of the S-IVB.
5	Earth Parking Orbit Insertion	A minimum of three parking orbits will be used to accurately establish orbit ephemeris and trajectory parameters.
6	Begin Transfer Ellipse to Synchronous Altitude	S-IVB restart at precise position. (Velocity to be gained is a critical value to reach synchronous altitude at desired longitude crossing.)
7	Coast to Station Location	S-IVB/LCSE will coast to the synchronous altitude along the coplaner transfer ellipse.
8	Circularization and Removal of Injection Errors	S-IVB restart to circularize orbit and make corrections to remove injection errors.
9	Begin Transposition and Docking	CSM will separate from LEM; the CSM maneuvers through 180 degrees and docks to the LEM.
10	S-IVB Stage Separation	The S-IVB stage and the Instrumentation Unit will be jettisoned from the CSM/LEM/LCSE.
	AAP ON STATION	
11	CSM Docking; Initiate ATM Erection	At least two orbits tracked for ephemeris; fine adjustment of orbit parameters accomplished with CSM.
12	ATM/LCSE Erection Completed Start Manned Operations	Control and monitoring of manned participation. Support of related experiments.
13	Astronauts De-orbit	CSM provides retro-force to LEM stage. CSM de-orbits and returns astronauts to earth.
14	LCSE Autonomous Operations using ATM and LEM Power Microwaves and Attitude Control	

of the LEM descent stage structure. While the requirements of low angular rates are important during the boom extend operations, the specific angular orientation is unimportant. The only requirement of angular orientation during the operation is that the sun rays should be entering the bottom of the LEM descent stage so that the EVA Astronaut who is monitoring the uncaging and boom extend operations has adequate light for observing the operation. The astronaut at the control console in the LEM is in voice link communication with the EVA Astronaut. By means of the control console and the voice cues from the EVA Astronaut, the Laser/Telescope and the ATM are deployed. The EVA Astronaut returns to the Command Module.

Step 5. LASER/TELESCOPE OUTGASSES

During the next 2 days, the equipment is allowed to outgas. No experiments are conducted. Angular rates should be kept low.

Step 6. ESTABLISH APPROXIMATE SUN ANGLE

Using sun sensors on the exterior of the Laser/Telescope, the approximate sun angle to the vehicle is established. The spacecraft attitude control system orients the spacecraft so that the Laser/Telescope is pointing at the sun and the angular rates are reduced to values near 0.1 degree/second.

Step 7. SUN ACQUISITION PROGRAM

All lasers are off and the telescope cap is in place covering the entrance aperture of the telescope. The sun seeker is activated, acquires the sun, and sends commands to the spacecraft attitude control system to point the Laser/Telescope at the sun.

Step 8. OFFSET LASER/TELESCOPE FROM SUN LINE BY KNOWN ANGLE

The ground station will telemeter an offset angle to the spacecraft. This offset angle will be programmed into the sun seeker head gimbal offset servos. As sun seeker head gimbal offset servo slowly rotates off from the initial zero, the commands from the sun seeker head to the attitude control system of the spacecraft request the spacecraft to move off the sun line by the same angle. The ATM gimbals are locked at this time so that the Laser/Telescope is offset in its pointing to the sun by the angle programmed into the system.

Step 9. OPEN TELESCOPE CAP AND FAST SHUTTER

The telescope cap is closed during all the sun operations in order to keep direct sunlight out of the telescope. The fast shutter is kept closed

until the Experiment Monitor Console in the LEM indicates that the experiment is ready to proceed. The fast shutter and lens cap are then opened. The ground laser beacon is turned on. The coarse guidance system is now ready to receive the 4880Å ground laser beacon when the telescope points within 1 degree of the ground laser beacon. In the coarse guidance mode, the telescope has a 1-degree field of view (FOV).

Step 10. ROTATE ENTIRE TELESCOPE ABOUT SUN LINE

With the sun seeker locked onto the sun and the programmed offset angle set into the system, the spacecraft rotates slowly about the sun line so that the offset telescope searches for the ground beacon on earth with its 1-degree FOV. The ground beacon laser beam will enter the coarse guidance system sometime during the 360-degree search.

Step 11. COMPLETE COARSE ACQUISITION OPERATIONS (Figures 5 and 6)

When the ground laser beam enters the coarse acquisition optics, the ground laser beam is divided by a fiber optic image divider. The up-down and left-right signals are developed by photomultipliers attached to the fiber optic bundles. The up-down and left-right signals are sent to the ATM stable platform, and the Laser/Telescope is oriented to center the image. Up-down and left-right signals are sent to the spacecraft attitude control system by the ATM to keep the ATM stable platform centered.

Step 12. ROTATIONAL REFERENCE ABOUT THE LINE OF SIGHT

The sun seeker tracks the sun during these operations with the ground laser beacon, and the two trackers in combination generate signals which provide a rotational reference about the line of sight. This rotational reference signal is developed in the onboard electronic coordinate converter which sends commands to the Risley prism servos used by the point ahead system. The coordinate converter commands into the Risley prism servos will drive the two prism servos, as a pair, off a pre-established zero position to compensate for spacecraft rotation about the line of sight. Slow and coarse rotations about the line of sight are provided by the spacecraft attitude control system in response to commands from the Risley prism servos.

Step 13. FINE GUIDANCE

With the earth laser beacon image being driven towards the center of the coarse guidance field by the ATM gimbals, the line of sight of the telescope is centered onto the earth laser beacon. Within 1 arc-minute of the center of the telescope line of sight, there is a hole in the coarse guidance fiber optic bundles. When the earth laser beacon image is driven towards the center, it moves toward the 2 arc-minute (plus/minus 1 arc-minute) hole. When the earth laser beacon image falls into the 2 arc-minute hole, the fine guidance

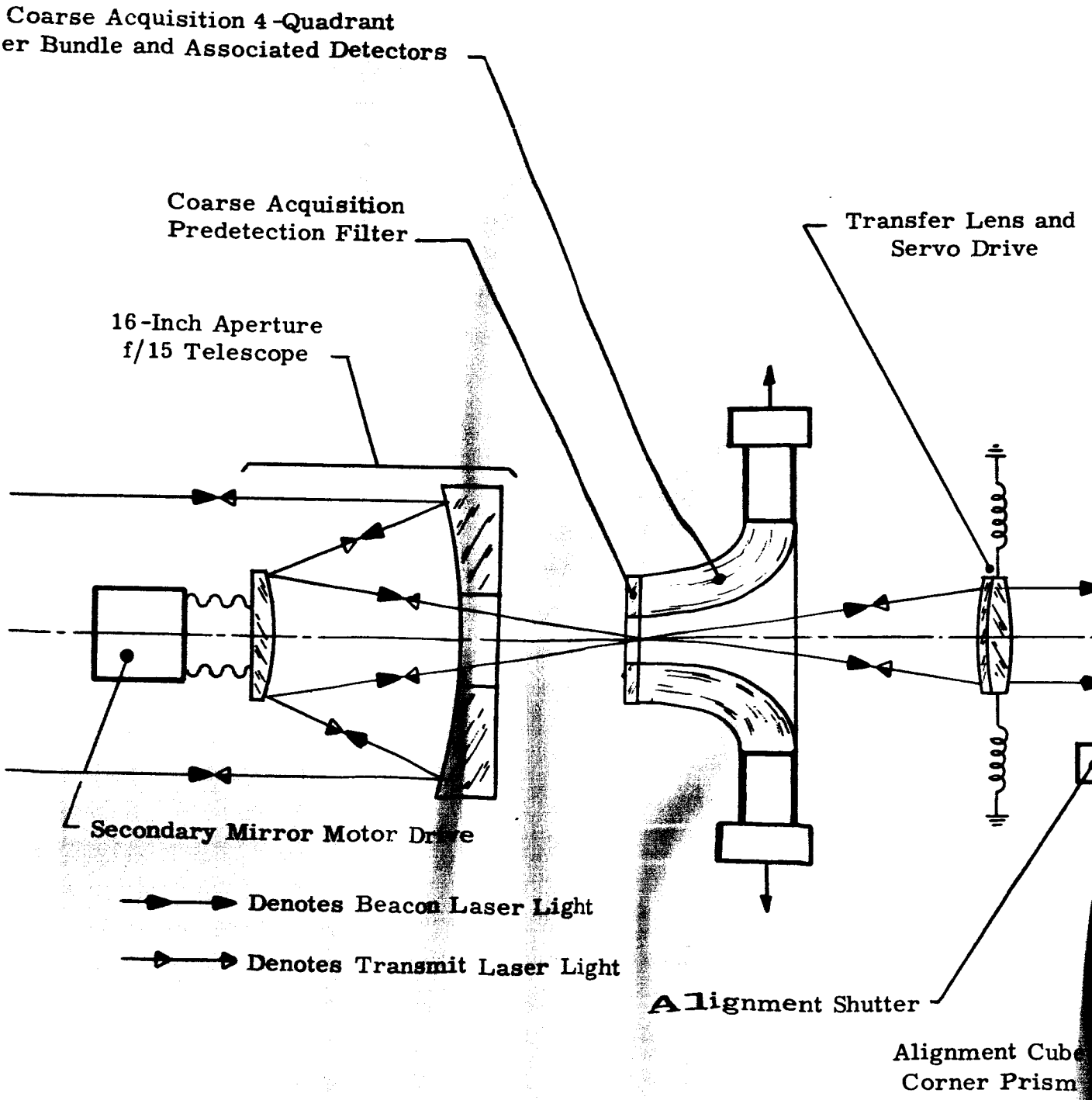
Coarse Acquisition 4-Quadrant
Fiber Bundle and Associated Detectors
Coarse Acquisition
Predetection Filter
Transfer Lens and
Servo Drive
16-Inch Aperture
f/15 Telescope
Secondary Mirror Motor Drive
Denotes Beacon Laser Light
Denotes Transmit Laser Light
Alignment Shutter
Alignment Cube
Corner Prism

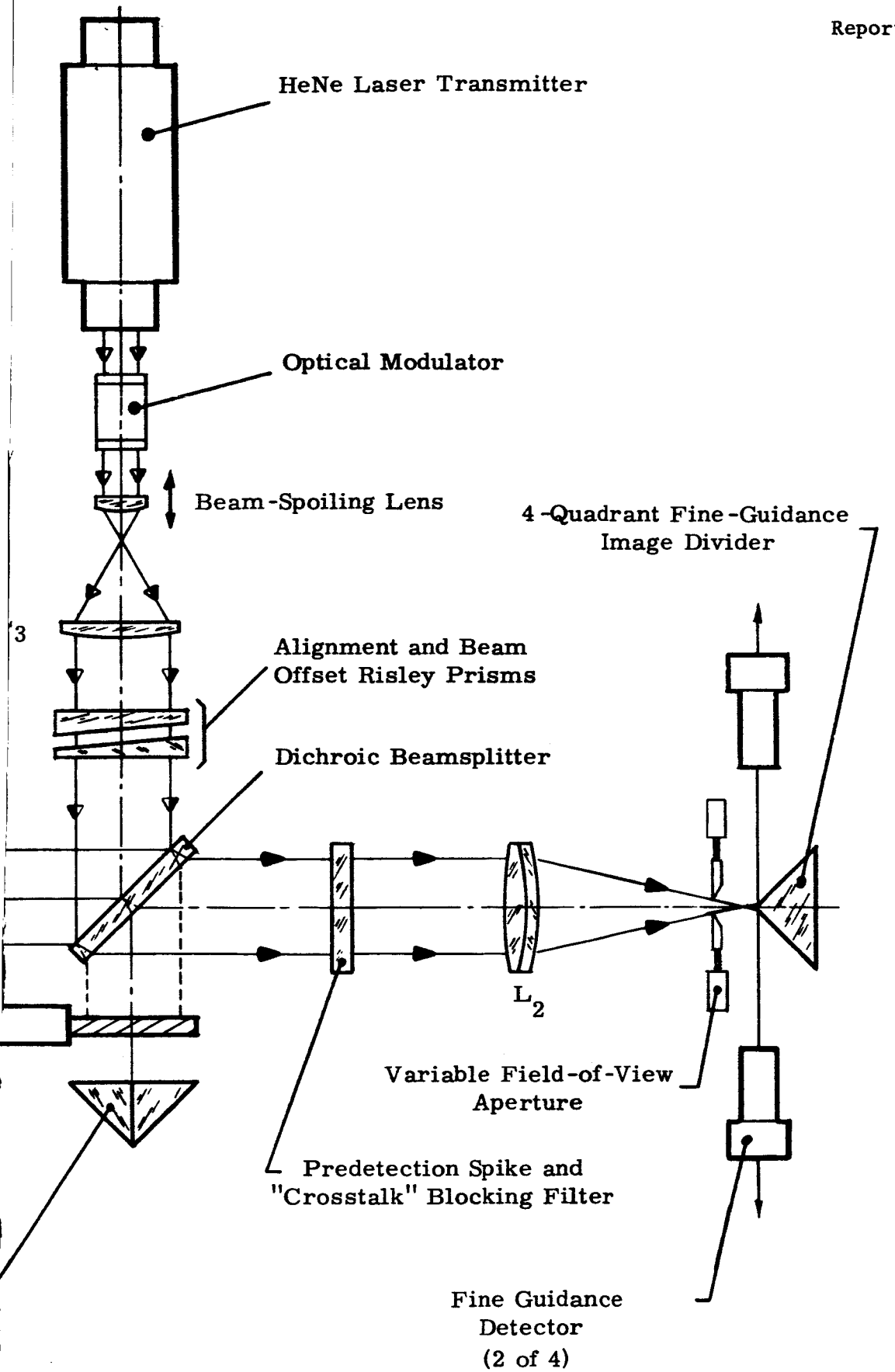

Figure 6. Layout of Basic Optical Communication System

system takes over. The light passes through a two-axis transfer lens and then to an image divider. The image divider breaks up the light into left-right and up-down signals which are sent to the corresponding left-right and up-down motors of the two-axis transfer lens. The transfer lens moves to center the image of the ground beacon onto the apex of the image divider prism. The transfer lens servos are fast and precise; and the transfer lens motions compensate for spacecraft or telescope motions about the line of sight. The image of the ground laser beacon is thus stabilized in space.

Step 14. POINT AHEAD (Figure 7)

With the telescope line of sight locked onto the earth beacon through the fine guidance system, and with the sun seeker locked onto the sun, the information is available to provide a rotational reference to the system. The rotational reference can be generated by knowing the geometry between the sun, the earth beacon, and the orbital parameters of the spacecraft. The point ahead angle is computed on the earth and telemetered to the spacecraft. The point ahead command is translated into differential rotations of the two Risley prism servos to provide a point ahead deflection to the transmit lasers before they enter the transfer lens.

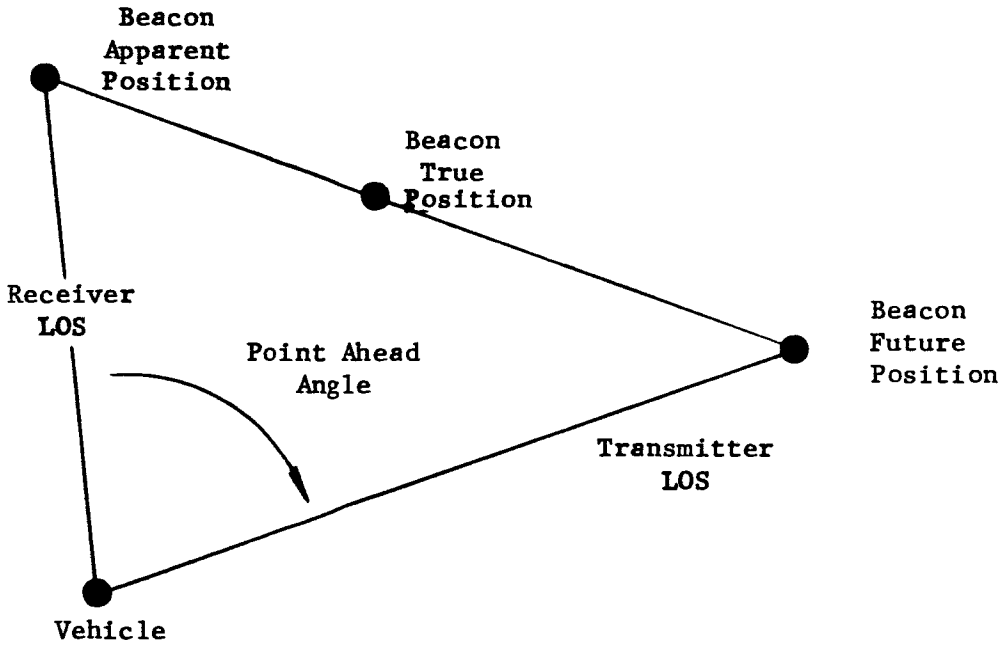

Figure 7. Point Ahead Geometry

Step 15. TRANSMIT LASER LIGHT FROM THE SPACECRAFT

One of the two helium-neon lasers in the laser telescope is turned on. The beam is modulated by the electro-optic crystal modulator with information from a video source (for example, a vidicon camera could be used to feed

analog video data to the PCM encoder which modulates the electro-optic modulator), or spacecraft housekeeping data could be telemetered down from the spacecraft. The laser beam leaves the modulator and goes through the Risley prism point ahead assembly and the beam spoiling lens assembly before it arrives at the transmit laser collimating lens. The laser light bundle is formed into a parallel bundle by the collimating lens before it is reflected off the dichroic beamsplitter. This element reflects the 6328Å light and permits the ground laser beacon (4880Å) to pass through it. The reflected 6328Å laser light then enters the two-axis transfer lens. This lens, which has been stabilized by the fine guidance servos to the line of sight of the earth argon laser beacon, transmits the laser light and effectively steers the laser beam from the telescope exactly stabilized to the incoming laser light from the earth beacon. This operation establishes the down-going laser communication link from the spacecraft and completes the procedural steps for the laser communication experiments. Data collection details are in Section 2.8.

Step 16. ASTRONAUT PARTICIPATION IN THE LASER COMMUNICATION EXPERIMENTS

The astronaut in an EVA mode can assist the Laser Communication Experiment in the following areas:

- In the event of mechanical difficulty in the launch mount uncaging operations, the astronaut can assist the equipment by guiding the Laser/Telescope structure away from the launch mounts and the LEM descent stage structure.
- The astronaut can provide assistance in the sun acquisition mode and function as a "sun sensor and orienter" or as a "sun sensor" only by voice link back to the Experiment Monitor Astronaut (in the LEM Life Cell).
- The astronaut can provide mechanical assistance in opening the telescope cap.
- The astronaut can provide mechanical assistance during the ground beacon acquisition mode (Step Number 10 above). He could either point the telescope himself or could provide voice link commands to the Experiment Monitor Astronaut.

Step 17. TELESCOPE MOTION EXPERIMENT (Refer back to Figure 4)

The laser communication link as presently conceived, would be able to lock onto the earth laser beacon in the presence of spacecraft vibration and motions induced into the telescope by attitude control system actuations. This is accomplished by the two-axis transfer lens stabilizing the line of sight to the earth laser beacon. Since the transmit laser light goes through

this stabilizing element simultaneously, the transmit laser light from the spacecraft will be stabilized in space and the earth receiver will be able to receive the down-going beam in the presence of typical equipment vibrations in the spaceborne structure. The astronaut can end a great deal of speculation about the narrow beam pointing performance of the laser communication system by inducing vibrations himself by either holding the instrument lightly or extremely tightly. The vibration and motion disturbances induced into the Laser/Telescope during these operations can be monitored and correlated with communication link performance.

Step 18. ASTRONAUT EARTH-VIEWING EXPERIMENT (Refer back to Figure 1)

After the communication link experiments are completed, and after the vibration inducing operations of Step 17 above are completed, the astronaut can go to the Astronaut's Grab Bracket on the exterior of the Laser/Telescope. At this location, he can remove the viewing port covers of the telescope structure, attach auxiliary optical eyepieces into the space provided and look through the telescope in a short focal length (1-degree field of view) or a long focal length (2 arc-minute field of view). He can conduct ground feature recognition experiments in cooperation with personnel at the ground station since his line of sight will be stabilized by the laser communication experiments guidance equipment. When viewing in the 1-degree FOV mode, the instrument is stabilized to plus/minus 10 arc-seconds. When viewing the earth in the long focal length configuration (f/70), the instrument is stabilized to 0.1 arc-second. Both viewing operations are conducted with the spacecraft helium-neon laser turned off, but with the earth laser beacon turned on. It would therefore be necessary to provide the astronaut with an optional 4880Å rejection filter so that he is able to distinguish features of the landscape without being overpowered by the intensity of the earth beacon. An auxiliary photographic system can simultaneously take photographs of what the astronaut observes. (The astronaut would take the films back into the command module for his earth return.) Also, if desired, an auxiliary TV camera can be incorporated into the external optical package attached to the Laser/Telescope by the astronaut. Real-time television could be sent down to the ground station at the same time the Laser/Telescope is guiding on the ground station beacon. The real-time TV signals would be coded by the PCM coder and these signals, in turn, would modulate the laser output.

2.3 FUNCTIONAL DISCUSSION OF THE LCSE LASER/TELESCOPE

The 18 procedural steps for the conduct of the proposed experiments which are described in Section 2.2 are accommodated by the block diagram of Figure 8. This block diagram shows the interrelationship between the key components of the optical communicator of the LCSE. The interfaces between the communicator and the LEM are:

- command decoder
- video signal for the optical PCM/PL link
- telemetry encoder for the diagnostic equipment.

The power and attitude control interfaces between the LEM and the LCSE are not shown in this figure. The dashed and dotted lines on the drawing show the path of the helium-neon laser output and the argon beacon input, respectively.

AUTOMATIC CHANNEL ALIGNMENT

After the LCSE has outgassed for 2 days (Step 5 of the Experiment Procedure), and before the functional operations of the laser communication experiments (Step 6 of the Experiment Procedure is the start of acquisition operations), the transmit and receive channels of the Laser/Telescope must be aligned with each other.

Temperature variations in the telescope tube wall and bulkheads will introduce alignment errors between the transmit (He-Ne) and the receive (argon beacon) channels. Also, continuous operation of the Risley prisms to compensate for the point ahead and telescope roll may introduce a bias error into the Risley prism actuator. The output of the position monitor on the Risley prism is telemetered to earth and compared with the value obtained from the monitor during the initial alignment. If this value is larger than expected, additional measurements will be made to determine the origin of the bias angular offset error.

For the conditions of zero point ahead, the apex of the image dividing prism in the receive channel must be conjugate with the focal point of the transmit laser. The technique that is utilized in the LCSE is based on laboratory work and procedures developed during the Laser/Optics Techniques Project (NAS8-20115).. The two problems of using a common telescope for both the transmitter and beacon receiver are channel separation and alignment. The work on the Laser/Optics Techniques Project has demonstrated a method of achieving the required channel separation (in excess of 100 db), and a technique for utilizing the fine guidance system for alignment of the channels. A cube-corner prism is located behind the main beamsplitter in line with the laser transmitter incident beam. Refer back to Figure 6 on page 21. In normal operation the cube-corner prism is covered by a shutter and the small but finite amount of transmitter beam passed by the beamsplitter is lost from the system. When the system is in this alignment mode of operation, the fast

shutter and telescope cap are closed to block the ground beacon and other background light, and the shutter in front of the cube-corner prism is opened to reflect the small amount of transmitter light back into the receiver channel. This reflected light impinges on the four quadrant pointing error sensor. The signals from the four photomultipliers in the error sensor are used to servo the Risley prisms so that the image of the transmitter laser is located precisely at the apex of the four quadrant divider. After the correction has been made, the alignment control electronics automatically close the shutter in front of the cube-corner prism, and open the shutter behind the primary mirror.

The time sequence and systems interplay of this channel alignment function are shown in Figure 9.

GROUND BEACON ACQUISITION

The definition of beacon acquisition includes the series of spacecraft maneuvers necessary to orient the satellite so that the diffraction-limited image of the ground beacon lies within the 2 arc-minute field of view of the fine guidance system. This acquisition can be divided into two stages:

Stage 1 - Obtaining the image of the earth beacon laser within the 1-degree field of view of the coarse guidance system. This is accomplished by a series of spacecraft maneuvers originating from the ground utilizing the sun as a unique star for guidance and developing spacecraft information from the LCSE Sun Tracker and Sun Indicators.

Stage 2 - After the earth beacon image is within the 1-degree field of view of the telescope, up-down and left-right commands originating in the coarse guidance electronics drive the image into the 2 arc-minute field of view of the fine guidance package by pointing the entire telescope with the ATM yaw and pitch servos.

The Stage 1 operations are controlled from the ground while the sequences of Stage 2 operations are controlled by the LCSE and will be described by the functional diagram of the LCSE subsystem used in coarse guidance.

The acquisition technique (Steps 6 through 11 on Page 19) consists of establishing the sun line at the satellite and offsetting the telescope's line of sight from this sun line by a specific angle which is telemetered to the LCSE from the earth station. The spacecraft then rolls about the sun line until the earth laser beacon appears in the 1-degree field of view of the coarse guidance system. Ground computer calculations using orbital data and earth-sun geometry are used to compute the offset angle to the sun line. To help distinguish the ground beacon from earthshine in both acquisition and tracking operations, the beacon will be modulated with a characteristic signature. During the station transfer experiment, each ground station laser will be modulated with a different signature.

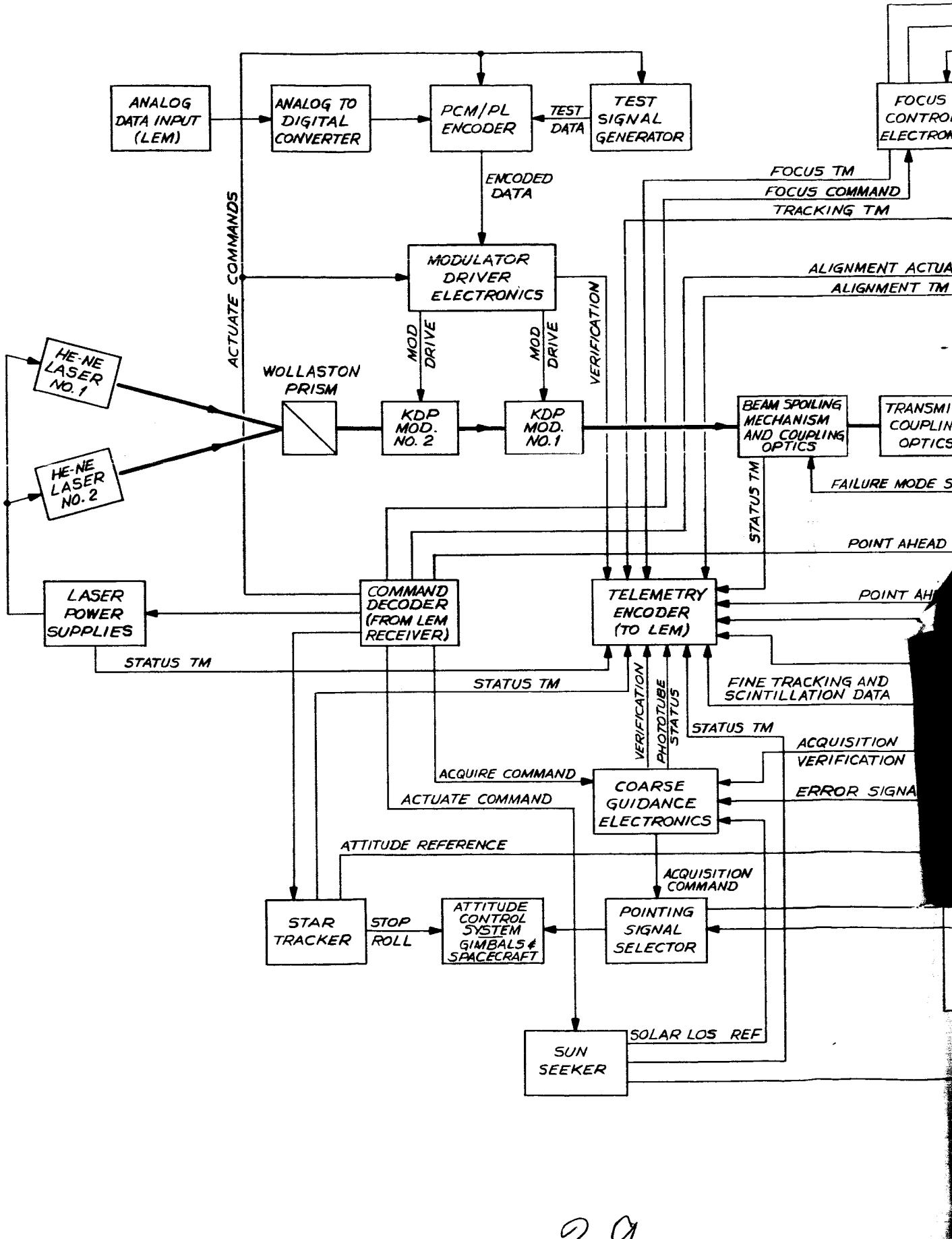
ANALOG DATA INPUT (LEM)
ANALOG TO DIGITAL CONVERTER
PCM/PL ENCODER
TEST DATA
TEST SIGNAL GENERATOR
FOCUS CONTRO ELECTRON
ENCODED DATA
FOCUS TM
FOCUS COMMAND
TRACKING TM
ACTUATE COMMANDS
MODULATOR DRIVER ELECTRONICS
ALIGNMENT ACTUA
ALIGNMENT TM
VERIFICATION
MOD DRIVE
MOD DRIVE
HE-NE LASER NO. 1
WOLLASTON PRISM
KDP MOD. NO. 2
KDP MOD. NO. 1
BEAM SPOILING MECHANISM AND COUPLING OPTICS
TRANSMI COUPLIN OPTICS
HE-NE LASER NO. 2
STATUS TM
FAILURE MODE S
POINT AHEAD
LASER POWER SUPPLIES
COMMAND DECODER (FROM LEM RECEIVER)
TELEMETRY ENCODER (TO LEM)
POINT AH
STATUS TM
STATUS TM
FINE TRACKING AND SCINTILLATION DATA
VERIFICATION
PHOTOTUBE STATUS
STATUS TM
ACQUISITION VERIFICATION
ACQUIRE COMMAND
COARSE GUIDANCE ELECTRONICS
ERROR SIGNA
ACTUATE COMMAND
ATTITUDE REFERENCE
ACQUISITION COMMAND
STAR TRACKER
STOP ROLL
ATTITUDE CONTROL SYSTEM GIMBALS & SPACECRAFT
POINTING SIGNAL SELECTOR
SUN SEEKER
SOLAR LOS REF

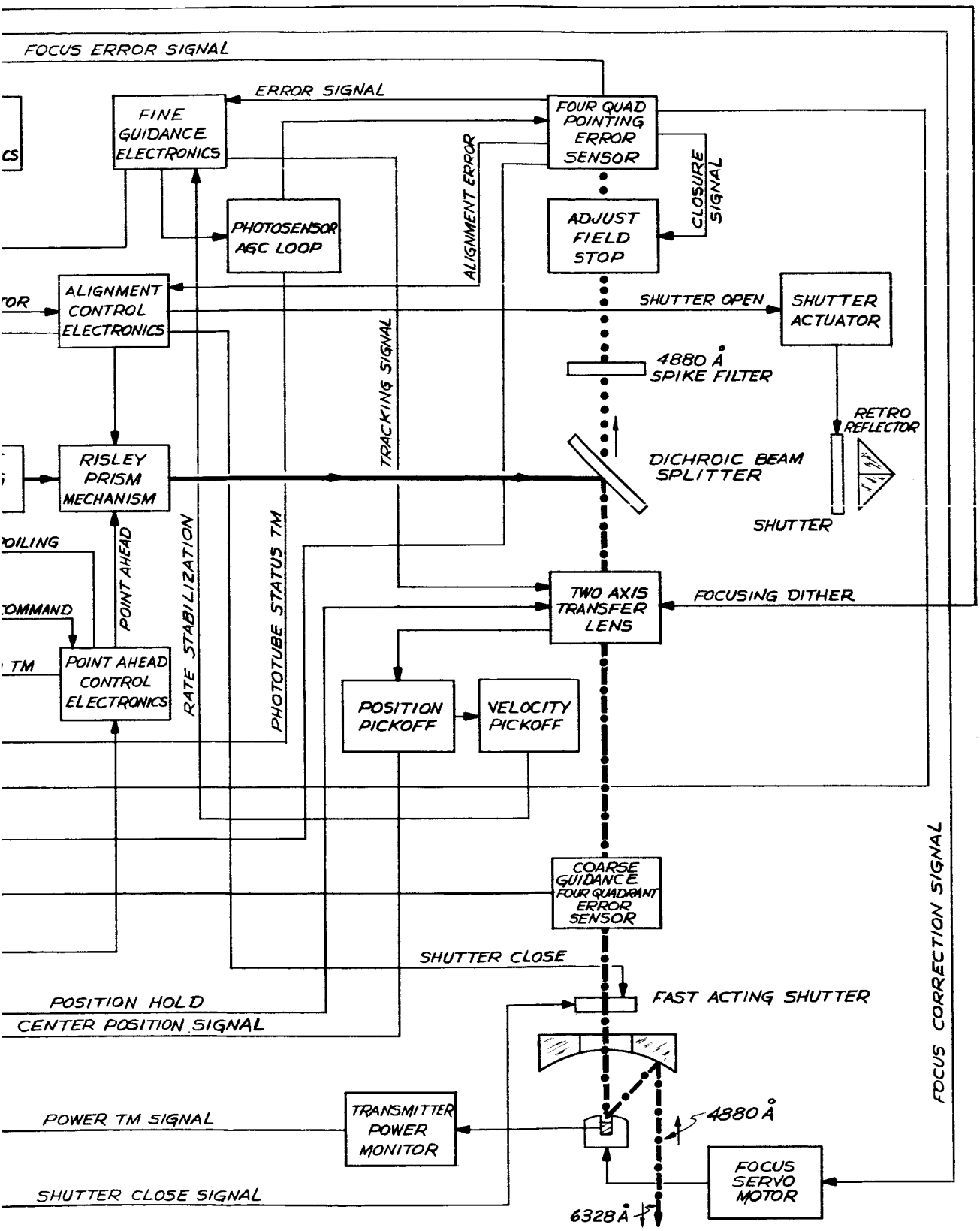

Figure 8. LCSE Functional Block Diagram

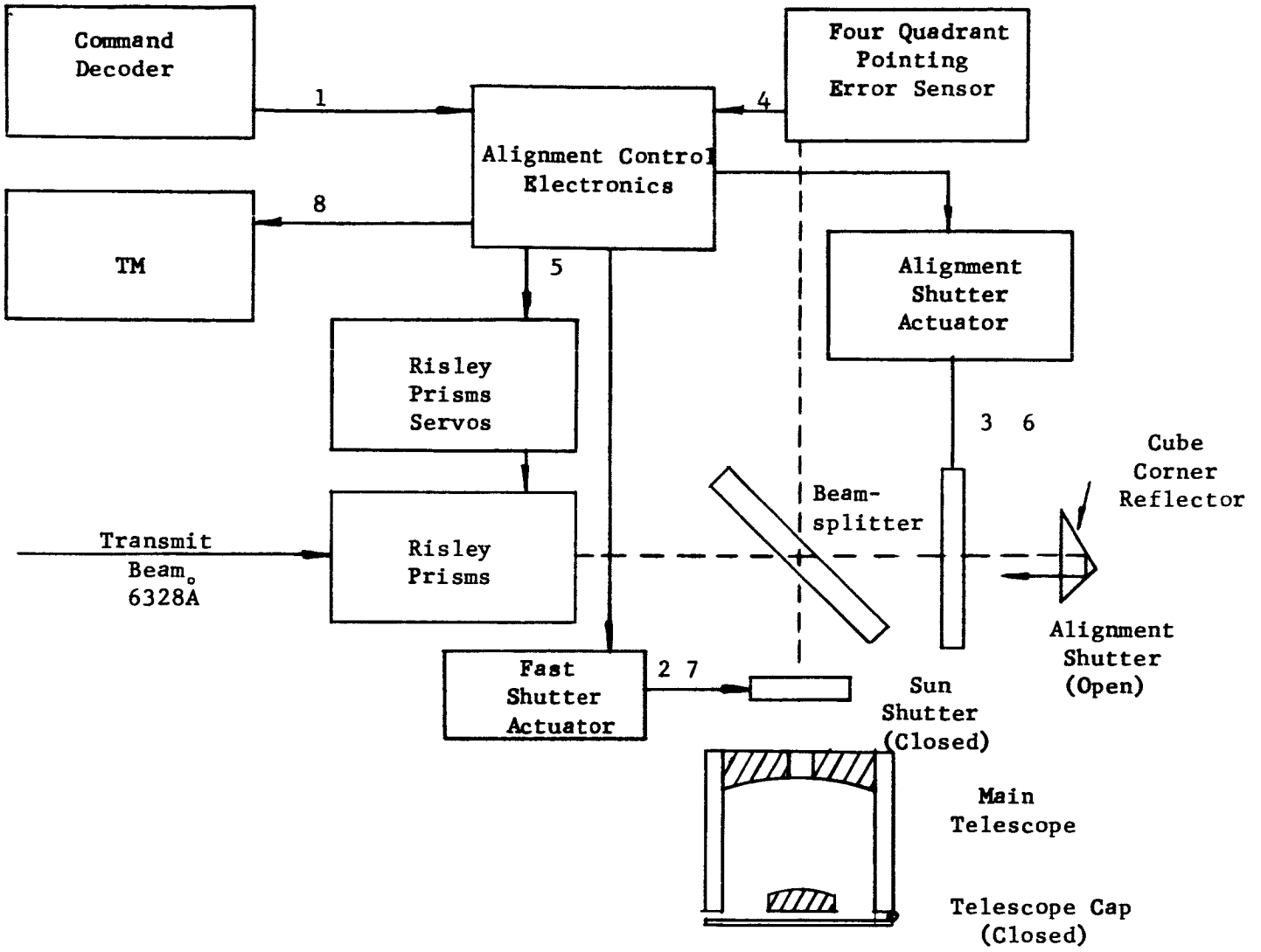

The numbered lines represent information paths and are as follows:

(1) Initiate alignment mode from command decoder to alignment control electronics.

(2) Shutter close signal from alignment control electronics to primary shutter actuator.

(3) Shutter open signal from alignment control electronics to cube corner shutter actuator.

(4) Error signal from pointing error sensor, proportional to offset of image of transmitter from apex of four quadrant divider, to alignment control electronics.

(5) Computed correction to Risley prisms from alignment control electronics to Risley prisms actuator.*

(6) Shutter close signal from alignment control electronics to cube corner shutter actuator.

(7) Shutter open signal from alignment control electronics to primary shutter actuator.

(8) Telemetry of completed function from alignment control electronics to telemetry electronics.

Figure 9. Functional Diagram of System Alignment

* Items 4 and 6 above represent a closed loop servo system and 5 and 6 change to drive 4 to zero. When 4 reaches a predetermined small value, the system proceeds to 7.

After completion and verification of Stage 1 operations of the coarse acquisition, the coarse guidance subsystem of the LCSE takes over to accomplish Stage 2 operations. This second stage of the acquisition operation is performed automatically and is controlled by the coarse guidance electronics in the satellite. Figure 10 is a functional diagram of the system and shows the information paths for the coarse guidance functional blocks.

Upon completion of the acquisition operations, beacon fine tracking operations take place. The fine guidance system has provisions to keep the beacon within a 2 arc-minute field of view. Acquisition mode sequences do not occur again until after a shutdown or loss of the ground beacon. Before examining the fine guidance tracking operation, the in-flight focusing sequence will be considered since it occurs next in the operational sequence of the satellite, and proper focus is necessary for the 0.1 arc-second tracking experiment.

IN-FLIGHT FOCUSING OF THE SECONDARY MIRROR

To maintain diffraction-limited performance of the optical system after launch, it is necessary to focus the system by adjusting the secondary mirror while tracking the 4880Å earth laser beacon. This is necessary because of the small tolerance allowable on the primary-secondary spacing. A displacement of 10^{-4} inches significantly reduces the performance of the telescope. The method employed in this subsystem involves the utilization of the ground beacon as a source and dithering the movable transfer lens. As the transfer lens is dithered, the fine tracking guidance system will automatically respond with a correction signal to the transfer lens which tends to cancel the dither. As this is being done, the secondary mirror is moved in and out by a servo motor. At the point of sharpest focus of the secondary, the displacement response of the fine tracking system will be maximum for a fixed dither amplitude. By adjusting the secondary to maximize this response the proper focus will be accomplished.

Figure 11 is a functional diagram of the in-flight focusing subsystem showing the information flow paths during operation. Note that this function, like alignment, is accomplished by a closed loop servo system which is inherently free of zero offset errors.

0.1 ARC-SECOND TRACKING OF THE EARTH LASER BEACON

Tracking the earth laser beacon to a fraction of an arc-second is necessary for deep space laser communications. The approach selected for the LCSE is the technique demonstrated in the laboratory at Perkin-Elmer in the Laser/Optics Techniques Project. The guidance system uses a four quadrant image divider to generate tracking error signals which are used to servo control a small and special optical element. This optical element, the transfer lens, is common to both the receiver and transmitter beams. In this system, the movable transfer lens has independent x and y motions and is located before the beamsplitter. As the telescope structure or primary vibrates, the transfer

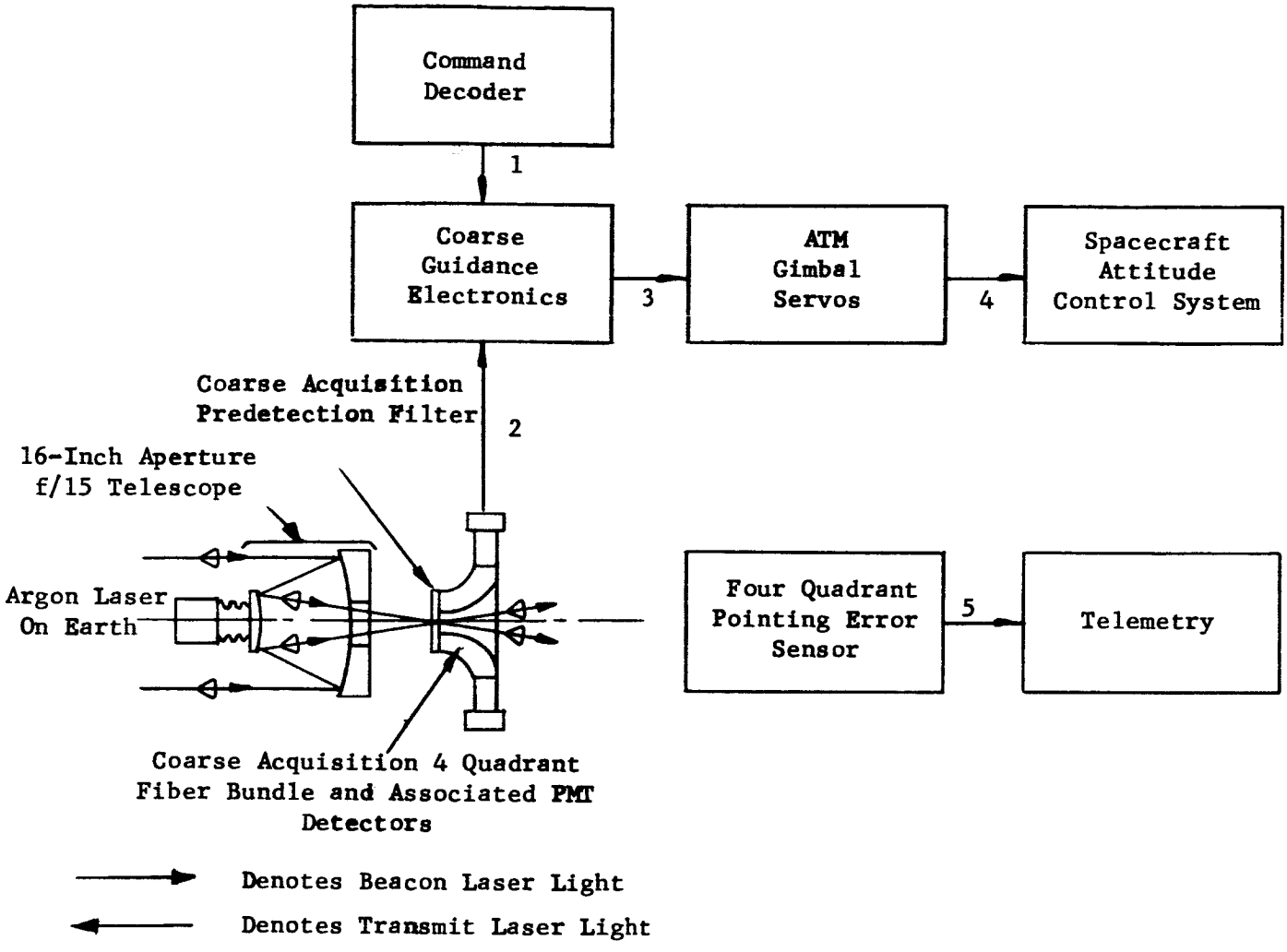

The information paths are:

(1) Ground command to activate Stage 2 of acquisition.
(2) Error signal developed from earth laser beacon image on quadrant image divider.
(3) Telescope attitude error.
(4) Attitude correction commands.
(5) Fine guidance acquisition confirmation upon completion of Stage 2 of coarse acquisition.

Figure 10. Functional Diagram for Coarse Guidance Acquisition

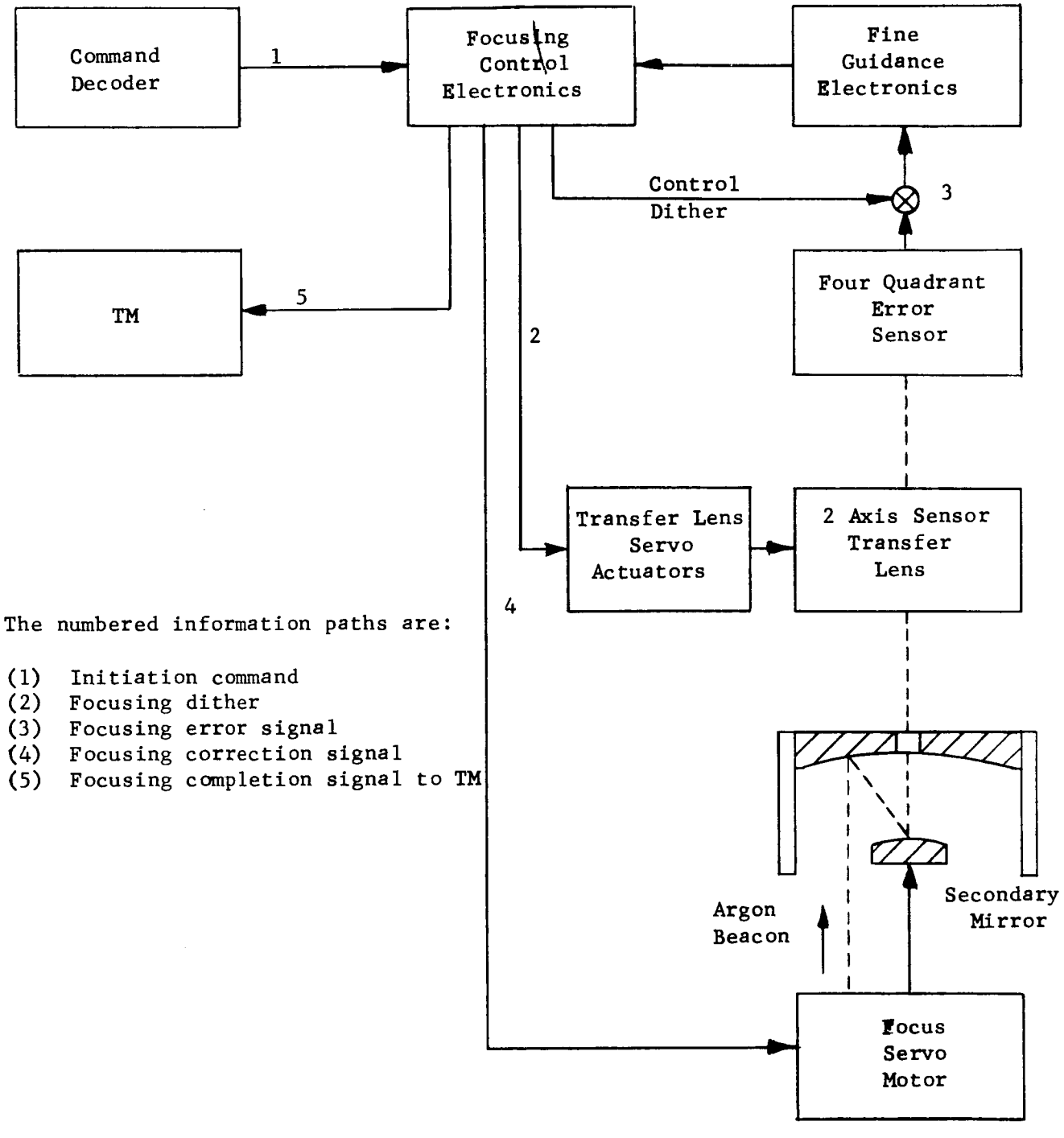

The numbered information paths are:

(1) Initiation command
(2) Focusing dither
(3) Focusing error signal
(4) Focusing correction signal
(5) Focusing completion signal to TM

Figure 11. Functional Diagram of In-Flight Focusing

lens is controlled to keep the diffraction-limited image on the apex of the four quadrant divider prism of the fine guidance system. The characteristics of this servo system have been reported elsewhere,* but the functional relationships of the components will be discussed here. Position sensors on the transfer lens generate signals which activate the ATM pointing control system in pitch and yaw to keep the lens operating in the general vicinity of its zero position.

By introducing the appropriate point ahead into the transmitted laser beam, the transmit laser beam can be pointed to the ground telescope on earth to demonstrate communication over diffraction-limited laser beams of fractional arc-second width. The accuracy which will be achieved with this tracking system is far better than necessary for near earth satellite communications where beam divergences can be large. However, for optical communication at interplanetary distances where beam divergence must be small, pointing (or tracking) to this precision is mandatory. Figure 12 is a functional diagram of the tracking (fine guidance) system.

POINT AHEAD

With the system telescope tracking the receiver beacon, only one function remains in establishing the optical link. To compensate for Bradley effects which cause appreciable pointing errors the transmitter beam must point at some point ahead angle, θ_p, ahead of the line of sight of the beacon. However, θ_p and the line of sight are not sufficient to specify a direction in space. The third piece of data needed to uniquely determine the direction in which the transmitter beam should be pointed is the rotational angle reference about the line of sight (RLOS) towards the beacon. A ground-based computer, can calculate the angles θ_p and ϕ (indicated in Figure 13) that are necessary for point ahead. The geometry of the earth laser beacon and the orbital parameters of the satellite (and the sun and the earth) are all known on earth. Therefore, the point ahead angle can be computed and telemetered to the spacecraft.

If the orbit is a synchronous equatorial orbit and the reference target for RLOS is a star at one of the celestial poles, then the point ahead angle is fixed and there are no earth computer requirements. However, since the sun is chosen as the RLOS reference, and at synchronous altitude the sun moves with respect to the spacecraft at 15 arc-seconds per second of time, the Risley prism servos will constantly be moving.

*Laser/Optics Techniques, Perkin-Elmer Report No. 8387, June 1966.

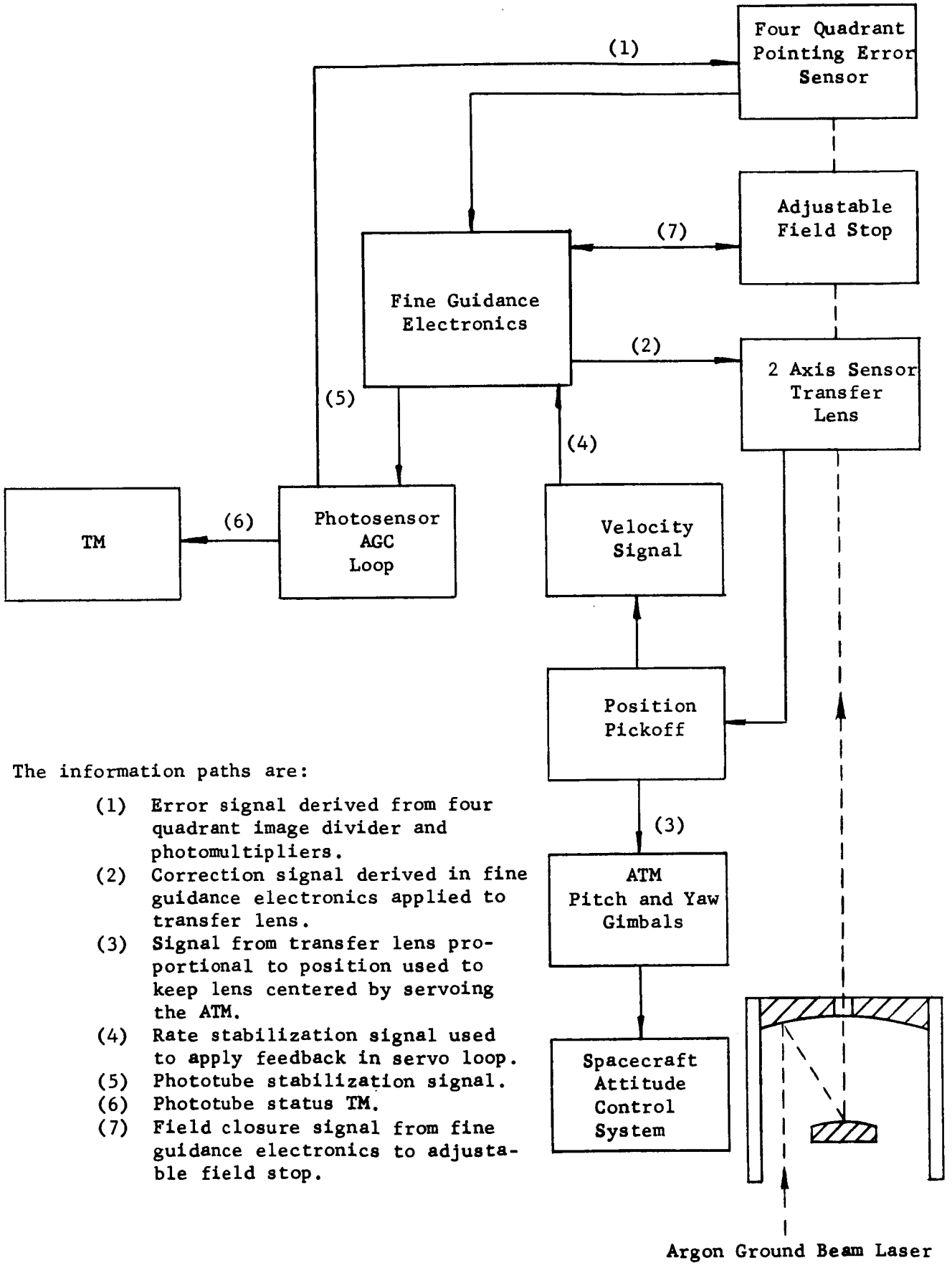

The information paths are:

(1) Error signal derived from four quadrant image divider and photomultipliers.
(2) Correction signal derived in fine guidance electronics applied to transfer lens.
(3) Signal from transfer lens proportional to position used to keep lens centered by servoing the ATM.
(4) Rate stabilization signal used to apply feedback in servo loop.
(5) Phototube stabilization signal.
(6) Phototube status TM.
(7) Field closure signal from fine guidance electronics to adjustable field stop.

Figure 12. Functional Diagram of Fine Guidance System

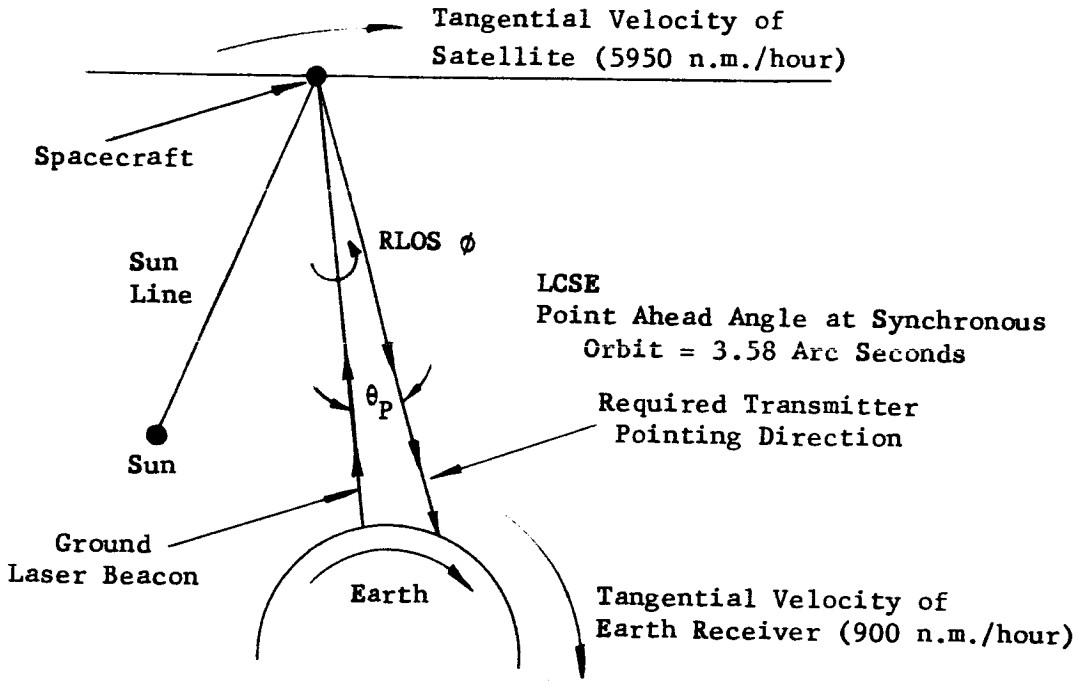

Figure 13. Geometry for LCSE Point Ahead Function

The problem of pointing separates into two functions. The first is determining a reference direction about the line of sight of the beacon (RLOS), and the second is transmitting the θ_p and $\emptyset$ commands from the ground based computer into precise changes in the transmitted beam direction.

At synchronous altitude, four optical techniques* for establishing RLOS are:

- using a sun tracker,
- star tracker,
- laser polarization sensing,
- and moire fringes.

Since it requires no additional hardware, the sun tracker is the most efficient and will be used to determine the RLOS. While tracking the ground beacon, the spacecraft attitude control system will introduce a roll about the line of sight of the beacon until the sun is acquired by the sun tracker. The offset angle, θ_p, between the line of sight of the beacon and the direction of the

*Previously analyzed in Report No. 8387, Loc. Cit.

sun is computed on the ground from orbital data and telemetered to the satellite. The sun is now the reference from which $\emptyset$ is measured while θ_p is measured from the line of sight of the beacon. Now that the coordinate system has been established, the θ_p and $\emptyset$ commands are sent to the satellite via the microwave link. Both θ_p and $\emptyset$ are slowly varying functions of time and the point ahead is periodically updated.

There are various ways of achieving the precise beam deflections necessary to perform point ahead. The one selected for the LCSE consists of servo actuated Risley prisms. This choice was made on the basis of simplicity and reliability and because the prism assembly requires no power to maintain a constant point ahead. The point ahead electronics receive the θ_p and $\emptyset$ commands and translate them into rotations of the prism by the required amount. Figure 14 is a functional diagram for the point ahead system.

BEAM SPOILING

The nominal diffraction-limited 3 db beamwidth of the 16-inch primary of the LCSE is 0.4 arc-second. This narrow beamwidth requires both accurate tracking and precise point ahead capability of the communicator optics. As a backup system for LCSE the point ahead can be eliminated by 4 arc-second beam spoiling. This reduces the energy density on earth. Since the system operates with a 20 db margin, communications are still possible with a 10:1 increase in the divergence to 4 arc-seconds.

TRANSMISSION OF 10^6 BITS/SEC OVER DIFFRACTION-LIMITED OPTICAL LINK

With the completion of the point ahead functions and the establishment of the optical link, high data transmission of digital information (10^6 bits/sec) from the onboard signal sources is used to collect engineering data on space optical communications. This operation constitutes one of the most important aspects of the flight.

To evaluate the 10^6 bits/sec, data rate communications verification of the received beam on earth is telemetered to the satellite. This is in the form of a series of commands which activate the PCM/PL modulator and the data handling electronics. The data is generated initially by the test signal generator and is not from an external input to the system. While the test data is being transmitted the laser output power and other diagnostic data are monitored and telemetered to earth. This enables a comparison between the calculated and the received signal-to-noise ratios.

Figure 15 is a functional diagram of the data handling chain.

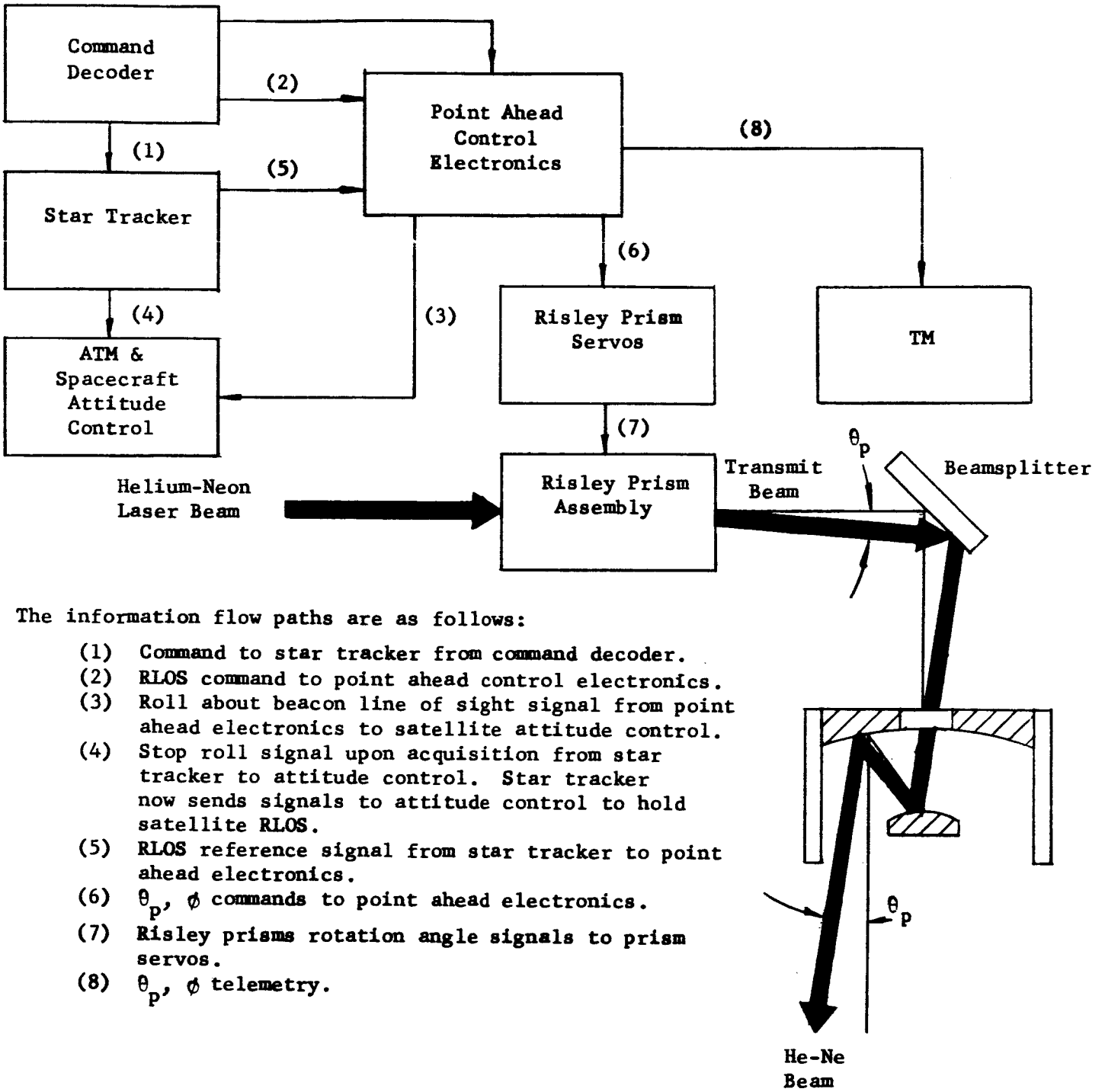

The information flow paths are as follows:

(1) Command to star tracker from command decoder.
(2) RLOS command to point ahead control electronics.
(3) Roll about beacon line of sight signal from point ahead electronics to satellite attitude control.
(4) Stop roll signal upon acquisition from star tracker to attitude control. Star tracker now sends signals to attitude control to hold satellite RLOS.
(5) RLOS reference signal from star tracker to point ahead electronics.
(6) θ_p, ϕ commands to point ahead electronics.
(7) Risley prisms rotation angle signals to prism servos.
(8) θ_p, ϕ telemetry.

Figure 14. Functional Diagram of Point Ahead System

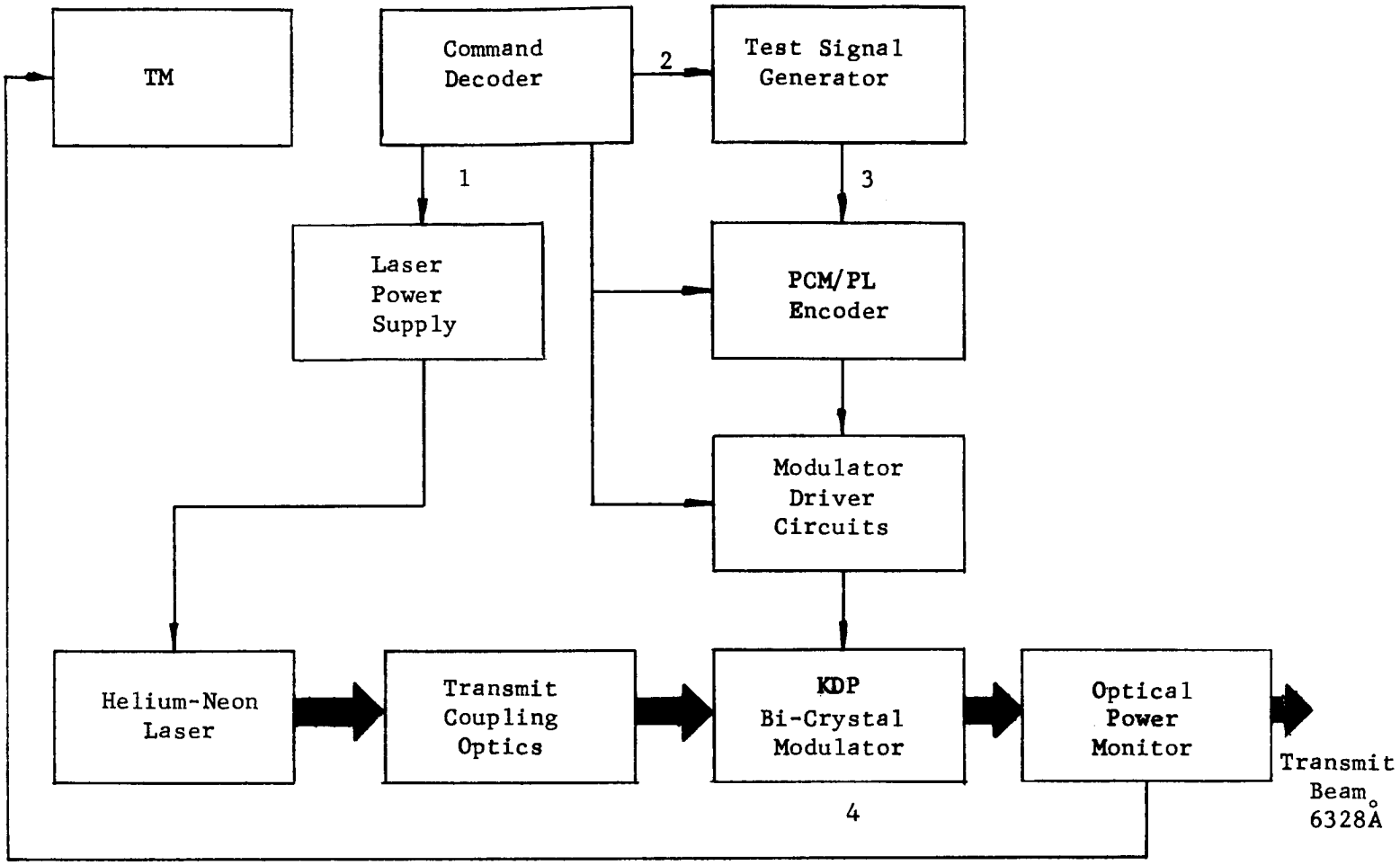

The information flow is as follows:

(1) Ground command to turn on one of the He-Ne lasers.
(2) Ground command to turn on test signal generator.
(3) Ground command to turn on PCM/PL encoder and modulator driver circuits.
(4) Telemetry of transmitter power from power monitor in center of secondary mirror.

Figure 15. Functional Diagram of Data Handling System

TRANSMISSION OF LIVE 10^6 AND 10^7 BITS/SEC DATA

After collecting the engineering data on the 10^6 bits/sec optical channel utilizing data from the test signal generator, the satellite will be available for the transmission of wideband live data. An input will be available for accepting analog video input or other analog information. This data will be sampled and digitized by the encoder. The increase in data rate by a factor of 10 is accompanied by a corresponding increase in power consumption of the LCSE from 85 watts to 130 watts. It is for this reason that 10^7 bits/sec transmission is not recommended for long periods of time.

The communicator satellite will be provided with an external connection whereby the astronaut can plug in a Vidicon or other source of live data. Provision is also made to switch the data handling system to internal mode of operation so that spacecraft housekeeping data can be telemetered to earth on the laser beam.

DEEP SPACE SIMULATION OF STATION TRANSFER

This experiment is included in the communicator satellite to measure the capability of the system to transfer the transmitted beam from one ground station to another without repeating the initial acquisition functions. The necessity for this capability arises from the occultion of the earth station to a deep space vehicle by either earth rotation or cloud cover. It is clear that in the deep space case where ranges are in the 10^8 mile category, that the transit time or Bradley aberrations for the two earth stations (estimated separation $\sim$ 4000 miles) are approximately the same. To simulate a deep space mission, station transfer will be accomplished between two earth beacons separated in angle (measured from the synchronous satellite) by an amount which corresponds to the angle for earth beacon separation ($\sim$ 4000 miles) for a deep space payload. This angular separation is approximately 8 arc-seconds or a station separation of about 4500 feet for a satellite at synchronous attitude.

The angular separation of both earth stations is small enough so that both will be within the field of view of the fine guidance system. Each ground station will have its own characteristic modulation. To accomplish station transfer when both beacon images are incident on the four quadrant image divider, a ground command to the fine guidance electronics switches between electrical filters which pass each one of the two signature modulations. As long as this switching occurs in a time that is short compared to the time for the spacecraft attitude to change sufficiently to shift the beacon images out of the two arc-minute field of view of the fine guidance system, transfer is accomplished without the loss of beacon acquisition.

An alternate procedure is to sequentially extinguish one beacon and turn on the second beacon. For this procedure, both beacons will have the same characteristic modulation. This technique has the disadvantage that track may be lost during the station transfer.

The operational sequences necessary to accomplish station transfer are as follows:

(1) Fine guidance system is tracking station A with signature modulation of frequency F_A.

(2) Station B with signature modulation of frequency F_B is received and its image is in the field of view of the fine guidance system.

(3) Circuitry in fine guidance package responds to presence of a photomultiplier signal of frequency F_B while tracking signal at F_A, and telemeters confirmation over microwave link.

(4) Command to switch tracking from signal at frequency F_A to signal at frequency F_B.

(5) Upon receiving command to switch to F_B, the fine guidance package checks for the presence of a signal at F_B and switches the necessary electronics filters. If a command is received to switch to a signal at a new frequency, the system will ignore the command unless that signal frequency is present in the fine guidance photomultipliers.

(6) The switching of the tracking frequency is telemetered to the earth station.

A functional diagram of the station transfer experiment is shown in Figure 16.

POINT AHEAD SIMULATION OF DEEP SPACE COMMUNICATION LINK

For a 10^8 miles communication link, transit time is of the order of 7-1/2 minutes one way and transit time aberrations become large enough to require point ahead by as much as 36 arc-seconds. This experiment is to measure point ahead precision of this magnitude while maintaining an accuracy of 0.1 arc-second. This will require a ground receiver located approximately 3.2 miles ahead of the beacon. The apparatus to accomplish this is included in the spacecraft optical system, and the Risley prism subsystem is designed to have a sufficient point ahead range to accomplish this deep space simulation.

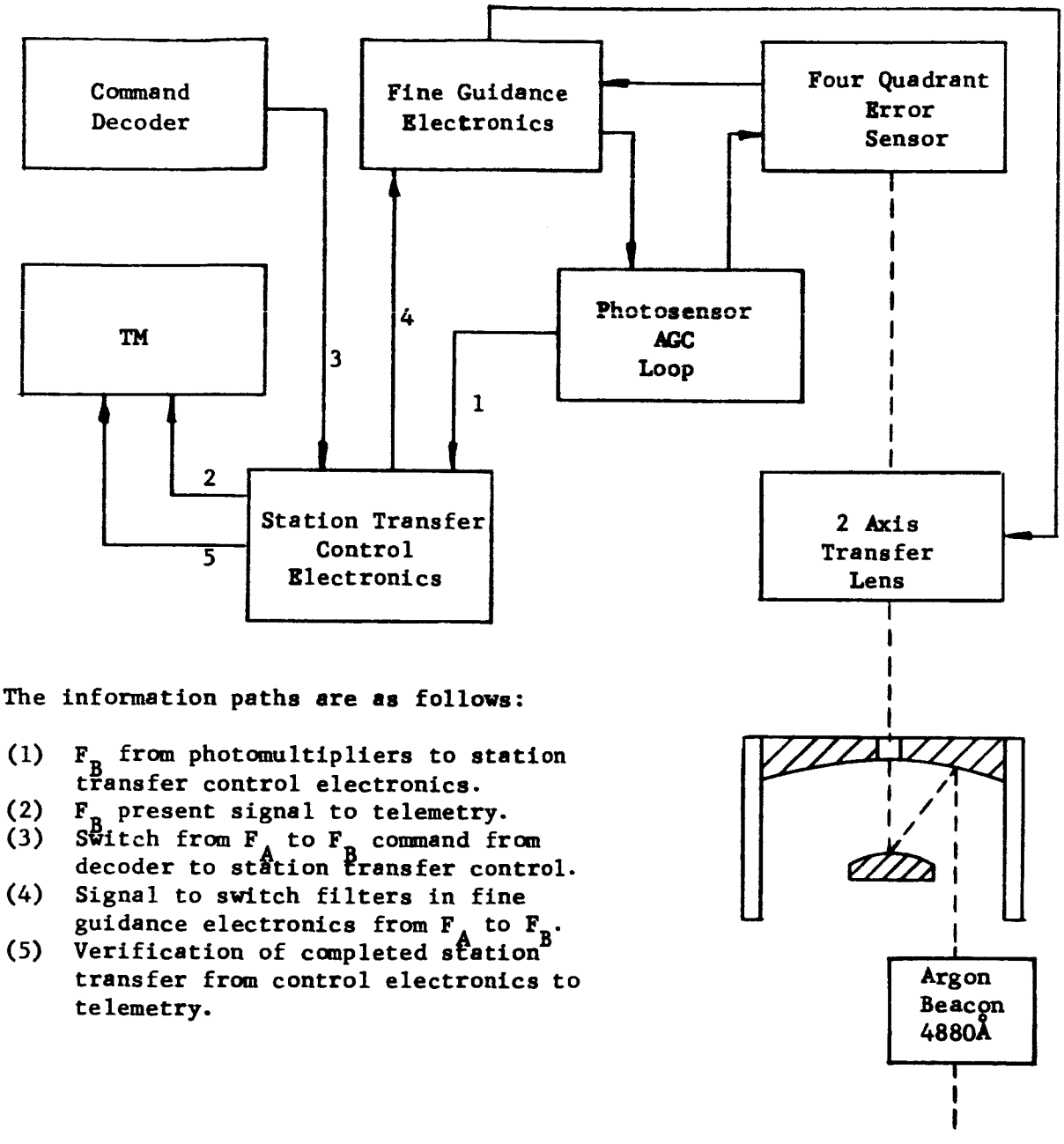

The information paths are as follows:

(1) F_B from photomultipliers to station transfer control electronics.
(2) F_B present signal to telemetry.
(3) Switch from F_A to F_B command from decoder to station transfer control.
(4) Signal to switch filters in fine guidance electronics from F_A to F_B.
(5) Verification of completed station transfer from control electronics to telemetry.

Figure 16. Functional Diagram of Station Transfer Experiment

BLANK PAGE

2.4 APOLLO SPACECRAFT MODIFICATIONS FOR THE LCSE

The required spacecraft modifications are assumed to be the responsibility of the Apollo Applications Payload Integration Contractor. The modifications are listed below, but the costs required to make the changes are not included in the cost estimates which are presented elsewhere in this report.

POWER SYSTEM

The existing fuel cell system is to be modified to provide power at the 3 month and 6 month operating periods. It is assumed that supplementary solar cells and storage batteries will be used if the present fuel cells cannot accommodate the requested 130 watt load for 8 days (during the first 14 days of the flight), 85 watts for 3 days at the end of 3 months, and 85 watts for 8 days at the end of 6 months. The total energy requirement for the experiments (laser communication and earth viewing) is estimated at 45,000 watt-hours. This power level of 85 watts is exclusive of the microwave communication, attitude control, and housekeeping power needed by LEM. The above comments apply to the Basic AAP Concept as shown in Figure 1. A summary of the LEM power required for the five concepts is listed below:

Concept	Electrical Power Load	Electrical Energy Requirement	Concept Illustrated
Basic AAP	85 watts	45,000 watt hours	Figure 1
Autonomous Vehicle	50 watts	200 watt hours	Figure 2
Pallet	85 watts	30,000 watt hours	Figure 3
Autonomous plus Boom/Gimbal	85 watts	30,000 watt hours	Figure 4
Integrated LEM	85 watts	45,000 watt hours	Figure 5

REACTION CONTROL SUBSYSTEM AND LEM GUIDANCE COMPUTER

The LEM RCS is to be augmented with additional propellants and pressurization gases to provide the attitude control for the LCSE. The RCS will provide the coarse pointing of the spacecraft during the initial earth laser beacon acquisition operations. The RCS will keep the spacecraft oriented within the gimbal limits or ATM angular travel limits as well. During this latter operation, since the telescope cap will be open, it is desired that the RCS use only cold gas jets for attitude control. At this point in time, the deposition hazard from the hot gas RCS to the Laser/Telescope optics is not known. However, according to some reports, the Gemini flight observation windows were covered with residue from the plumes of rocket motors.

The LCSE will generate the fine pointing error signals needed for the RCS. In four of the five concepts (the Autonomous Vehicle Concept is the exception) boom/gimbal systems or the ATM are used in operational modes. The Guidance Computer should be modified to accommodate a requirement of the experiments that the spacecraft have pitch and yaw motions about the center of rotation of the telescope, as contrasted with the center of mass of the combined system.

APOLLO MICROWAVE COMMUNICATION SYSTEM

The Apollo-LEM 2.3 Gc data link has the capability to transmit 51.2 kbps of data over a 210,000 mile range with an output power of 20 watts and using a 2 foot vehicle antenna and an 85 foot ground antenna. Decreasing range to a synchronous altitude results in a 19.2 db power excess. Decreasing power output from 20 watts to 0.75 watt, by deleting the power amplifier and using only the solid state exciter output, will decrease the power excess to 4.9 db. Decreasing the antenna size to 1.2 feet will bring the excess to zero. If a 30 foot ground antenna were used, the Apollo-LEM S-band system with the 0.75 watt exciter would handle 20 kbps instead of the 51.2 kbps.

The microwave telemetry required for the LCSE totals about 1.5 kbps when time is shared between the operational, status and diagnostic channels. The list of the signals for each channel follows:

Operational Diagnostic Telemetry

1. Laser Power Output
2. Coarse PMT Difference Output in Up-Down
3. Coarse PMT Difference Output in Left-Right
4. Fine PMT Difference Output in Up-Down
5. Fine PMT Difference Output in Left-Right
6. Coarse PMT Summation of all 4 Outputs
7. Fine PMT Summation of all 4 Outputs
8. Transfer Lens X Position
9. Transfer Lens Y Position
10. ATM Pitch Angle
11. ATM Yaw Angle
12. Spacecraft Pitch Angle
13. Spacecraft Yaw Angle
14. Spacecraft Roll Angle
15. Sun Seeker Offset Angle (Gimbal)
16. Sun Seeker Cross Offset Angle (Gimbal)
17. Sun Seeker Sensor Output Signal
18. Sun Indicator #1
19. Sun Indicator #2
20. Sun Indicator #3
21. Sun Indicator #4
22. Sun Indicator #5
23. Sun Indicator #6

24.	Sun Indicator #7
25.	Sun Indicator #8
26.	Sun Indicator #9
27.	Sun Indicator #10
28.	Risley Prism Servo #1 Angle
29.	Risley Prism Servo #2 Angle
30.	Astronaut ATM Pitch Command
31.	Astronaut ATM Yaw Command
32.	Astronaut Spacecraft Roll Command
33.	Astronaut Voice Monitors
	Operational Status Telemetry
34.	Laser #1 On
35.	Laser #2 On
36.	KDP Modulator #1 On
37.	KDP Modulator #2 On
38.	Beam Spoiler Location
39.	Alignment Shutter Location
40.	Astronaut Folding Beamsplitter (Fine Guidance Path) Location
41.	Astronaut Folding Beamsplitter (Coarse Guidance Path) Location
42.	Primary Mirror Caging Sensor
43.	Fast Shutter Status
44.-49.	Silica Rod End Status (3 Rods)
50.	Secondary Focus Control
51.-53.	Secondary Launch Isolator Cage Status
54.	Telescope Cap Status
55.	Telescope Cap Angle
56.-65.	Programmer Status
66.-67.	PCM Encoder Status
68.	Fine Guidance Servo Loop Gain
69.	ATM Gimbal Lock Status Pitch
70.	ATM Gimbal Lock Status Yaw
	Diagnostic Status Telemetry
71.	Laser #1 Power Supply Voltage
72.	Laser #2 Power Supply Voltage
73.	KDP #1 Modulator Temperature
74.	KDP #2 Modulator Temperature
75.	Risley Prism Servo Power Supply Voltage (#1)
76.	Risley Prism Servo Power Supply Voltage (#2)
77.	Risley Prism Servo #1 Error Voltage
78.	Risley Prism Servo #2 Error Voltage
79.-86.	PMT #1 through #8 Power Supply Voltage
87.-94.	PMT #1 through #8 Tube Currents
95.	Transfer Lens Error Voltage X-axis
96.	Transfer Lens Error Voltage Y-axis
97.	Transfer Lens X-axis Displacement Signal
98.	Transfer Lens Y-axis Displacement Signal
99.	Transfer Lens Displacement Sensor Power Supply Voltage

100.	Primary Temperature
101.	Secondary Temperature
102.	Structure Temperature
103.	Behind the Mirror Structure Temperature
104.-107.	Launch Accelerometer Readouts (4)
108.	Sun Seeker Power Supply Voltage
109.	Sun Seeker Servo Error Voltage - Offset Gimbal
110.	Sun Seeker Servo Error Voltage - Cross Offset Gimbal
111.-120.	Electronic Boxes Temperatures
121.	Risley Prism Servo Assembly Pressure
122.	Sun Seeker Assembly Pressure
123.	Secondary Focus Assembly Pressure
124.	Sun Shade Mechanism Assembly Pressure
125.	Beam Spoiler Mechanism Assembly Pressure
126.	Fast Shutter Mechanism Assembly Pressure
127.	Launch Mount and Attenuator Status
128.	Launch Mount and Attenuator G Indicator

MECHANICAL, STRUCTURAL AND ELECTRICAL MODIFICATIONS TO THE APOLLO SPACECRAFT

Basic AAP Concept (Figure 1)

The LEM descent structure would require appropriate modifications to accommodate the ATM.* In addition, the launch mounting clamps which soft mount the Laser/Telescope and the folded ATM during launch must be attached to the inside of the LEM descent structure. Inside the LEM, provisions must be made to mount the Laser Communication Satellite Experiment Monitor (and control) Station. Hard line electrical interconnections exist between the LCSE and LEM during all operational modes.

Autonomous Vehicle Concept (Figure 2)

The modifications are similar to the ones described above for the Basic AAP Concept except that there are no provisions to mount the ATM (it is not used) and there are no provisions for hard line electrical interconnections between the LCSE and the LEM during checkout and operation. Local RF link TM would be needed.

Pallet Concept (Figure 3)

The pallet area of the Service Module must be modified to provide the soft launch mounts for the equipment and the necessary hard line electrical interconnections to power and control the Laser/Telescope. The Laser Communications Satellite Experiment Monitor Station must be mounted inside the Command Module in this configuration.

*ATM or equivalent LCSE Mission Boom and Gimbals.

Autonomous Spacecraft Separable From Boom and Gimbal Concept (Figure 4)

The modifications for this concept are identical to those required for the Basic AAP Concept except that attitude control signals and electrical power for the LCSE will not originate in the LEM. However, for this concept, the LCSE Monitor Station will be more elaborate than the Basic AAP Concept since the check-out functions will include check out of the LCSE attitude control system, power supplies and collectors and the microwave communication system.

Integrated LEM Concept (Figure 5)

Extensive modifications will be required in the LEM descent structure to mount the LCSE gimbals, laser telescope and the soft mounts for launch. The Monitor Station is located inside LEM as in the Basic AAP Concept and consequently the hardline electrical modifications will be similar to the ones previously indicated.

BLANK PAGE

2.5 THE SPACE-TO-EARTH COMMUNICATION LINK EXPERIMENTS

In this section, calculations of the expected power requirements for the space-to-earth communication link are presented. The specifications for the various components in the optical path are listed in Table IV along with source references, where applicable. The calculations assume worst case conditions. That is, under the expected operating environment, the average signal level will not decrease below the signal level derived in this section. The assumptions used for the worst case link included:

- Daytime operation (no clouds)
- Earth receiver tracking 60 degrees from the zenith
- Data rate of 10^6 bits per second (equivalent analog bandwidth of $\approx 10^5$ cps)
- Bit error rate less than 0.001
- Large atmospheric turbulance
- All components are current state of the art
- Transmit power safety factor in excess of 20 db
- Laser source of 3.0 milliwatt in TEM_{oo} mode.

The calculations in the next section indicate that a PCM/PL synchronous satellite-to-earth link, under the assumed conditions above, is feasible.

To determine the sensitivity of the maximum obtainable data rate with a variation of a given system parameter, a series of graphs are plotted with coordinates of data rate versus the system parameter being investigated. These graphs verify the importance of the 0.1 arc-second pointing requirements and the requirement of diffraction-limited optics.

The definition of the optical communicator freezes many of the system parameters. However, further analysis was required to determine some of the other parameters needed for the link calculations. This section will discuss the limiting factors which determine the value of these parameters.

RECEIVER FIELD OF VIEW, β

The value of the receiver field of view (β) will be determined by the limiting aperture in the earth-based optical system. The communicator receiver on earth will have an iris that will limit the background radiation. Ideally, the iris could be reduced to less than an arc-second without a reduction in the signal power. However, the uncertainty caused by atmospherics and the telescope vibrations will determine the practical limitation for the

TABLE IV

SPACE-TO-EARTH COMMUNICATION LINK

VARIABLE	SYMBOL	VALUE	UNITS	REFERENCE OR COMMENT
Range	R	21,500 34,060	miles Km.	Receiver viewing 60° to zenith
Wavelength	λ	0.6328	microns	
Transmitter Optical Power	P_s	0.0030	watts	Measured at laser output
Transmitter Beam Divergence 1.2 λ/D	α	2×10^{-6} 0.4	radians arc-seconds	
Diameter of Transmitter Aperture	D	16 40	inches centimeters	
Receiver Field of View	β	9.7×10^{-5} 20	radians arc-seconds	
Atmospheric Transmission	τ_A	0.70	60° from zenith	Table 3-1 NASA CR-252
Transmitter Optical System Transmission	τ_{OT}	0.33		
Receiver Optical System Transmission	τ_{OR}	0.75		
Diffraction Loss	τ_D	0.5		
Prediction Optical Filter Transmission	τ_F	0.40		For filter bandwidth $\Delta B = 1.5\text{Å}$
Diameter Receiver Aperture	d	24 61	inches centimeters	
Blue Sky Background	P_B	2×10^{-3}	$\frac{\text{watts}}{\text{cm}^2\text{- ster-}\mu}$	Table 3-5 NASA CR-252
Average Star Field	P_F	5×10^{-10}	$\frac{\text{watts}}{\text{cm}^2\text{-ster-}\mu}$	Table 3-5 NASA CR-252
Venus	P_V	2×10^{-10}	$\frac{\text{watts}}{\text{cm}^2 - \mu}$	Figure 7-16 NASA CR-252
Scintillation	τ_s	0.4		
Receiver PMT @ -70°C (RCA 7265)	P_p	2×10^{-15}	watts	Radiant input power equivalent
PMT Quantum Efficiency	η	0.05		Conservative Value
Safety Factor	M	110		
Speed of Light	c	3×10^8	m/sec	
Data Rate	C	10^6	bits per sec	
Planck's Constant	h	6.62×10^{-34}	joule-sec	

field of view. The value of 20 arc-seconds is quite conservative for a 24-inch ground telescope and really reflects the receiver FOV that can be obtained with the 10-meter aperture need for a deep space link. However, the use of a much smaller field of view or the use of an image dissector tube will not significantly increase the obtainable data rate because the link is very close to quantum noise limited.

TRANSMITTER OPTICAL SYSTEM TRANSMISSION, τ_{OT}

Losses in the transmitter optics can be attributed to the 20% obscuration of the secondary mirror, 10 air-glass interfaces, the truncation of the gaussian intensity distribution output from the laser, and the reflectivity of the primary and secondary mirrors. The pointing requirements of the optical communicator dictate that the output of the laser must be in the TEM_{00} mode. Thus, the spatial intensity distribution across the laser output will be approximately gaussian.

Preliminary calculations indicate that both the central obscuration and the truncation of the gaussian will introduce losses of at least 0.5. Methods are available for mapping the gaussian intensity distribution into a more optimum distribution.* Since the efficiency of the laser radiation is always of concern, the special mapping optics will be included in the optical design work of the LCSE. Thus, the value of $\tau_{OT} = 0.33$ is a conservative estimate of the losses in the transmitter optics. The use of antireflective coatings plus the referenced mapping techniques can increase τ_{OT} to 0.66. However, after 6 months in space there will be some degradation of the optical reflectance and the dielectric coatings. For this reason, the 0.66 value was reduced to 0.33 for the calculations.

RECEIVER OPTICAL SYSTEM TRANSMISSION, τ_{OR}

The wavefront impinging on the earth receiver will have a uniform average intensity across the aperture.** Thus, the energy loss resulting from the secondary obscuration will be approximately 20% if a cassegrain telescope is used at the receiver. The losses from the silvered mirror surfaces and the air-glass interfaces will not introduce significant additional losses. Thus, the value $\tau_{OR} = 0.75$ is reasonable for the optical losses at the receiver.

DIFFRACTION LOSS, τ_D

The far field pattern of an unobscured circular aperture is the classical Airy pattern. As discussed previously, both secondary obscurations and the nonuniform illumination of the transmitter aperture will distort

*"Laser Light Redistribution in Illuminating Optical Signal Processing Systems", J. L. Kreuzer, Optical and Electro-Optical Information Processing, MIT Press 1965.

**This statement assumes the effects of atmospherics will be small.

the far field distribution on the earth. Both effects will decrease the width of the central maximum in the far field and will increase the energy contained in the "side lobes" of the diffraction pattern. The energy contained outside the half power point of the far field pattern of the ideal uniformly illuminated aperture* is 0.4. Thus, a value of $\tau_D = 0.5$ will be expected as the loss in the far field at the optical system due to diffraction effects. No techniques are available for significantly reducing this system loss.

COMMUNICATIONS LINK CALCULATIONS

Equation (1) states the average number of signal photoelectrons detected during a bit interval.

$$S = \left(\frac{d}{\alpha R}\right)^2 \times \left(\frac{\lambda P_s \eta}{hcC}\right) \times \left(\tau_D \tau_A \tau_{OT} \tau_{OR} \tau_F \tau_S\right) \frac{1}{M} \text{ counts/bit} \qquad (1)$$

$$= \begin{pmatrix}\text{ratio of receiver and} \\ \text{illuminated areas}\end{pmatrix} \times \begin{pmatrix}\text{conversion of optical} \\ \text{power to counts/bit}\end{pmatrix} \times \begin{pmatrix}\text{system} \\ \text{efficiencies}\end{pmatrix}$$

Equation (2) states the average number of noise photoelectrons (N) detected during a bit interval.

$$N = \frac{\lambda \eta}{hcC} \left\{ 2 P_P + \left(P_F \tau_A + P_B\right)\left(\frac{\pi d^2}{4}\right)\left(\frac{\pi \beta^2}{4}\right) \Delta\lambda \, \tau_O \, \tau_F + \left(P_A + P_v\right)\left(\frac{\pi d^2}{4} \, \Delta \, \pi \, \tau_{OR} \, \tau_F \, \tau_A\right)\right\} \qquad (2)$$

$$= \begin{pmatrix}\text{conversion to} \\ \text{counts/bit}\end{pmatrix} \left[\begin{pmatrix}\text{noise of both phototubes + average} \\ \text{blue sky and star background}\end{pmatrix} + \begin{pmatrix}\text{Venus and Sirius A} \\ \text{"point sources".}\end{pmatrix}\right]$$

The variables in Equations (1) and (2) are defined in Table IV.

Under normal daytime operation, the blue sky background noise power, N_p, will limit the optical communication link. Neglecting P_p, P_A, P_F, P_v, substitution of the values of Table IV into Equation (2) yields

$$N = \frac{.6328 \times 10^{-6} \times 5 \times 10^{-2}}{6.625 \times 10^{-34} \times 3 \times 10^{8} \times 10^{6}} \left[2 \times 10^{-3} \, \pi \left(\frac{61}{2}\right)^2 \left(\frac{\pi}{4}\right)\left(9.7 \times 10^{-5}\right)^2 \times 1.5 \times 10^{-4} \times .75 \times .40 \right] \qquad (3)$$

N = 3 noise counts/bit (blue sky)

*Born and Wolf, Principles of Optics, Macmillan, New York (1964) p. 398.

The noise count resulting from the phototube dark current, Venus at conjunction, and the star, Sirius A, will now be computed. Substitution of the values of Table IV into Equation (2) yields the average noise count per bit listed below:

$N = 0.7$ from Sirius A

$N = 17$ from Venus at conjunction

$N \sim 0$ from phototube dark current

Noting the large safety factor for the proposed link, the optical communication system will still operate even when a star or planet is in the field of view of the receiver telescope.

Figure 17 shows the required signal count for a system with a given background noise and bit error rate. The derivation of these error rate curves for PCM/PL assume that both the signal and noise photoelectrons are Poisson distributed. Note that as the noise approaches zero, the signal count approaches a minimum. For example, this minimum is an average of 6.22 signal photoelectrons when a system operates with a bit error rate of 0.001. Thus, when one reduces the noise count much below N = 1/2, one can expect a significant reduction in the signal count required.

For daylight operation (N = 2), Figure 17 states that the signal count required for a PCM/PL system with a bit error rate of 10^{-3} is S = 10. Assuming 0.003 watt of optical power transmitted from synchronous orbit, Equation (1) is satisfied when the safety factor of M = 110. That is, the system has a 20.5 db safety factor during daytime operation. Since the minimum average signal count allowed is 6.22 per bit, the safety factor will be increased to $M = 110 \times \frac{10}{6.22}$ or 22.5 db for quantum noise limited operation.

PARAMETER TRADEOFFS

The values for the parameters listed in Table IV were chosen on the basis of the present state of the art and tradeoffs between the system parameters. To demonstrate the effect of varying some of the parameters, a series of graphs are derived and discussed in this section. To judge the relative effect of varying each parameter, all the graphs have Data Rate as the ordinate. The system will be background limited during daylight hours and will be quantum noise limited during night operation. That is, the system will be operating in the regions A and B (Figure 17) during nighttime and and daytime, respectively. Thus, two curves are required for each graph to demonstrate background and quantum noise limited performance.

The background noise power admitted to the PCM/PL detector is independent of the data rate (information bandwidth). Thus, even with a decade increase in the data rate, the noise power admitted by the optical filter and field stops, P_B, remains constant. However, Equation (2) states that increasing

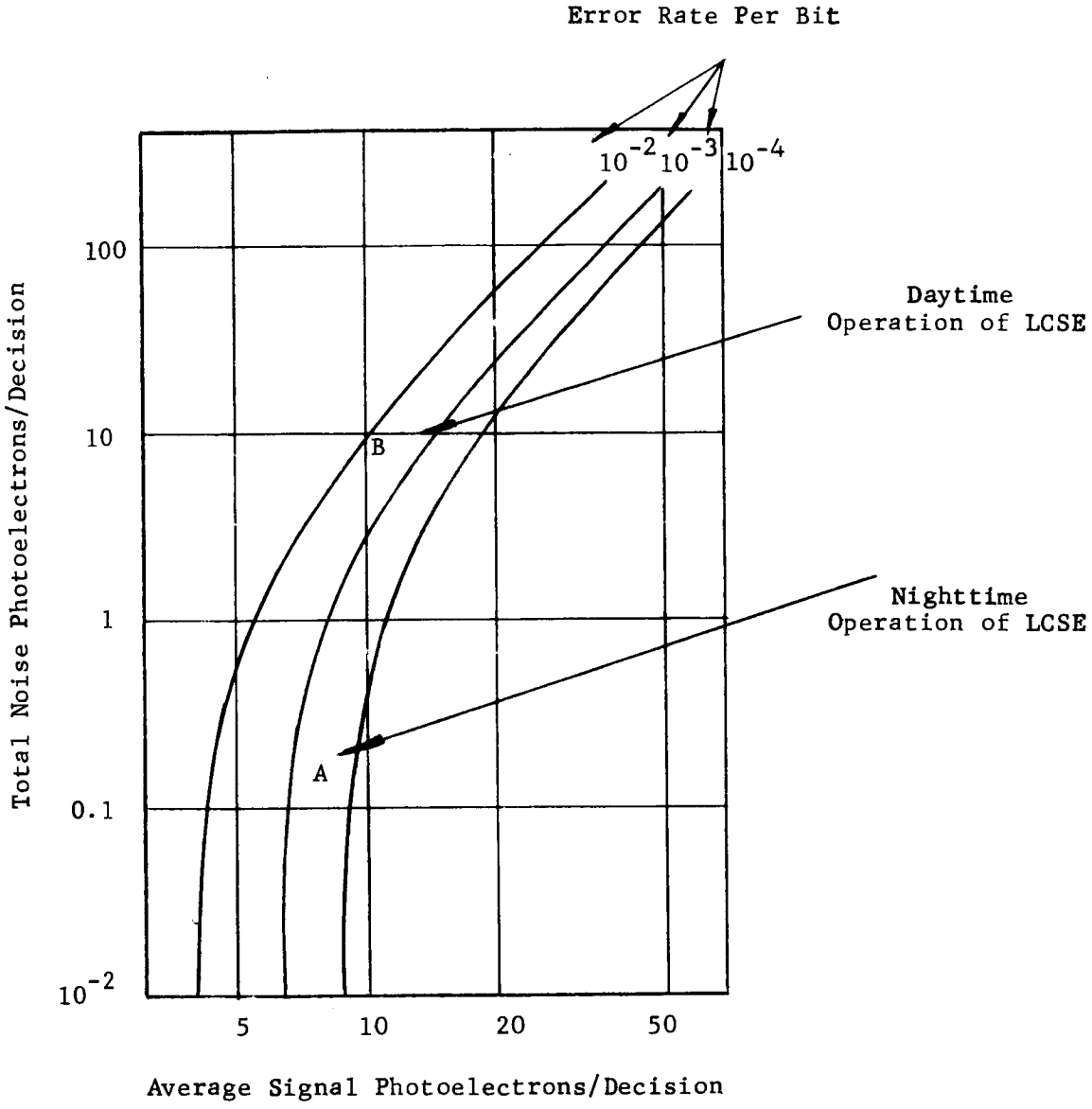

Figure 17. The Effect of Background Noise on the Number of Signal Photoelectrons Needed in a PCM/PL System for a Decision

the data rate, C, by a decade will reduce the average noise count per bit. As demonstrated in Figure 18 the data rate for daylight operation approaches the quantum limit (night operation) when the data rate is increased.

The reference in Figures 18 — 26 is a 10^6 bit per second PCM/PL system operating with the parameters listed in Equation (3), (worst case - daytime). For example, in Figure 18 the daytime curve crosses 10^6 bit per second when D = 16 inches, the value listed in Table IV.

TRANSMITTER APERTURE

The diffraction-limited beamwidth, α, from an aperture of diameter D is $\alpha = \frac{1.2}{D}\lambda$. Variation of α in Equation (1) shows that the received signal power varies proportionately with the square of the transmitter aperture. Figure 18 shows the dependence of the data rate on the transmitter aperture.

TRANSMITTED OPTICAL POWER

The received signal power is proportional to the transmitted optical power (Equation (1)). The dependence of data rate on the signal is shown in Figure 19.

PRIMARY MIRROR RMS FIGURE ERROR

In an imaging system, the intensity I at some point in the image may be expressed in the form

$$I \sim 1 - \left(\frac{2\pi}{\lambda}\right)^2 \Delta_\omega^{\,2}$$

where Δ_ω is the rms deviation of the wavefront about the spherical reference wavefront.* This equation is valid only for rms deviations much less than a wavelength. Since the wavefront is reflected from the primary mirror, a mirror deformation of Δ_m will introduce a wavefront error of $\Delta_\omega = 2\Delta_m$. Thus, the reduced intensity at a point in the central image is

$$I \sim 1 - \frac{16\,\pi^2 \Delta m^2}{\lambda^2}$$

Using $\lambda/50$ as the reference for the rms mirror error, Figure 20 gives the dependence of the data rate on the rms primary figure error. In determining the specification of the primary, allowances must be made for the mirror quality

*Born and Wolf, Principles of Optics, MacMillan, New York (1964)

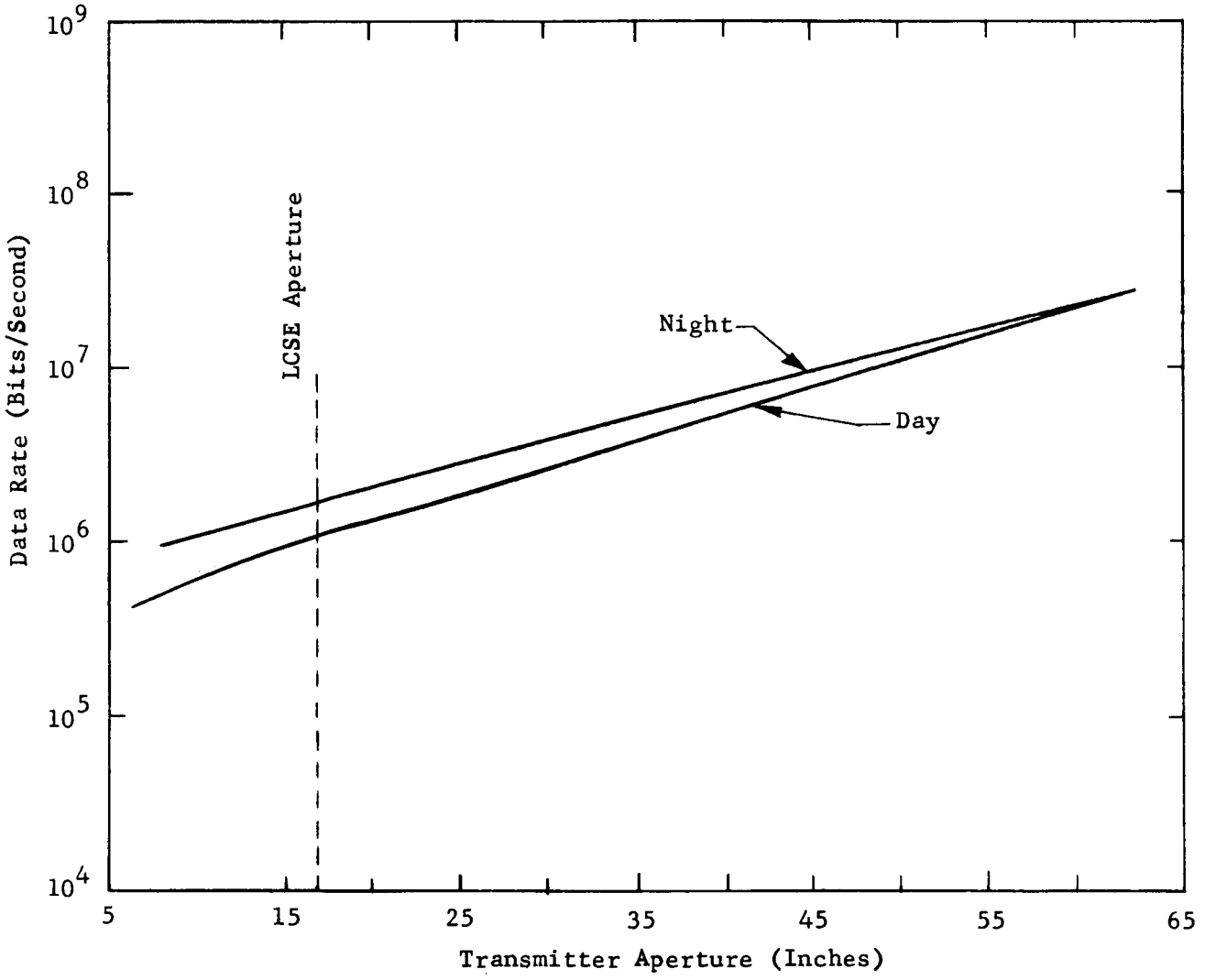

Figure 18. LCSE Transmitter Aperture Selection

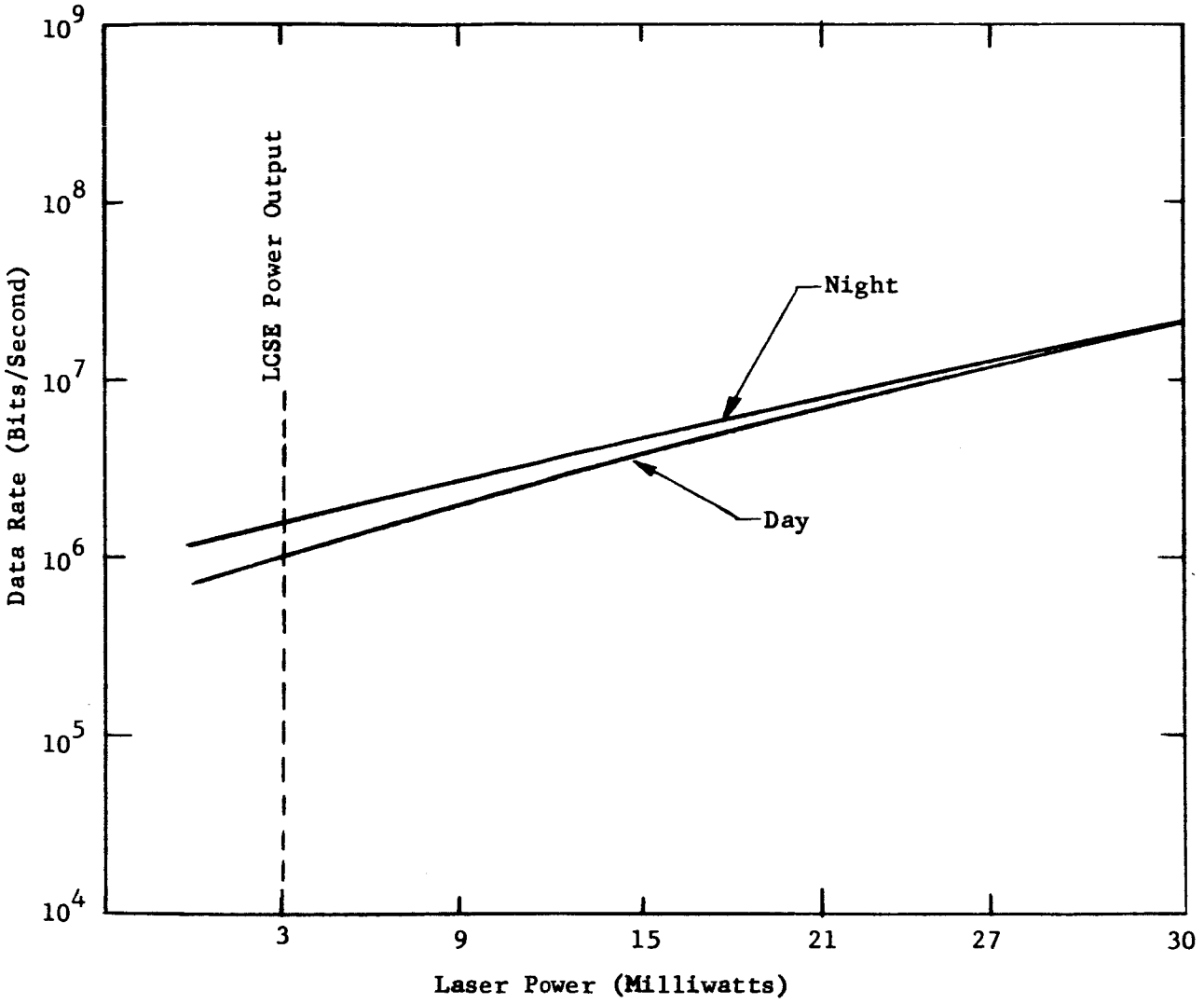

Figure 19. LCSE Laser Output Power Selection

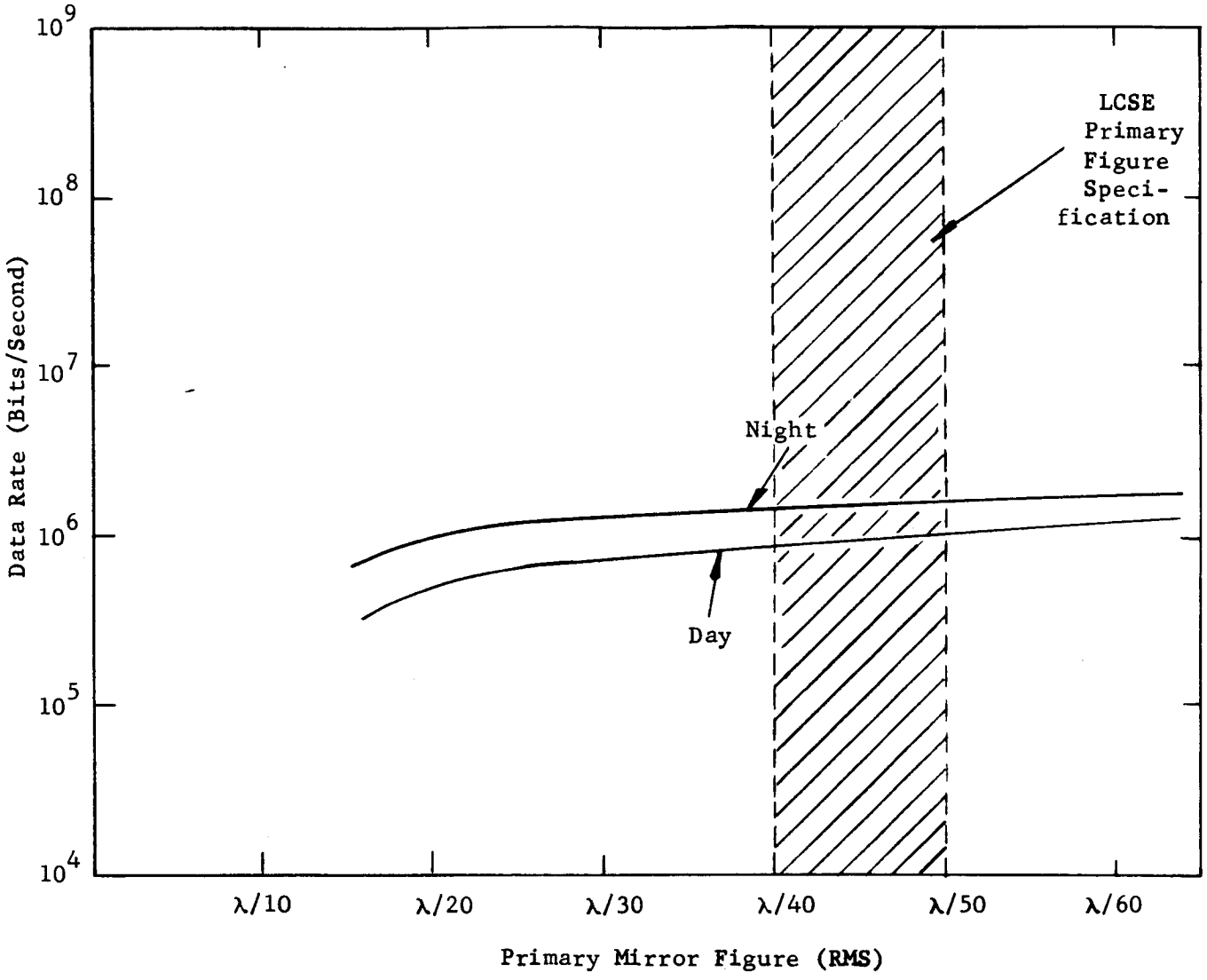

Figure 20. LCSE Figure Error

required by the LCSE tracking subsystem and mirror errors introduced by temperature gradients, zero gravity, and the launch environment. Thus, an rms figure error of $\lambda/40$ to $\lambda/50$ will be required to guarantee diffraction-limited performance of the telescope.

BEAM SPOILING

A device to spoil the transmit beam was inserted in the optical communicator to insure a backup mode of operation to the fine tracking, RLOS, and point ahead subsystems. If the beam is spoiled to 4 arc-seconds, the link is operative (although at a reduced data rate in the daytime) even if the aforementioned subsystems are inoperative or only partially operative. The reduction of data rate is shown in Figure 21. Since the link has a safety factor greater than 20 db, the link will support a one megabit data rate at night when the beam is spoiled to operate without the RLOS or point ahead subsystems.*

TRANSMITTER POINTING ERROR

The far field pattern of the laser radiation transmitted by the optical communicator is determined by intensity and phase distribution across the telescope aperture, plus the obscuration of the central portion of the aperture by the secondary. The free space loss calculations require knowledge of the absolute energy density at the center of the far field pattern. The specifications of the pointing subsystems require knowledge of the relative change of the energy density in the far field as one introduces small angular alignments.

The light distribution across the output of a laser operating in the TEM_{oo} mode is approximately a truncated gaussian. Calculations indicate that the far field distribution near the center of the far field pattern of a telescope with a gaussian distribution across the aperture does not vary significantly** from

$$I_o \sim \left(\frac{J_1(x)}{x}\right)^2$$

where I_o is the far field distribution of a uniformly illuminated aperture with no obscuration. This idealized distribution was used to compute the variation in data rate when a pointing error is introduced (Figure 22).

RECEIVER ZENITH ANGLE

The satellite, as viewed from earth, will describe a tilted figure eight on the earth surface with a period of 24 hours. The zenith angle will

*This statement is true only when the transmit-receive channel alignment procedure is carried out.

**Personal Communication, J. Kreuzer.

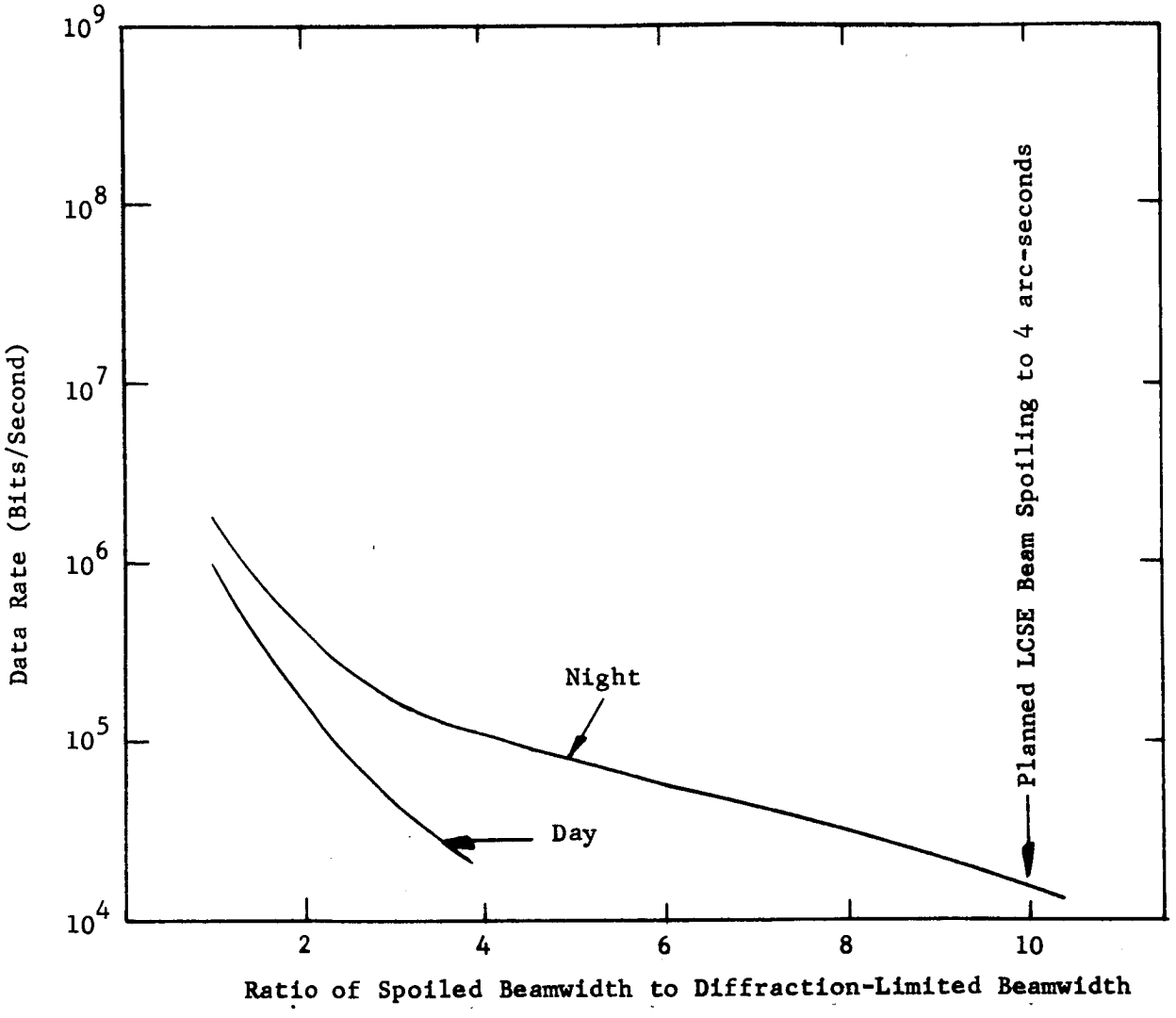

Figure 21. LCSE Beam Spoiling Selection

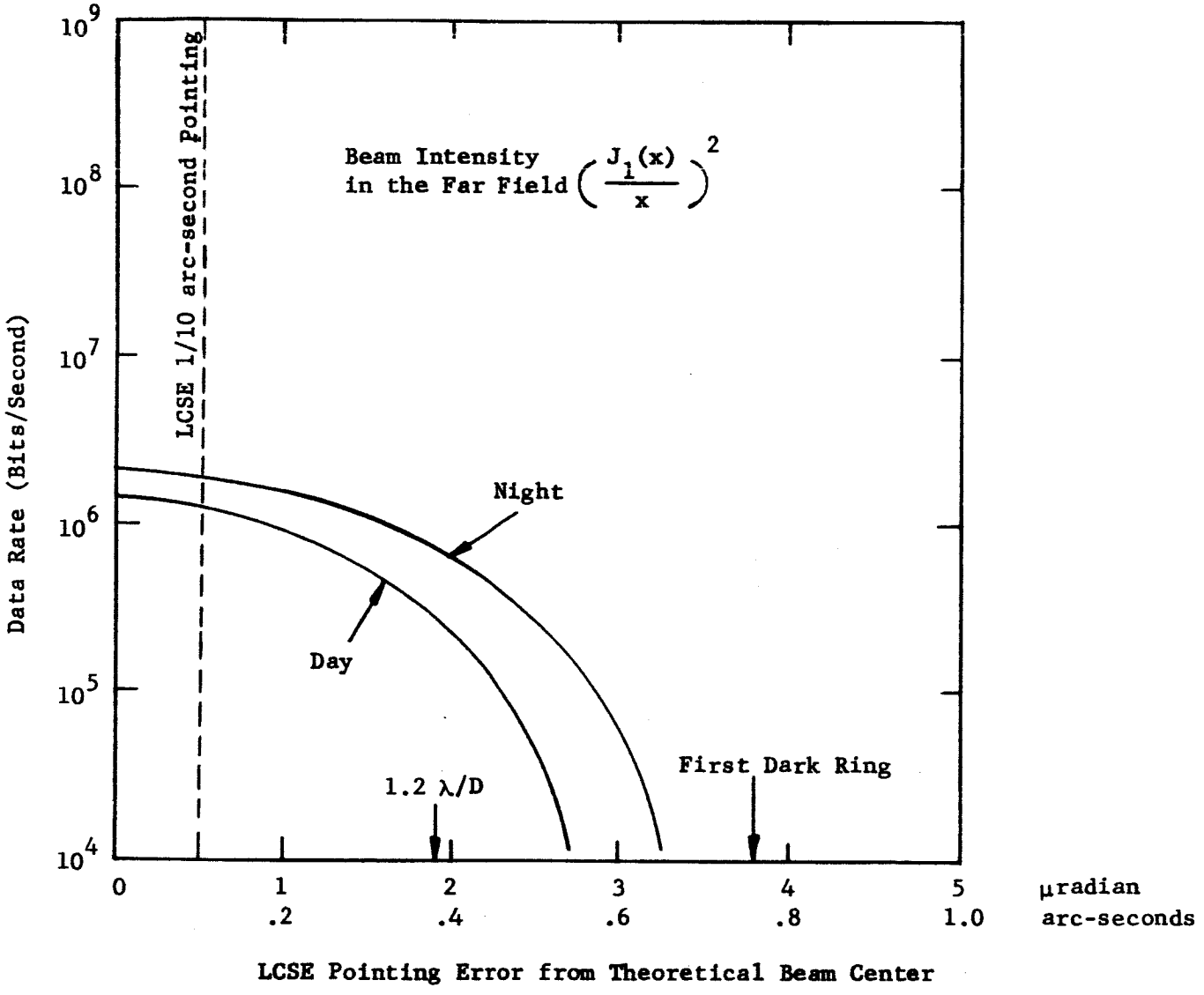

Figure 22. Pointing Requirements for LCSE

be determined by the location of the ground station with respect to the orbital position of the LCSE. Angles greater than 60 degrees from the zenith are not expected. Two effects reduce the data rate as the angle from the zenith is increased. First, the range increases with the corresponding increase in the free space loss. Secondly, the absorption of the atmosphere increases as the zenith angle increases.* The absorption varies approximately as the secant of the zenith angle. Both effects were considered in the plot of Figure 23.

PREDETECTION OPTICAL BANDWIDTH

The optical filter preceding the PCM/PL detector in the earth-based receiver should have, ideally, a bandwidth equal to the signal bandwidth. However, the narrowest optical filters have a bandwidth which is many orders of magnitude larger than the signal bandwidth. Ultra-narrow Lyot optical filters (less than 1Å) are available, but the transmission is reduced to approximately 15%. Since the light input to the Lyot filter must have a single polarization, the PCM/PL receiver is required to have two Lyot-type filters for the two orthogonal polarizations. Lyot filters are sensitive to small temperature changes and, for this reason, careful thermal control of the filter is always an important requirement.

Recently, filters have been developed which are basically a Fabry-Perot cavity in series with a multilayer filter to suppress the unwanted modes of the cavity. Although these filters have a bandwidth larger than the Lyot filter, the increased temperature tolerance and higher transmittance of the Fabry-Perot filter makes them more suited than the Lyot filter for the proposed LCSE system. The field of view requirements of the LCSE optics limit the use of ultra-narrow interference type filters. This is discussed in more detail on page 101.

Figure 24 shows the variation of the data rate when different filters are substituted at the receiver. The filters considered for LCSE are:

- Lyot-transmission = 15%, bandwidth = 0.5Å
- Dobrowski-transmission = 40%, bandwidth = 1.5Å
- Harriott**-transmission = 50%, bandwidth = 2Å
- Multilayer-transmission = 80%, bandwidth = 5Å

The PCM/PL system will be limited by quantum noise during night operation. The only way to reduce this noise is to increase the detected power. The above values indicate that the filter transmission (i.e., detected power) increases as filters with larger bandwidths are used. Thus, during night operation, it is advantageous to have a filter with a high transmission as contrasted with a narrow spectral bandwidth.

---

*Table 3-1, Determination of Optical Technology Experiments for a Satellite, NASA CR-252 (NAS8-11408).

**Harriot, D.R., Filters, Waveplates, and Protected Mirrors, 50th Meeting, Optical Society of America, Washington, D.C.

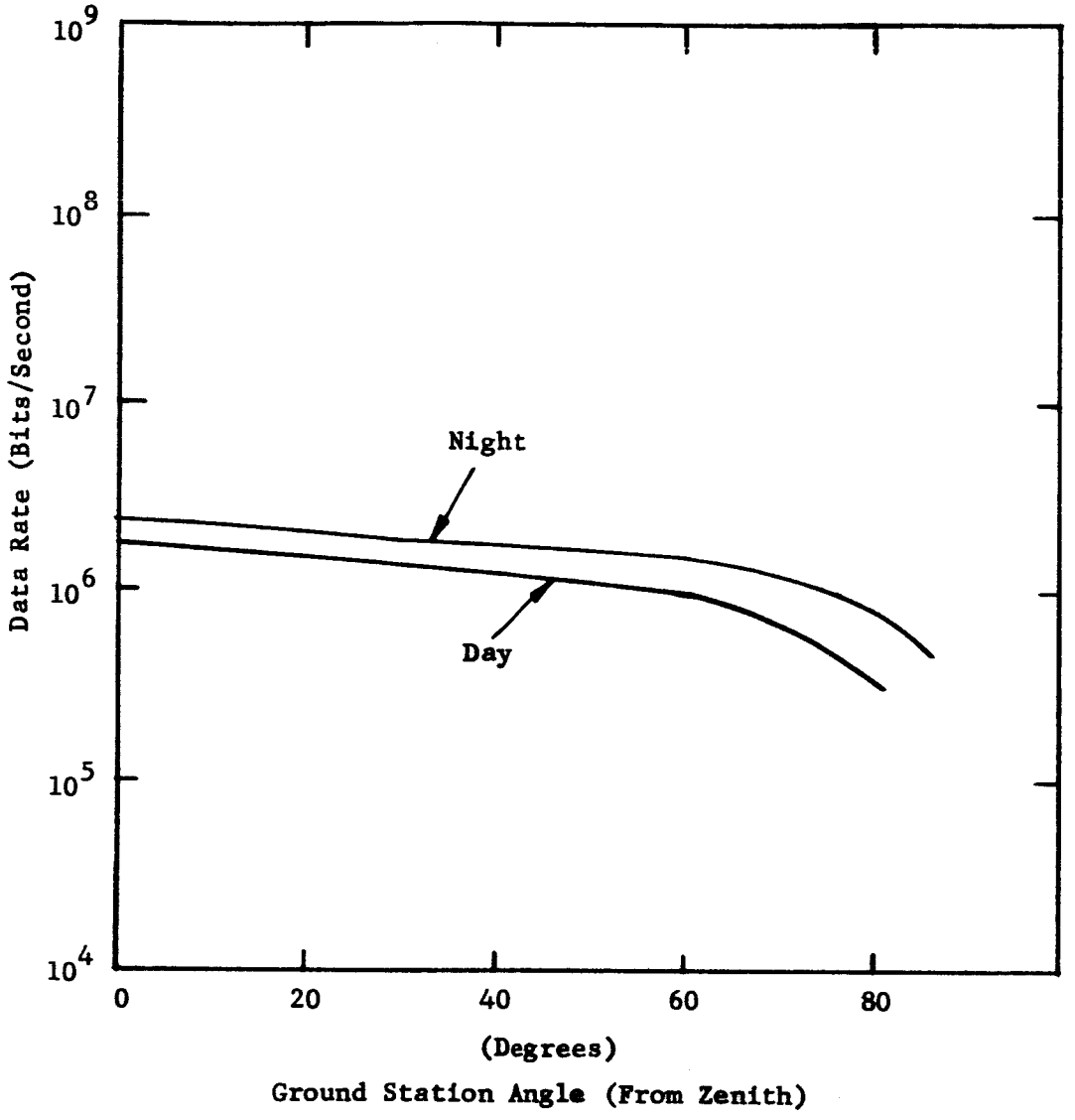

Figure 23. Up-Looking Angles Effect

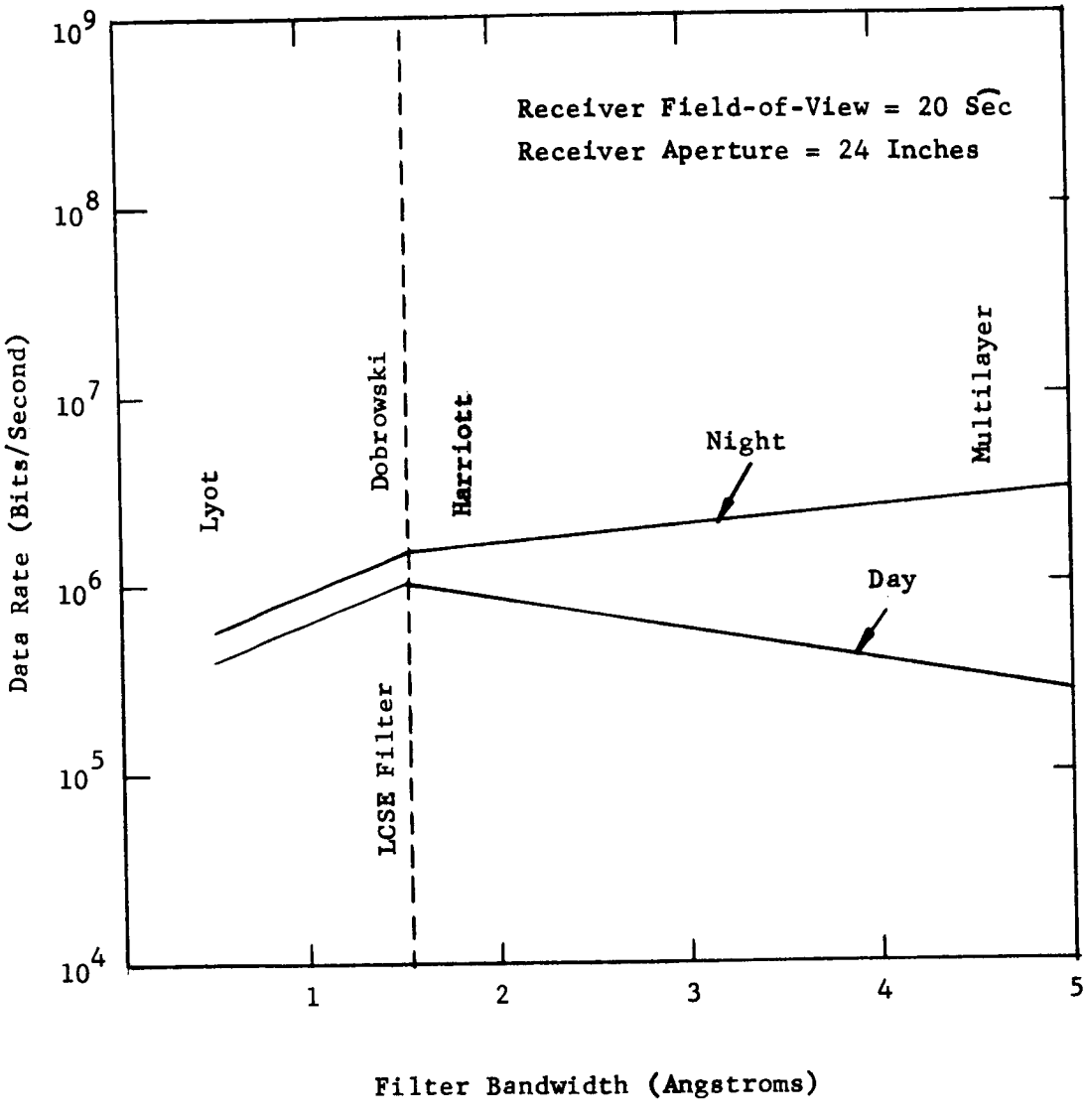

Figure 24. Ground Station Filter Selection for LCSE

The PCM/PL system will be limited by background noise during day operation. This noise source is reduced by inserting a narrow bandpass optical filter before the detector. For the parameter values assumed in Table IV, Figure 24 shows that it is adequate to use the Dobrowski-type filter. However, it must be emphasized that any increase in the background, or increase in the receiver field of view will increase the background noise. Under one of these conditions, it will be more advantageous for the LCSE ground station to use the narrower bandwidth Lyot filter.

EFFECT OF SCINTILLATION ON DATA LINK

A star viewed from the earth suffers from image dancing and blurring plus scintillation. Since the PCM/PL receiver is an energy detector (i.e. quantum counter), image dancing and blurring will not degrade the PCM/PL system as long as the received signal is incident on the photoemissive surface. The scintillation, however, will introduce fading in the received signal. Under special conditions, 100% amplitude modulation of a star's image has been observed. No empirical data or theory exists to determine the scintillation of a monochromatic laser light beam propagating vertically through the atmosphere.

A rather complete theory of star scintillation along with confirmation data has been published by Tatarski*. The theory states that the star's detected energy, I, has time varying statistics which are log normal. The probability density function is

$$P(y) = \frac{1}{2\pi\sigma} \exp\left[\frac{-y^2}{2\sigma^2}\right]$$

where σ^2 = variance of scintillation

$y = \ell n \frac{I}{\bar{I}}$

I = intensity of light wave on surface of the objective.

$\bar{I}$ = average light intensity

The value of σ is greatest for viewing of stars near the horizon with a small aperture telescope. As the aperture is increased, several uncorrelated field inhomogeneities fit in the aperture. This effect (aperture averaging) reduces the scintillation by averaging the fading over several inhomogeneities.

The effect of scintillation on the error rate of the PCM/PL signal will now be discussed. Knowing the instantaneous received signal level of the time varying PCM/PL signal, the PCM/PL error rate equations ** will give a

*V. I. Tatarski, Wave Propagation in a Turbulent Medium, Chapter 13.

**See NASA CR-252 (NAS8-11408).

corresponding bit-error rate. This method is legitimate only when the bit interval (1 microsecond) is small in comparison to the shortest period of the fading ($\approx$ 1 millisecond). Thus, stating that the instantaneous signal must be in excess of S_o for 0.999 of the time is equivalent to stating that the bit error rate will be less than P_B (S_o, N) for 0.999 of the time. Figure 17 may be used to find the relationship between S_o and N when P_B (S_o, N) = 10^{-3}.

Doing the necessary transformation, the relation between the instantaneous power S_o and the average power $\bar{S}$ is

$$\ell n \frac{\bar{S}}{S_o} = 2\sigma \ \text{erf}^{-1} (2 \times 0.999-1)$$

where $\sigma \cong 0.08$ for zenith viewing winter atmosphere 24-inch receiver

$\sigma' \cong 0.08 \sec \theta^{3/2} = 0.22$ for viewing 60 degrees from zenith

erf^{-1} = inverse error function

Substituting the above values into Equation (1) states that the power ratio $\frac{\bar{S}}{S_o}$, will be approximately 1.5 db and 4 db for zenith and 60 degrees to zenith viewing, respectively.

The value of σ increases when the aperture is reduced because the effect of aperture averaging is reduced. Figure 25 shows the dependence of the data rate on the receiver aperture. In addition to scintillation, the variation of the receiver aperture changes the value of blue sky background and the received signal power. Both of these values are proportional to the square of the aperture. The effects of all three sources of error were considered in plotting Figure 25 and the 24-inch aperture ground station telescope is indicated.

SAFETY MARGIN

The safety margin (in db) is defined as

$$M_{db} = 10 \log_{10} \frac{\eta N_S}{CS}$$

where N_S = number of photons incident on PMT

η = PMT quantum efficiency

C = data rate

S = signal counts per decision for PCM/PL detection (See Figure 17)

A plot of data rate versus safety margin is shown in Figure 26. The LCSE experiments require transmission of 10^6 bits per second. Both a pseudorandom digital sequence and slow scan video will be transmitted. Figure 26 shows safety margins of 21 db and 23 db for the worst case day and

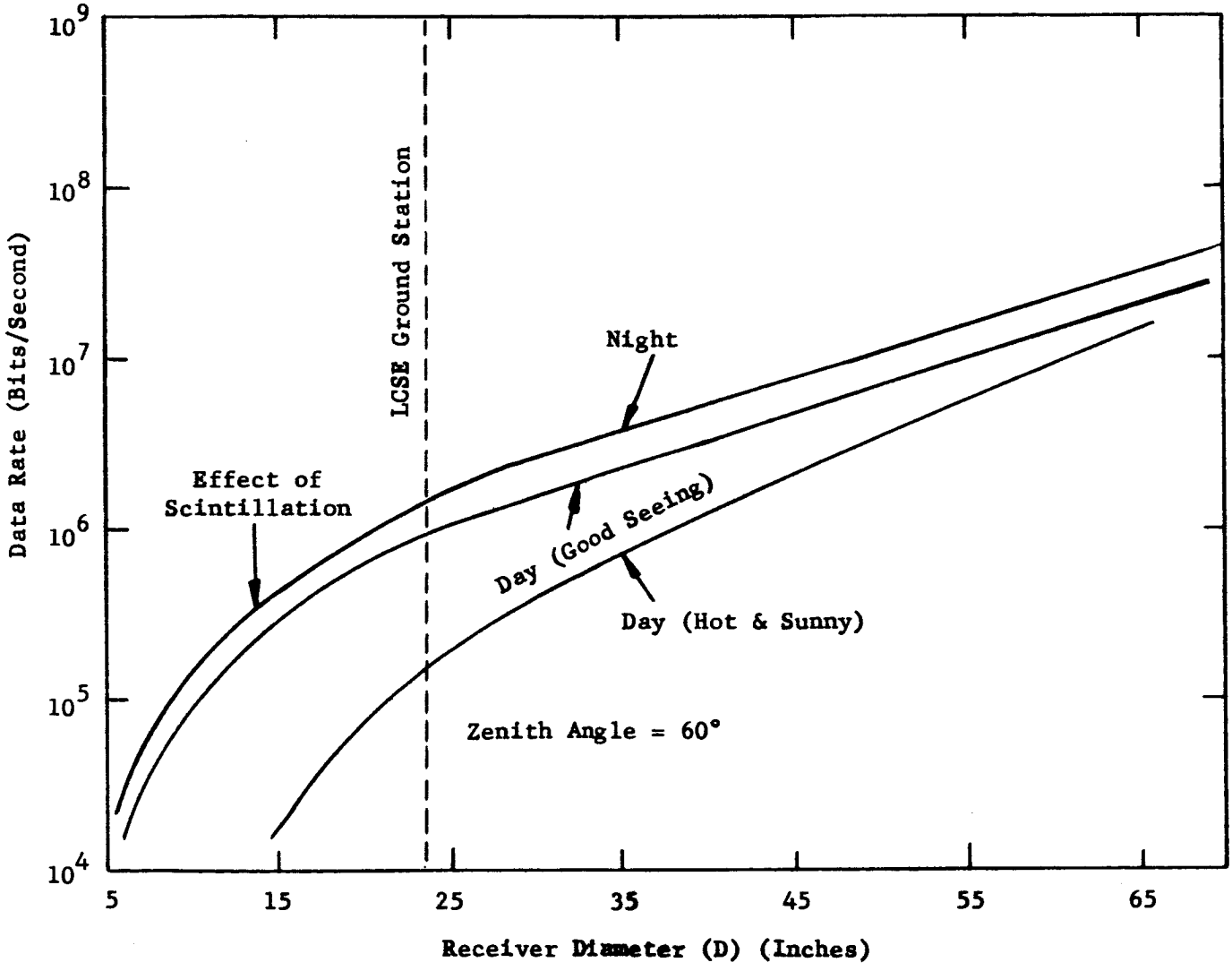

Figure 25. Earth Receiver Aperture for LCSE

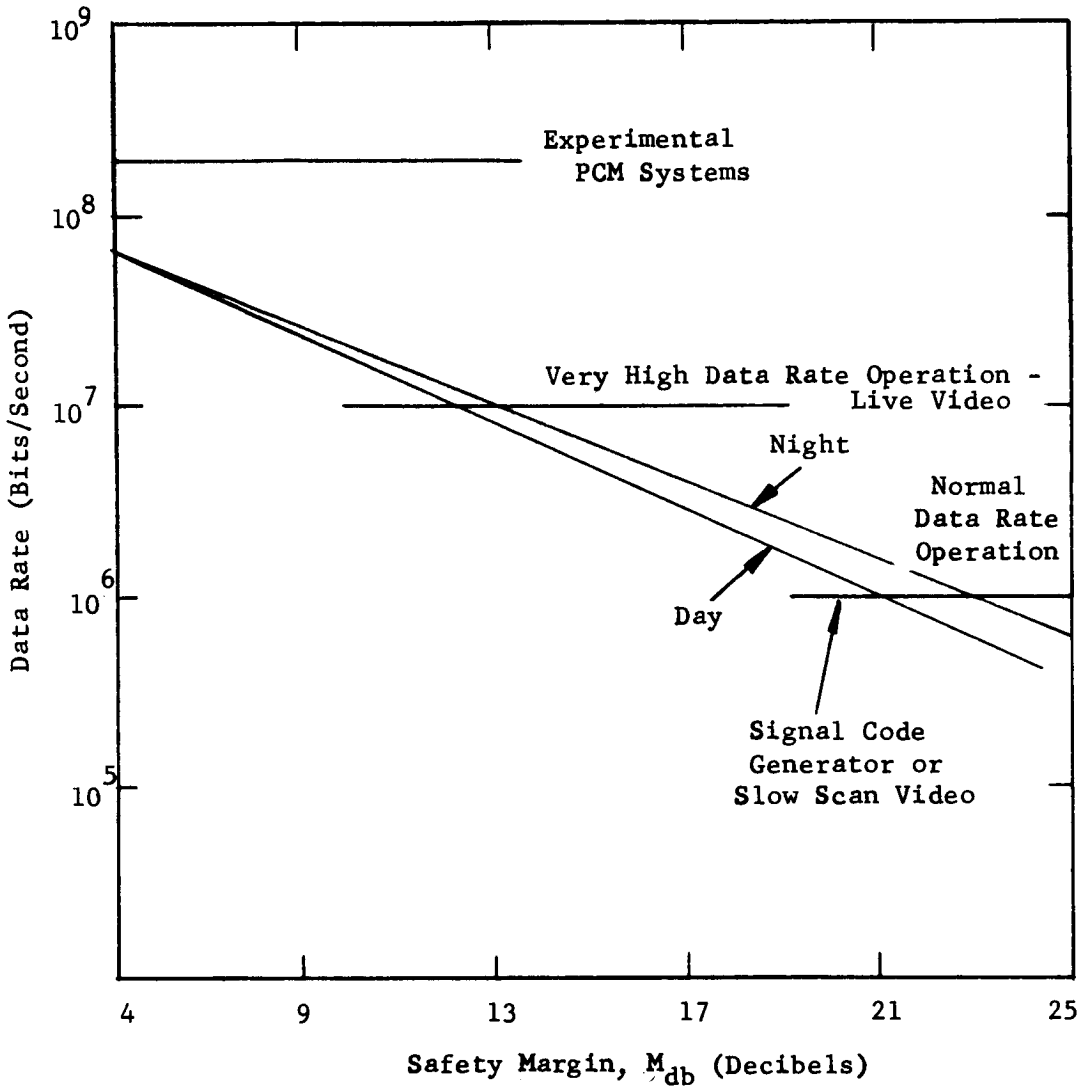

Figure 26. LCSE Safety Margin

night operations, respectively. Assuming night operation, no scintillation, zenith viewing, and optimum predetection optical filter, a large safety margin (over 20 db) will be available at 10^6 bits/second and an adequate safety margin (over 10 db) at 10^7 bits/second.

If the data rate capabilities of the laser link are extrapolated to 0 db of safety margin, the LCSE hardware intercepts sufficient laser energy for a 200 megabit digital system. This data rate can not be programmed into the LCSE program because of the present state of the art of such key components as the modulators, all solid state PCM/PL encoders and PMT detectors. However, the LCSE is a space verification of techniques for a deep space link. In the deep space case, the present state of the art laser communication system is quantum noise limited in the vicinity of a million bits/second. Therefore, the very high data rates of over 10^7 bits/second are either academic or of interest to near space missions.

BLANK PAGE

2.6 LCSE COMPONENTS TECHNICAL REQUIREMENTS AND PARAMETERS

MAIN TELESCOPE

The main telescope of the LCSE performs two key functions. It collects and images beacon light for the fine-guidance operations and it radiates laser light back to the earth. In this section, some of the considerations that point to a specific design for the LCSE are evaluated and compared.

From an optical system point of view, the totally reflective telescopes are most attractive because these forms are inherently free from chromatic aberrations. Even though the optical system will be used with laser sources, different wavelengths are required. One wavelength is used for the spaceborne laser transmitter and a different wavelength is used for the ground beacon. Also, multiple laser wavelengths may be employed for non-communications experiments with the LCSE; e.g. scintillation measurements. Thus, chromatic aberration is a consideration in the LCSE since it is not an all reflective system even though monochromatic sources are used.

Telescope Type - Basic Configuration

Perfect imagery of the telescope is required within a relatively small field of view (FOV). The most critical FOV is the central 2 arc-minutes used for fine guidance. An outer annular FOV of 1 degree is used for coarse acquisition. There are three different basic telescope configurations for narrow-field applications. These are the Newtonian, the Cassegrainian, and the Gregorian configurations. All are two-mirror systems based on parabolic, hyperbolic or ellipsoidal reflector figures. They exhibit perfect (aberration-free) imagery on-axis, but the useful field is restricted because of off-axis aberration.

The various catadioptric systems, which have been pioneered by Schmidt, Maksutov, and others, form a separate category of reflecting telescopes. They employ a spherical primary and feature a transmissive corrective element, covering the entire primary aperture. These systems are used when large angles of view (larger than 1 degree) are required and where the aforementioned simpler configurations are field-angle limited. However, field-angle limitations are distinctly not a LCSE problem and the more complicated catadioptics systems have no special merit over the two-mirror systems.

A fundamental requirement of the telescope follows from its dual function as a transmit/receive antenna, namely to provide a real image of practical magnification in an accessible region where the electro-optical apparatus of the transceiver system is located. Figure 27 illustrates the geometrical relations of the three basic telescope configurations considered that employ an f/3 primary mirror and a secondary amplification of 5 to yield an f/15 focus.

A Newtonian form comprises a paraboloidal primary and a flat to fold the converging beam to the side. An additional magnifying lens provides the required f/15 focus. (The prime focus shown by dotted lines has insufficient space to mount the transceiver apparatus in an axial position.) The Cassegrainian configuration uses a paraboloidal primary mirror in conjunction with a convex hyperboloidal secondary mirror located in front of the focus of the primary. The Gregorian form consists of a paraboloidal primary mirror and a concave ellipsoidal secondary mirror located behind the primary focus.

To yield an overall structure of tubular shape and a very compact arrangement of the optical components of the LCSE, the transceiver instrumentation is best located behind the primary mirror. Thus, side mounting of the transceiver package via a folding flat, as would be necessary with the Newtonian arrangement, presents additional mechanical support and alignment problems. Furthermore, the usable field of a Newtonian system is considerably smaller than of the other configurations, which is plausible as it utilizes the corrective power of only one aspheric surface.

The essential difference between the Cassegrainian and the Gregorian configuration is the different location of the secondary. This aspect, however, is of major concern as mounting and maintaining the secondary within the extreme tolerances for diffraction-limited telescope performance represents the most severe problem of the telescope structure. Every effort should therefore be taken to keep the distance between the vertexes of primary and secondary mirror as short as possible to facilitate the structural design. A primary/secondary separation of 56 inches for the Gregorian in Figure 27 compares with only 40 inches for the Cassegrainian of the same imagery. In view of these considerations, the basic Cassegrainian configuration is preferable.

Modification of the Cassegrainian Form

The conventional parabolic-hyperbolic combination of the Cassegrainian form corrects for spherical aberration and exhibits perfect axial imagery. However, the limiting off-axis aberration is coma. This form of image degradation is most detrimental to guidance systems owing to the asymmetric shape of the comatic flare which restricts the use of the conventional Cassegrainian configuration to a relatively small field of view.

As illustrated in Figure 28 there are several variations of the conventional Cassegrainian form which retain the advantages of the compact primary-secondary mirror arrangement but exhibit either a considerably larger corrected field or other features.

A modification that is used occasionally is the Dall-Kirkham design. An ellipsoidal primary mirror is combined with a spherical secondary to provide correction of spherical aberration. Its useful field is also limited by coma

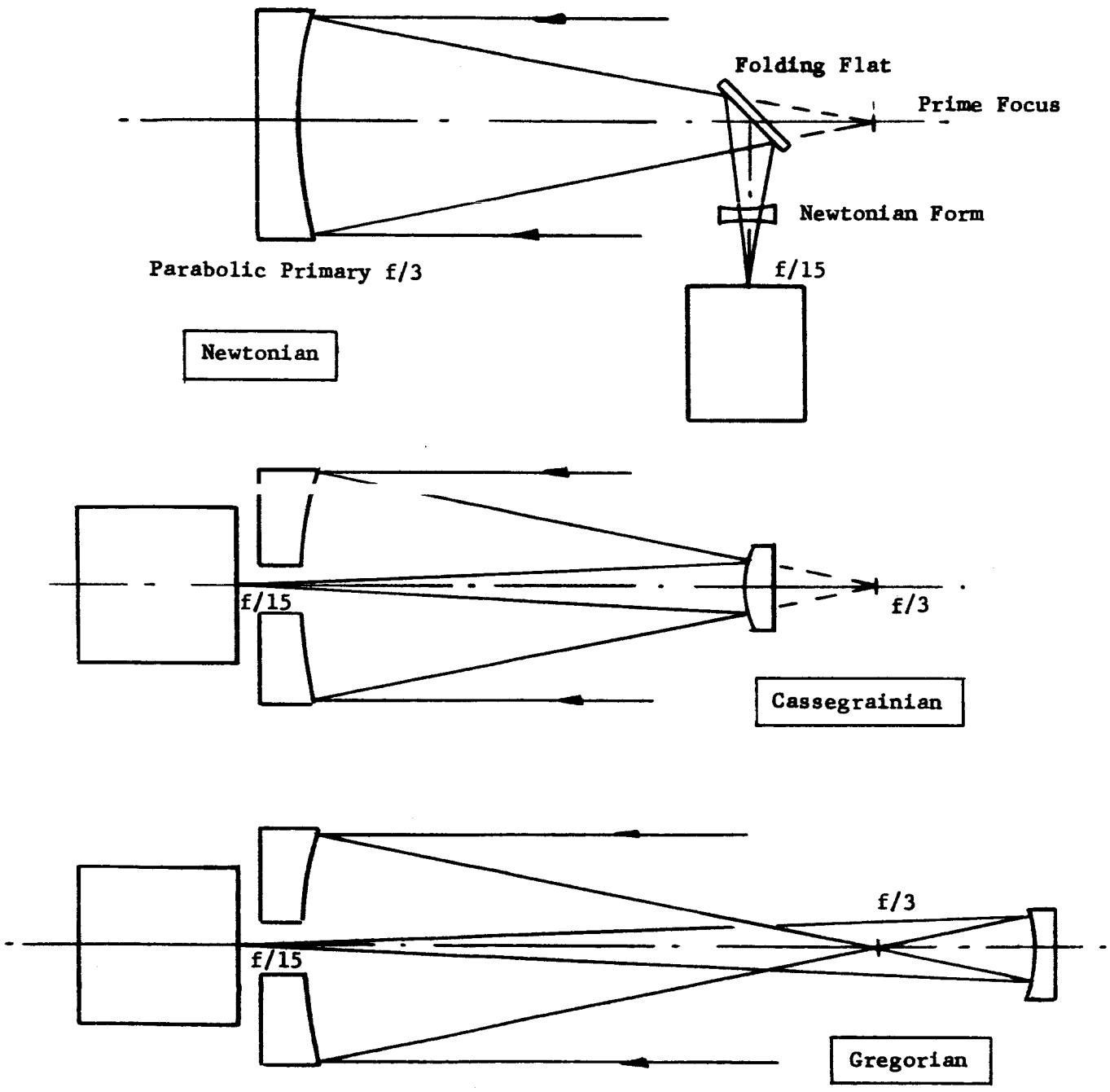

Figure 27. Geometry of Conventional Telescope Configuration and Possible Location of Optical Transceiver Package, Primary Mirror f/3, Effective System Focus f/15.

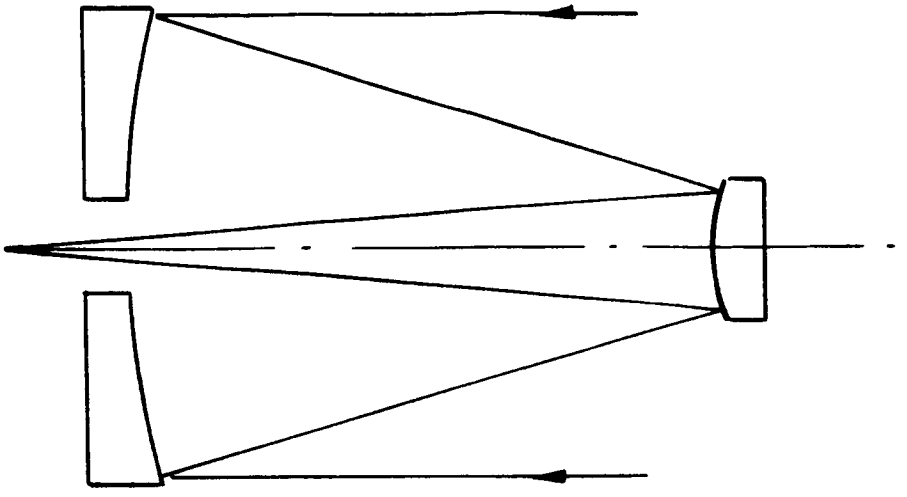

Variant of Cassegrain	Primary Mirror	Secondary Mirror	Corrected For	Useful Field Limited by
Conventional Cassegrain	Parabolic	Hyperbolic	Spherical Aberration	Coma
Dall-Kirkham	Ellipsoidal	Spherical	Spherical Aberration	Coma
Ritchey-Chretien	Hyperbolic	Hyperbolic	Spherical Aberration and Coma	Astigmatism

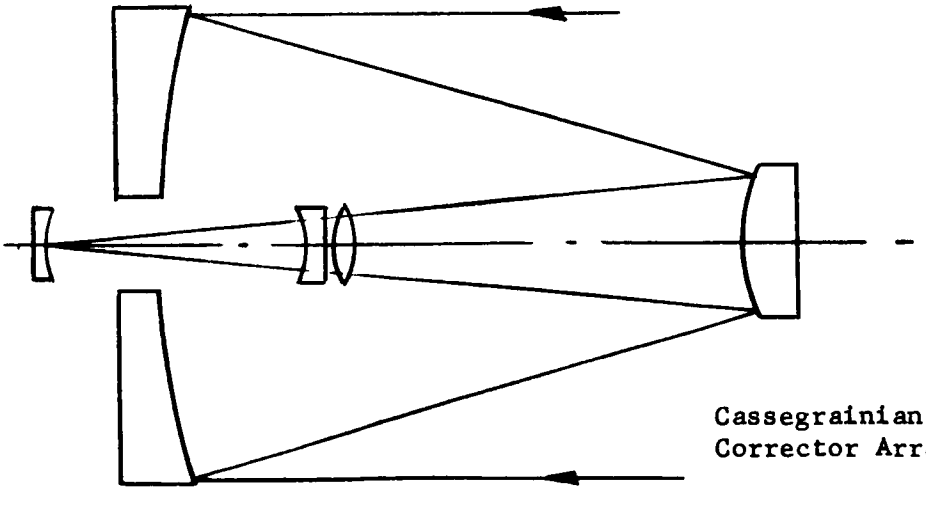

Cassegrainian Form With Corrector Array

Figure 28. Variants of Cassegrainian Configuration

and is generally worse than a normal Cassegrainian. However, the advantages offered by the spherical secondary in fabrication, alignment and test are significant enough to recommend this lens form in cases where its narrow field suffices.

Currently, a very popular Cassegrain-type form is the Ritchey-Chretien which employs a hyperbolic primary and a hyperbolic secondary. This design provides complete correction not only for spherical aberration but also for coma. Only astigmatism limits its useful field. The Ritchey-Chretien design is consequently capable of good performance over a wider field of view than the true Cassegrain.

There have also been a number of Cassegrain field correctors proposed during recent years which may be mentioned in this context*. These consist of an array of refractive elements of spherical or aspherical shape near the Cassegrainian focus. They are capable of providing large-aperture, near-diffraction-limited performance over fields as large as 30 arc-minutes, but at the expense of complex alignment problems associated with the additional optical elements.

PRIMARY MIRROR SIZE AND APERTURE

The limiting aperture of the LCSE is the primary mirror and has been set at 16 inches.

In choosing an aperture size, one must consider three questions:

- Will the link support a 10^7 bit per second data rate?
- Can 0.1 arc-second pointing of the fine tracking subsystem be verified?
- Can the results of the experiment be extrapolated to determine the performance of anticipated deep space optical communication systems?

The 20 db safety margin of the PCM/PL link was obtained with a conservative choice of laser and of earth receiver aperture. An aperture of 16 inches results in a satisfactory laser data link.

*Rovin, S., J. Opt. Soc. Am., 51, 331, 1961
Wynne, C.G., Appl. Opt. 4, 1185, 1965

To provide 0.1 arc-second tracking, a diffraction-limited aperture of approximately 16 inches is required for the LCSE. In addition, the temporal variations of the beacon, temperature gradients in the spacecraft, and telescope aberrations will reduce the resolution (and, thus, the tracking accuracy) of the communicator. Therefore, the 16-inch aperture is needed to establish the feasibility of high precision optical tracking systems in space.

The basic configuration of the LSCE tracking, telescope, and laser-modulator subsystems can be used in anticipated deep space optical communication links. The extensive diagnostic data received from the primary-secondary mirrors and the telescope structure will be invaluable in determining the validity of the thermal and mechanical analyses. These data will allow extrapolation from the 16-inch primary mirror to mirror sizes of approximately 1 meter for deep space optical communication link applications.

The f-number of the primary mirror is the major factor determining the length of the telescope tube. A primary with a lower f-number (i.e., faster primary) results in a closely spaced secondary and, as such, in a shorter system. A primary/secondary separation of 99 cm for an f/3 primary compares with 65 cm for a f/2 primary employing the same secondary magnification (Table V).

Increasing the speed of the primary mirror, however, also has negative aspects. Above all there is the dominating influence of the primary f-number on the mounting tolerances of the secondary mirror. As was stated earlier, mounting and maintainance of the secondary within the tolerances of diffraction-limited performance are extremely difficult tasks. The tolerances for the axial dislocation Δz and for the decentration $\Delta\rho$ of the secondary mirror were calculated. The exact expressions are given in Figure 29 and show Δz proportional to the square and $\Delta\rho$ proportional to the cube of the primary f-number. A secondary mirror facing an f/3 primary, for instance, would have to meet tolerances such as $\Delta z \approx \pm 3.5\mu$, $\Delta\rho \approx 80\mu$. for a maximum wavefront deviation of $\lambda/10$.

A further constraint on the choice of the primary speed is the well known fact that figuring an aspheric surface such as a paraboloid becomes increasingly difficult with smaller f-numbers. A 16-inch paraboloid with a relative aperture of f/3, for instance, involves considerable efforts when figured to the required RMS value of $\lambda/50$. The fabrication of an f/2 paraboloid of same size and figure quality, however, would be more expensive and time consuming and would provide only small increases in system performance.

The advantage of a somewhat shorter telescope tube for the payload volume was weighed against these shortcomings and a value of f/3 was selected as a judicious compromise between program performance and cost.

TABLE V

BASIC LCSE SPECIFICATIOI S FOR
VARIOUS PRIMARY/SECONDARY MIRROI COMBINATIONS*

f-number of Telescope	Effective Focal Length (m)	f-number of Primary	Primary/ Secondary Spacing (m)	Diameter of 1 degree Coarse Guidance Field (cm)	Diameter of 2 arc-min. Fine Guidance Field (cm)	Max. Shift of Peak Wavelength of Interference Filter in Coarse Guidance (Å)
f/15	6.09	f/3	0.99	10.6	0.35	2
f/10	4.06	f/3	0.90	7.1	0.24	4
f/10	4.06	f/2	0.65	7.1	0.24	3
f/7	2.84	f/2	0.60	5.0	0.17	7

*Cassegrainian Type With a 16-inch Primary and a Focal Plane 15cm Behind the Primary Apex.

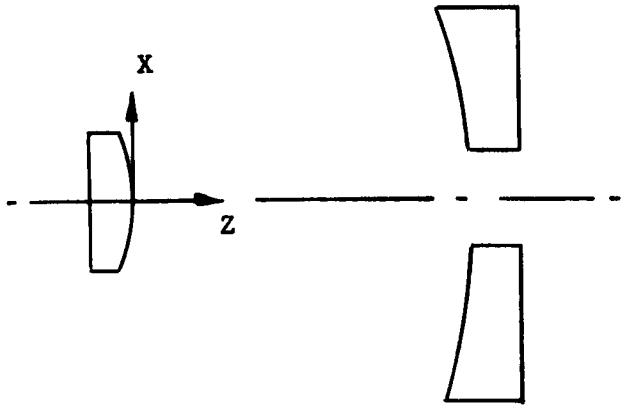

Axial Dislocation:

$$\Delta z = \pm \left(\frac{\lambda}{n}\right) \frac{8m^2f^2}{1+m^2} \approx \pm \left(\frac{\lambda}{n}\right) 8f^2$$

Decentration:

$$\Delta\rho = \Delta x^2+\Delta y^2 = \left(\frac{\lambda}{n}\right) \frac{64\ m^2f^2}{m^2-1}$$

where:

f = primary f-number

m = secondary magnification

λ/n = maximum wavefront deviation in fractional wavelength

Figure 29. Mounting Tolerances for Secondary Mirror in Cassegrainian Configuration

SECONDARY MIRROR CONSIDERATIONS

The basic specifications for the secondary mirror including diameter, secondary magnification, axial location, etc., are determined by considering the various implications of the resulting telescope magnification and f-number.

The first component in the optical train of the transceiver apparatus connected to the telescope is the coarse guidance image plane dissector. It is positioned immediately behind the primary mirror. The secondary has to be dimensioned so as to locate the image plane of the telescope at the plane of the image plane dissector. This brings the focal point of the telescope to about 15cm behind the primary mirror apex.

The coarse guidance image plane dissector first functions as a field stop restricting the overall field of view of the telescope to 1 degree. This field is then divided into an annular shaped outer section for the coarse guidance channel and a circular shaped central section for the fine guidance and transmit channel. The diameter of these fields in the focal plane of the telescope depends on the focal length of the telescope. Table V gives numbers for some possible primary/secondary combinations. An effective focal length of 6.09m (for a telescope speed of f/15), for example, is associated with a field of 10.6cm diameter to be covered by the coarse guidance channel. This necessitates rather bulky optical elements for relaying and detecting the coarse guidance field information, and may therefore be considered the upper limit to keep the coarse guidance subsystem of practical size. It is desirable to stay close to this limit so that the much smaller fine guidance field is still of reasonably large size in the f/15 focal plane and is not adversely affected by mechanical tolerances.

TELESCOPE PARAMETERS

There are clearly a number of primary/secondary combinations which yield a basic Cassegrainian configuration and comply with the requirement indicated. The geometrical parameters of some of them are listed in Table V. They are based on a 16-inch primary with a relative aperture of f/2 or f/3. They possess a focal plane 18cm behind the primary apex and an effective focal length between 4m to 6m (or a main focus with an f-number between f/7 and f/15).

An additional column in Table V refers to the permissible optical filtering of background radiation seen by the coarse guidance channel. We assume a Fabry-Perot type interference filter mounted in front of the coarse guidance image dissector as is the case with the fiber optics design. These filters are inherently sensitive to the angle of the incident radiation. The wavelength λ of peak transmission at zero angle of incidence shifts to a shorter wavelength $\lambda - \Delta\lambda$ for an angle of incidence α according to the relationship.

$$\Delta\lambda = \frac{\lambda \alpha^2}{2n^2}$$

where $\alpha \ll 1$ and n is the refractive index of the spacer. The wavelength intervals in Table V (last column) state the shift in peak transmission for the maximum angle of incidence occurring in the coarse guidance field for the respective f-number. The bandwidth of the interference filter employed for the coarse guidance channel should not be significantly narrower than the wavelength intervals indicated. Too narrow a filter would affect the coarse guidance system in the same way as a decrease in aperture diameter.

The system parameters chosen for the LCSE are shown in Table VI and resulted from all of these considerations.

Telescope Design

A standard Cassegrain telescope design was worked out and employed in the Laser/Optics Technique Project . This choice was based on computer-aided calculations that showed clear advantages over the Dall-Kirkham design but only a marginal advantage (unwarranted by the requirements of that particular project) over the Ritchey-Chretien design. However, as coma is the particular concern for coarse acquisition purposes, the improvement in off-axis performance to be expected by employing the Ritchey-Chretien design warrants the somewhat greater manufacturing difficulty it entails. Therefore the LCSE will employ a 16-inch clear aperture Ritchey-Chretien telescope with an f/3 primary and with a secondary mirror of 5X magnification.

Telescope Mirror Material

Fused silica is designated as the material for the LCSE primary and secondary mirrors. Experience has shown this to be the best choice for this size, since it takes on an excellent polish, an accurate and stable figure, and has good thermal characteristics. The weight of the primary mirror can be minimized by curving the rear surface of the primary mirror. A dish-shaped primary mirror results which is deep in the middle where it needs to be for structural reasons, but which is relatively thin at the periphery, where thickness is not beneficial. A solid mirror is chosen for the LCSE over the eggerate since the weight saving of the latter in this 16-inch diameter is not significant enough to warrant the additional cost.

TABLE VI

LCSE LASER/TELESCOPE OPTICAL PARAMETERS

Clear Aperture of Main Telescope	16 inches
f-number of Primary Mirror	f/3
Secondary Magnification	5X
Location of f/15 Focal Plane	7 inches behind vertex of primary mirror
Field of View for Coarse Acquisition	1 degree
Fine-Guidance Field of View	2 minutes
Magnification of Image Transfer Optics (Resulting in Final f/70 Image)	4.67X
Diameter of 2-Minute Field at f/15	0.14 inch
Diameter of 2-Minute Field at f/70	0.65 inch
Diameter of 1-Degree Field at f/15	4 inches
Operating Wavelengths	6328Å, 4880Å
Image Quality	Diffraction-limited pointing and tracking capability over central 2-minute field.

COARSE ACQUISITION GROUP

Field Splitter

As indicated in Figure 6 on page 21, and in Table V the coarse acquisition and fine guidance field of views are separated by the field splitter at the f/15 focal plane of the telescope. The annular ±1 arc-minute to ±0.5 degree field is intercepted by a cluster of four pie shaped fiber optic bundles. Each bundle intercepts one quadrant of the coarse acquisition field and directs the accepted light to its respective photomultiplier detector.

Each fiber bundle changes from a pie shape at the focal plane to a cylindrical shape at the PMT end of the bundle.

Predetector Filter

A predetection filter with a matching central hole is situated in front of the fiber optic field splitter.

The half-bandwidth has been set at 5Å, which, for reasons mentioned earlier, is a minimum value established by entrance cone angle considerations. In particular, the coarse acquisition predetection filter receives rays spreading up to ±4 degrees from normal incidence.

Cone Condensers

Space qualified photomultipliers are immediately available with a maximum useful photocathode area of about 1 inch^2. As each relayed quadrant of the 1 degree, f/15 coarse acquisition field occupies an area of about 3 inches^2, it will be necessary to precede each coarse acquisition photomultiplier with a tapered cone condenser. This will necessitate elongating the four coarse acquisition "arms". This will also tend to diffuse the beacon light across an entire photocathode and to reduce the gain variations associated with nonuniform photocathode sensitivity.

FINE GUIDANCE GROUP

The basic elements of the fine guidance group are illustrated in Figure 6 on page 21 and the system parameters are listed in Table VI. A 16-inch aperture telescope acts as the front end of the system and is used for both transmission of helium-neon laser light and reception of argon laser beacon light. The coarse acquisition fiber bundle and associated PMT's are located at the f/15 focus of this telescope. It divides the field of view into a 2 arc-minute fine guidance field (transmitted through the hole in the fiber optics bundle) and a 1-degree coarse acquisition field (piped by the fibers to four PMT's).

The focal plane of the first lens, L_1, beyond the field dividing fiber bundle lies in the focal plane of the telescope. This produces a region of collimated light to the right of L_1 with an axial bundle diameter equal to the clear aperture of the telescope multiplied by the ratio of the focal length of L_1 to the effective focal length of the telescope.

The next item in the optical chain is a dichroic beamsplitter, designed for maximum reflectance at 6328Å and maximum transmission at 4880Å. Two conjugate light paths are produced which are separated according to color on transmission and on reflection. The beamsplitter merges a reflected red beam and a transmitted blue beam in the reverse direction and makes them collinear. This arrangement implements the concept of optical duplexing.

Two additional lenses, L_2 and L_3, form conjugate f/70 images at the apex of a fine-guidance image-divider prism and at an equivalent image of the transmit laser, respectively. The required point-ahead function of the system is implemented by a pair of Risley prisms. Relative and joint rotation of these prisms accomplishes two-coordinate angular offset of the transmitted laser beam from the line of sight of the receive channel (RLOS).

Telescope pointing errors are sensed by the fine-guidance image-divider and associated photomultipliers illustrated in Figure 6. The resulting error signals are used to close a feedback loop that causes an x-y servo drive to translate lens L_1 and reposition the beacon image on the apex of the image-dividing prism. In this way, the system can point at and track an earth beacon to within the diffraction limit of the telescope. The transmit channel is made conjugate to the receive channel which constrains the light transmitted back to earth to point and track to the same accuracy.

The predetection filter is located in the receive channel between the dichroic beamsplitter and lens L_2 and acts as a narrowband filter centered on the beacon wavelength. It serves to block background light on either side of the passband and blocks stray light that originates from the transmit channel.

A variable aperture stop is located in front of the fine-guidance image channel. Its purpose is to restrict the field of view from a nominal 2 arc-minutes down to as little as a few arc-seconds. FOV reduction is carried out in this way after beacon acquisition. This increases the ratio of signal to background noise and improves the performance of the fine-guidance servos and, therefore, tracking accuracy.

The auxiliary cube-corner prism and retractable shutter are used as discussed on page 27 to ensure that the two channels are accurately boresighted.

Design Requirements of the Image Transfer Optics

A preliminary design of the image-transfer optics for the LCSE has already been carried out under the Laser/Optics Techniques Project. It was specified that the design be achromatized for helium-neon laser light at 6328Å and argon laser light at 4880Å and 5145Å. It was further specified that the image transfer optics provide a net magnification of 4.67X and result in an f/70 diffraction-limited image of the main telescope's central 2-minute field. In addition, because these optics are required for use with laser light, it was specified that a minimum of surfaces be used and that parallel or concentric surfaces be avoided. A computer-aided design was obtained which meets these criteria and consists of a special doublet at L_1 with a focal length of about 6cm and another doublet at L_2 with a focal length of 28cm. Between these lenses is a region of collimated light 10 to 20cm long in which zero-power, zero-distortion, beamsplitters, Risley prisms, filters, etc., can be located without introducing aberrations into the system.

These doublets resemble, and in a sense act as, telescope objectives. The first, which we have designated the transfer lens, collimates an image falling within the central 2-minute field of the telescope. The second lens decollimates light from the first and forms the f/70 image required for fine-guidance and tracking purposes.

Lens L_3, which works with a conjugate image formed by the transmitter channel may be considered identical to L_2.

The diameter of an axial bundle of the relayed collimated light is about 4mm, which is a demagnification of 100X of the 16-inch (400mm) entrance pupil of the main telescope.

Field angle considerations lead to a minimum clear aperture of about 12mm for L_1 and a similar value or greater for L_2, depending on the spacing between L_1 and L_2.

Optical Tolerances

The optical system of the LCSE must be capable of pointing and tracking to within a fraction of the angular diffraction spread of its 16-inch aperture telescopic front end. Optical tolerances must therefore be held to an extent which insures that the final f/70 image, falling on the apex of the fine-guidance image divider, contains an adequate amount of energy symmetrically disposed within the focal spot. This spot ideally corresponds to the area enclosed by the first dark ring of the f/70 Airy pattern; a theoretical maximum of 84 percent of the total light intensity in the image can be so enclosed.

If the theoretical peak intensity at the prime image of a telescope mirror is I_o, then the ratio of the expected intensity peak I to I_o is given by the expression

$$I/I_o = 1 - 4\pi^2 \Delta^2 \lambda^{-2}$$

where λ is the wavelength of operation and Δ is the rms (root mean square) wavefront departure of the wavefront from a sphere centered on the image; i.e., Δ is twice the rms mirror figure error.*

It follows from this expression that, to result in a peak intensity, I, of 94 percent of theoretical, the rms figure error cannot exceed $\lambda/50$. This exceedingly stringent tolerance was selected for the 36-inch aperture primary mirror of Stratoscope II because its principal function is to carry out celestial photography in such a way that resolution in the recorded image is limited mainly be the finite primary mirror diameter.

Diffraction-limited pointing and tracking functions, where the need is to locate and lock onto the centroid of an image, is best accomplished with optics made to the same tolerance. This insures the most efficient collection of the beacon energy for tracking purposes and the most efficient transmission of light from space to earth.

The LCSE imcorporates an image-position sensor subsystem at the f/70 fine-guidance image plane. One such subsystem was previously illustrated in Figure 6 page 21 by a pyramid-shaped prism and four photomultipliers. Basically the same function can be carried out be a variety of techniques. A brief comparison of the different techniques suited to the needs of the LCSE is given in Table VII. Only the most immediately relevant properties of each are highlighted.

The technique to be used in the LCSE consists of an optical image divider in conjunction with four photomultipliers. This technique originated with Stratoscope II and is capable of exceedingly accurate performance.

The original Stratoscope image divider design consists of a modified cube-corner retroreflector. A star image is divided four ways on retroreflection from a cube-corner prism whose three reflective surfaces depart by a calculated amount from mutual orthogonality. The design results in the ability to discriminate image motions that are small compared with the size of the diffraction-limited star image. Image division occurs at the point of intersection of three planes of one glass element, and as this point can be made to have a blunt region of less than 5 microns diameter, only a correspondingly small fraction of light in the image fails to reach the four photomultipliers.

*Scott, R.M., Applied Optics, Vol. I, p. 387, July 1962

TABLE VII

COMPARISON OF IMAGE DIVIDERS AND TRACKERS FOR LCSE

DEVICE DESCRIPTION	
Magnetically focused image dissector (e.g., IIT Type FW-146, F4011, etc.)	
PROPERTIES	**CONSEQUENCES OF PROPERTIES**
Furnished with fixed aperture sizes ranging from 0.0005 inch to 0.350 inch. Typical equivalent photocathode aperture sizes: 0.005 inch.	Aperture can function as a virtual image stop. This eliminates noise due to background light in remainder of image. But as a concomitant property this necessitates a search mode if image is not centered.
Senses image position by magnetic scanning of electron image across aperture.	Necessity for scanning decreases available signal power in each of two axes by 1/2 for 100% modulation. Requires magnetic coil power supplies and drive circuitry.

DEVICE DESCRIPTION	
Electrostatically focused image dissector (e.g., C.B.S. Type CL-1147 Reconotron).	
Aperture fixed as in above device. Typical aperture diameter 0.002 inch for a typical useful photocathode diameter of 0.75 inch.	As for all image dissector devices the virtual image-stop is not adjustable. This limits the field of view drastically and requires a scanning mode for initial acquisition and for acquisition on loss of track.
Senses image motion by electrostatic deflection system.	Low power requirements but worse resolution than by magnetic focus and deflection. Also loses useful signal power by the need for position modulation by electron image.

TABLE VII (Continued)

DEVICE DESCRIPTION

EMR Quadrant Multiplier Phototube (e.g., Model 568A-01-14)
(consists of 4-quadrant photocathode followed by a common multiplier chain)

PROPERTIES	CONSEQUENCES OF PROPERTIES
Sensitive area of photocathode 0.4 in dia. gap size (dead region between quadrants) 0.0015 inch + 0.0005 - 0	Maximum number of resolution elements limited $\frac{0.4}{0.0015} = 270$ in either axis.
Image position determined by sequential switching on of each quadrant.	Losses 75% of available signal power.

DEVICE DESCRIPTION

ITT Quadrant Multiplier Phototube (e.g., Model F4002)
(consists of 1 photocathode followed by a splitting reticle and 4 multiplier chains)

Useful cathode diameter 0.97 inch. The splitting reticle is used to direct photoelectrons from each quadrant of the photocathode into their respective multiplier chain. A relatively large loss area (unspecified by the manufacturer) exists near the electrical center of the photocathode.	Unspecified but probably small numbers of resolution elements.
Functions as four photomultiplier tubes in one package.	No loss of signal power except at electrical center of photocathode. Compact unit as compared with four separate photomultipliers.

DEVICE DESCRIPTION

Optical Image Divider with Associated Photomultiplier Tubes
(e.g., Perkin-Elmer retrodivider design for Stratoscope II)

Image division takes place at intersection point of three optically polished planes. Useful apertures in excess of 1.5 inches readily obtained with essentially no dead zone at apex, (i.e., apex can be made to have a blunt region no greater than a few microns in diameter.	No loss of signal power as each quadrant of divided image falls on its own photomultiplier tube. Tremendous number of resolution elements. No appreciable amount of signal power lost when image is centered.

TABLE VII (Continued)

DEVICE DESCRIPTION - (Continued)

Optical Image Divider with Associated Photomultiplier Tubes
(e.g., Perkin-Elmer retrodivider design for Stratoscope II)

PROPERTIES	CONSEQUENCE OF PROPERTIES
Entire field of view is exposed to photomultipliers.	Tracking information available over entire field of view. Requires an additional image stop if field of view is to be reduced to cut down on noise due to background light. Field of view can be adjusted by external stop.
Requires external photodetectors.	The choice of detector is not restricted. This technique allows selection of optimum photomultipliers in semi-redundant configuration.
Critical manufacturing tolerances can be maintained with optical precision.	The finished optical element is basically rugged and the critical surfaces can be so constructed as to be self-protecting. Other mechanical tolerances (e.g., positioning of photodetectors) are non-critical as a result of the optical design at the divider.

DEVICE DESCRIPTION

Optical Image Divider with Associated Quadrant Multiplier Phototube (e.g., Perkin-Elmer retrodivider design for Stratoscope II with ITT Model F4002 Quadrant Multiplier Phototubes.)

Image division is still carried out optically, but sensing is carried out as if by four photomultiplier tubes in one envelope.	Uses signal power as efficiently as four photomultipliers yet mechanical configuration is much more compact. Reliability of quadrant multiplier phototube is not as high as four semi-redundant individual photomultipliers.
Requires image stop if noise due to background light must be reduced by reducing the field of view.	The field of view can be varied at will by changing the size of the image stop. Hence, an added versatility of this technique.

Because of space restrictions, an image divider of this type was employed in the Laser/Optics Techniques Project on transmission, not on reflection as is more usually the case. This modification carries the divided image out to a region behind the divider where photomultipliers can be mounted conveniently, and is easily accomplished with the Stratoscope divider by leaving two of its three reflecting surfaces uncoated. The LCSE can use the divider in either configuration but the Laser/Telescope Layout (Figure 6 page 21) shows the image divider as a refraction divider. The features of the transfer-lens-servo-fine-guidance approach are illustrated in Figures 30 and 31.

The field of view of the main telescope is shown relayed by the transfer lens to the plane of an image-splitting element. This element divides the field into four quadrants and reflects each quadrant to a respective photomultiplier. The apex of the image divider is exceedingly sharp, and is capable of quadrisecting the diffraction-limited beacon image without appreciable loss of light intensity.

When the beacon image is centered on the apex of the image divider, all four photomultipliers receive equal amounts of signal light. When the image is slightly off center, the light divides proportionately. When the image is completely off to one side, the position-proportional nature of the signals is lost, nevertheless, the photomultipliers sense a saturation signal that indicates the quadrant in which the beam is located.

The electronics are designed to process this information and reposition the transfer lens optics so as to bring the beacon image from any point in the fine-guidance field to the apex of the image divider. This servo system has a linear discriminant when the image is nearly centered and each photomultiplier receives a finite share of the light. Beyond this linear range the servo is saturated, and the electronics are arranged to drive the transfer lens back in the direction that tends to center the beacon image on the divider apex where linear servo operation occurs.

The image divider apex defines the axis of the entire optical system. When the transfer lens is in its central position, an image of the hole in the coarse-acquisition fiber bundle is formed in the plane of the image divider. The image divider, therefore, need be only nominally centered with respect to this image.

Image-Position Sensor Requirements

The ability to accomplish diffraction-limited pointing and tracking in practice requires the technique employed for sensing beacon image position in the receive channel. If the angular diffraction-limit of the telescope front end is 1/3 arc-second, then the image-position sensor must be able to detect pointing errors on the order of 1/30 arc-second. It must be capable of this remarkable level of performance throughout the fine-guidance field of view.

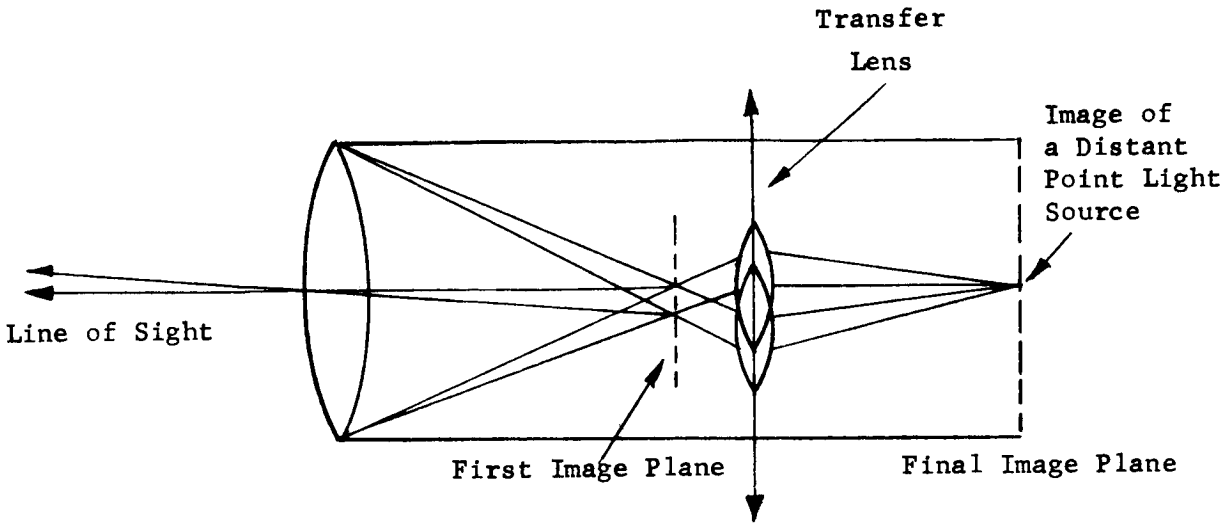

Figure 30. Transfer Lens Motions Which Compensate for Image Motions Due to Telescope (or Object) Movements.

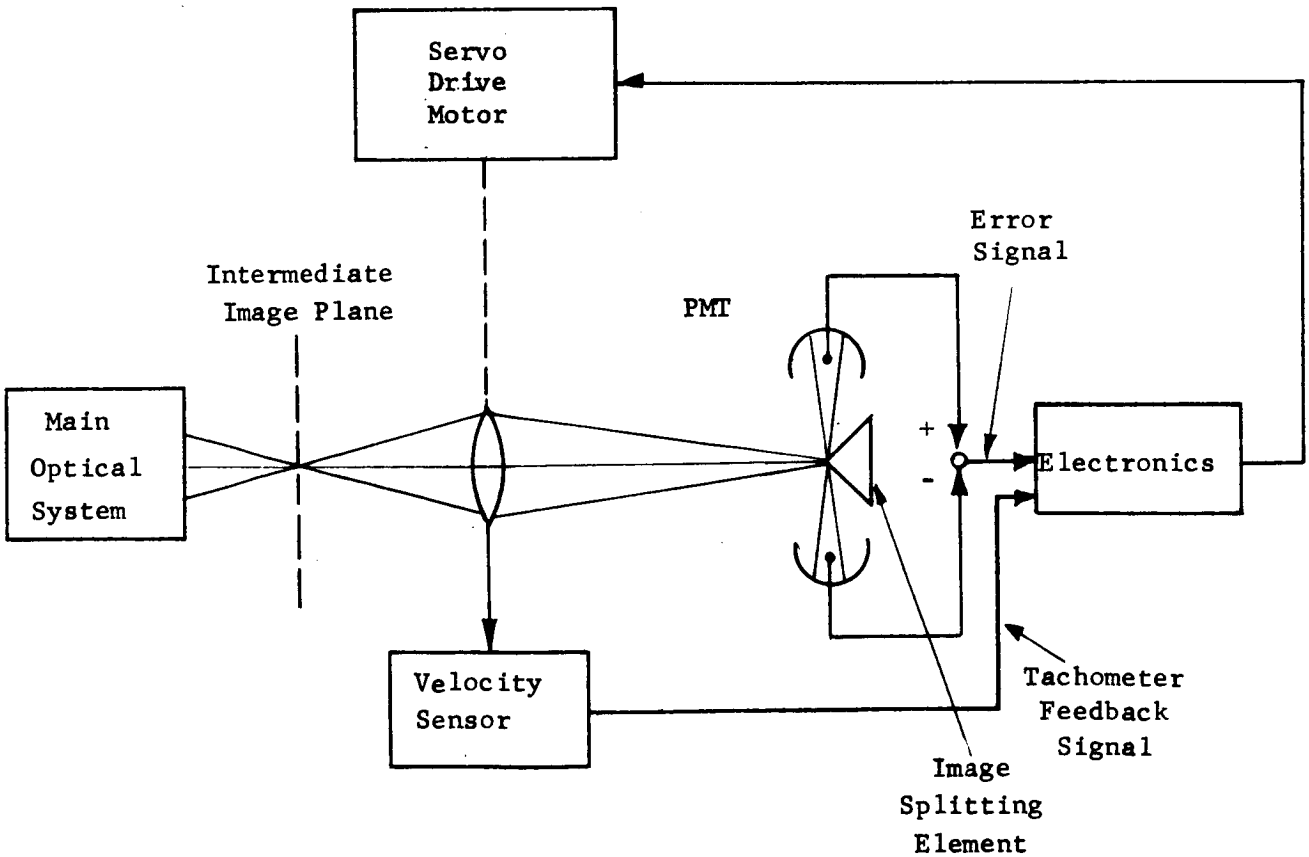

Figure 31. Single Axis Arrangement Illustrating The Stratoscope II Star Tracking Method

In terms of resolution elements, assume the fine-guidance field of view is 2 arc-minutes x 2 arc-minutes. This area contains 13 million 1/30 arc-second x 1/30 arc-second elements.

Photomultipliers

The prime function of the photomultipliers employed in the image position sensor subsystem is to detect argon laser beacon light at 4880A. They must carry out this function in the presence of whatever residual red light at 6328A is incompletely blocked from the transmitter channel. Because of the channel separation problem it is desirable to choose receive-channel photomultipliers that not only have maximum blue response but also minimum red response.

It was shown in the Laser/Optics Techniques Project that adequate channel separation can be obtained without relying too heavily on choosing photomultipliers with poor red response. Because of the high quantum efficiency of the S20 surface to the argon beacon wavelengths this is the recommended surface for the LCSE photomultipliers. As compared with the S11 and S surfaces, this choice requires that an additional factor of 10 or more of attenuation at 6328A be provided by the LCSE dichroic beamsplitter or predetection filter (Figure 32.) The improvement in quantum sensitivity to argon beacon light is about 1.5X and 2X, respectively.

Space qualified photomultipliers with matched solid state power supplies are available. Care must be taken in choosing four phototubes which have emissive surfaces which do not vary in sensitivity from point to point. The exact area over which uniformity is required is determined by the linear response region of the fine tracking servos. The dark current of the tubes operating at ambient temperatures is sufficiently smaller than the received signal power.

Transfer Lens Servo

As indicated in Figure 6 on page 21, fine-guidance is carried out not by maneuvering the telescope but by two-axis electromechanical translations of the transfer lens L_1.

An appropriate LCSE transfer lens servo subsystem was designed constructed, tested and incorporated into the breadboard of the Laser/Optics Techniques Project. The most important characteristic of this design is that it does track to less than the 1/10 arc-second requirement.

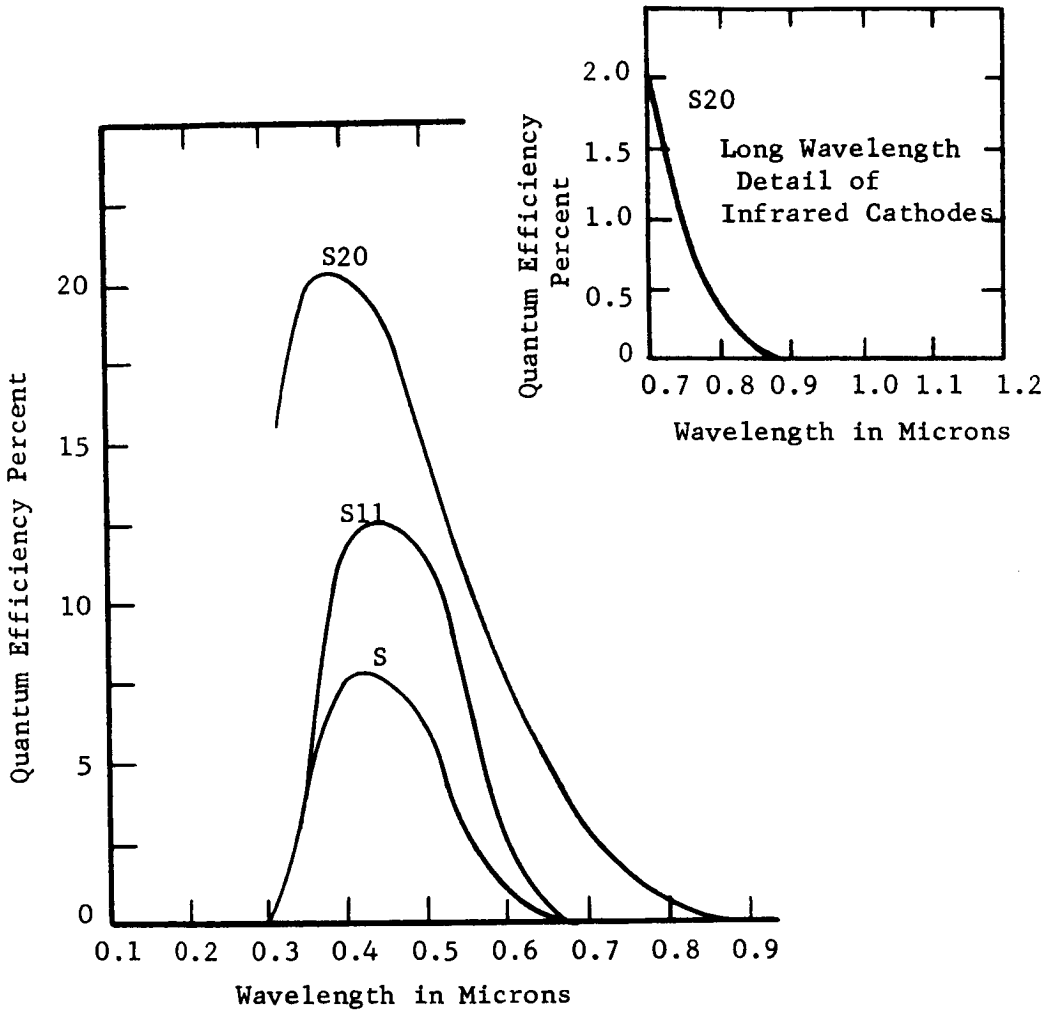

Figure 32. Photocathode Spectral Response Curves

Other principle features are:

- The transfer lens cell is supported by flexure bearings that are so arranged as to allow only translation in an x-y plane. This assembly is driven by x-y magnetic drives in response to signals from the image position sensor subsystem.

- The mounting arrangement is compatible with the hard vacuum space environment and has zero stiction as a result of the flexure bearings.

- A top view of the Laser/Optics Techniques transfer lens mechanism situated in place behind the main telescope is shown in Figure 33. The photograph is a time exposure and shows graphically how focused light from the 10 milliwatt He-Ne laser is collimated by one lens (L_3 of Figure 6), deflected at right angles by the dichroic beamsplitter and this is focused to a spot in the f/13 focal plane of the system after which it diverges to "fill" the telescope.

- The servo has approximately the response we would expect to be needed by a spaceborne beacon tracker. The measured 3 db bandwidth is approximately 38 cps, and the low frequency response is very stiff. (See Figure 34).

- Unique capacitance-operated position-pickoff sensors are utilized for position feedback and the position signal is differentiated for velocity feedback.

- The transfer lens servo subsystem is used in setting optimum system focus.

System Focus

By considering the depth of focus at each focal plane of the project optical system, it becomes evident that only the spacing of the secondary mirror to the primary is critical for correct system focus. At f/70, for example, the focus tolerance ΔZ is $\simeq \pm 5$mm as given by*

$$\Delta Z \simeq \pm \frac{1}{2} (f/a)^2 \lambda$$

where f/2a is the f-number and λ is the wavelength (4880Å).

* Born and Wolf, Principles of Optics, Macmillan, New York, 1964

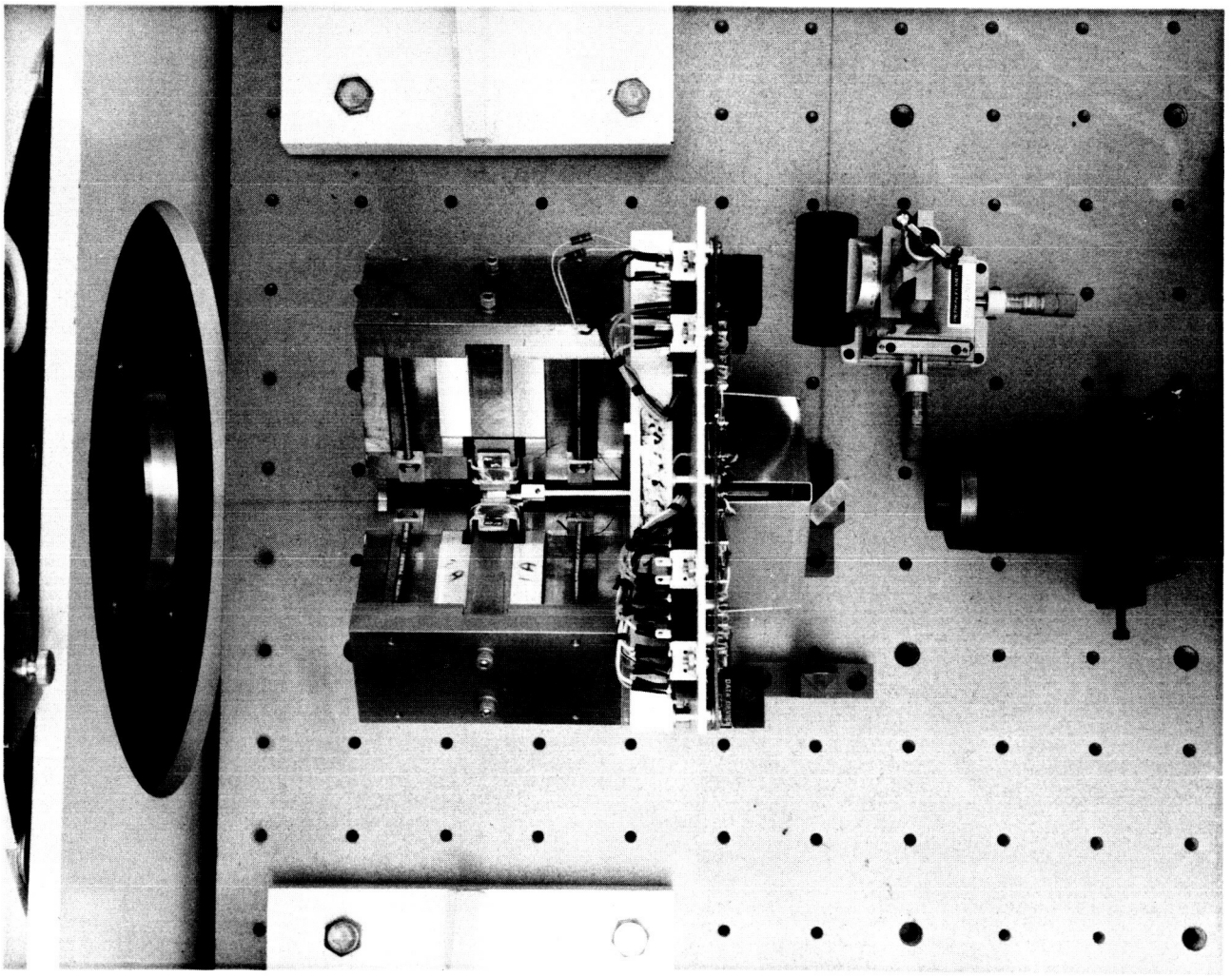

Figure 33. Path of He-Ne Transmit Laser Beam in Region of Transfer Lens

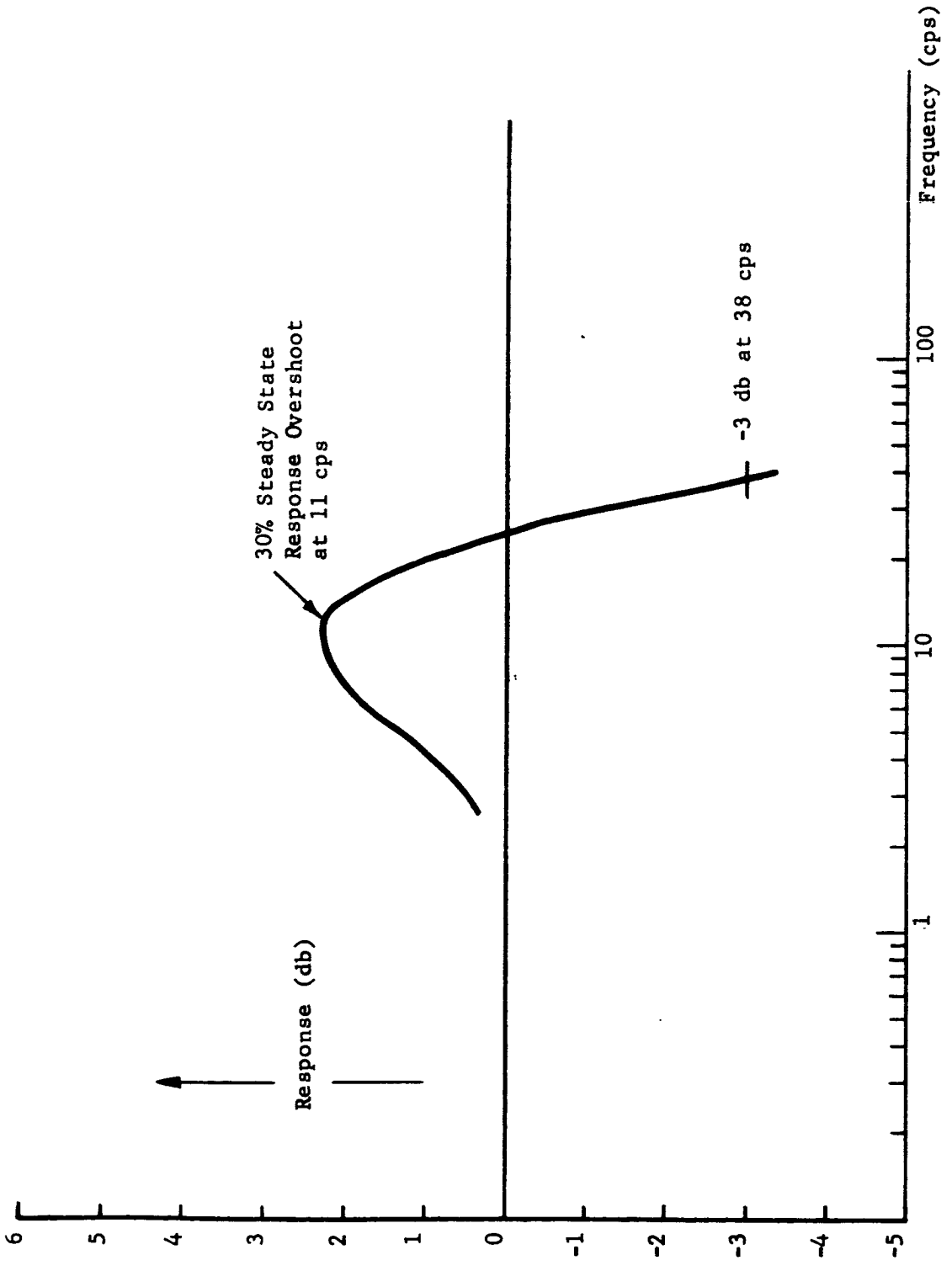

Figure 34. Major Loop Response Characteristic, $\frac{\theta_o}{\theta_i}$

At f/15 the focus tolerance is ±0.23mm (±0.009 inch). But at the f/3 prime focus of the telescope the tolerance is only ±.009mm ($3x10^{-4}$ inches). It therefore follows that all of the image transfer optics can be mechanically positioned and fixed with respect to the primary mirror if system focus is left to be accomplished by adjusting the position of the secondary mirror. A motor drive, shown in Figure 6, is incorporated into the LCSE for this function. An in-flight procedure for achieving correct system focus for the LCSE is discussed on page 32.

Remote Focus

As discussed above, with the exception of the secondary mirror, all of the optical elements can be permanently spaced with respect to the primary mirror. This leaves the axial spacing of the secondary mirror as the one parameter to vary to readjust the system focus. A motor drive mechanism is provided in the LCSE for this purpose.

The motor drive, then, is the system focus actuator. Detection of focus errors is accomplished by the transfer lens servo subsystem. The focusing procedure is carried out while the complete system is tracking the earth beacon or its equivalent. An electrical dither signal is injected into one axis of the transfer lens servo drive. The response of the closed loop is to exactly compensate for the electrical dither by moving the transfer lens. This motion produces an equal and opposite error signal in the image position sensor subsystem, since the dither acts on the servo drive the same as would a sinusoidal torque disturbance on the telescope. The motion of the transfer lens is then monitored while the secondary mirror is moved in and out of focus by the motor drive. At optimum focus the f/70 beacon image has a minimum diameter and the transfer lens experiences minimum dither induced displacement. In practice this is a rather broad minimum. On either side of focus, the beacon image is broadened and the transfer lens has to move further to produce the same compensation. This relationship is illustrated in Figure 35.

Position pickoff sensors are incorporated into the transfer lens servo subsystem and may be used to monitor displacement magnitude during focus operations. In practice it is preferable to determine a position of the secondary mirror on either side of focus each of which results in the same dither-induced lens motion. Then the secondary mirror is moved to the half-way position, which is taken to be optimum. It also turns out to be preferable, for reasons of accuracy in the presence of spacecraft disturbances, to measure dither-induced velocity of the transfer lens rather than position. This technique has been used successfully in Stratoscope II, OAO-C (Princeton Experiment Package), and the Laser/Optics Techniques Project.

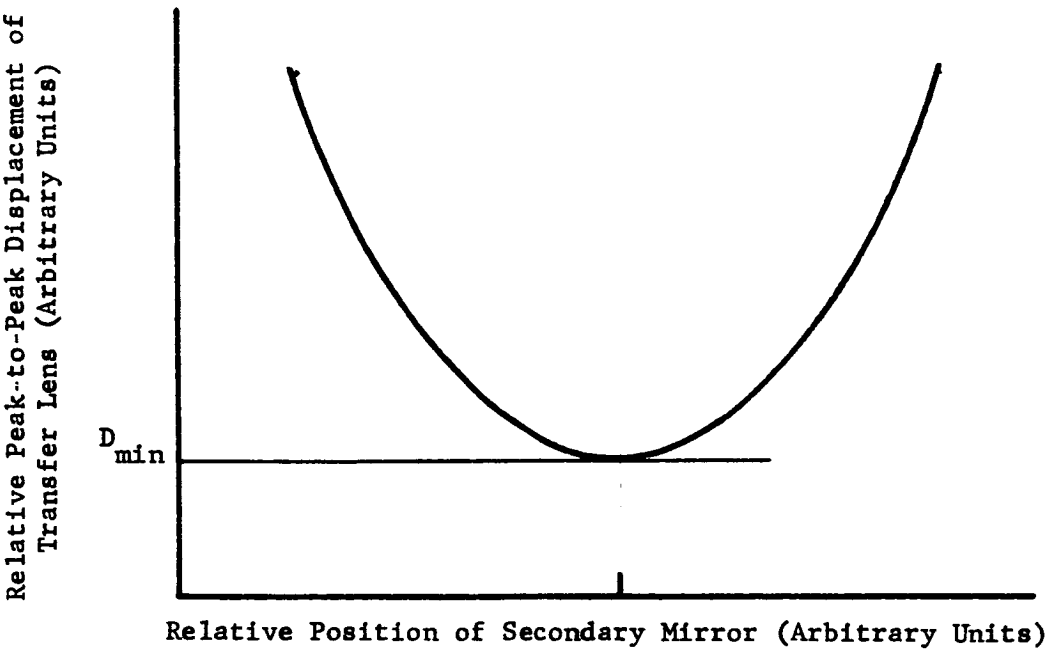

Figure 35. Relationship Between Dither Induced Peak-to-Peak Displacement of Transfer Lens and System Focus as Determined by Secondary Mirror Position

Channel Separation Requirements

Utilization of effective techniques for adequate channel separation is the key to using common telescope optics for both the receiving (beacon tracking) function and the transmitting function of a spaceborne optical communications system. The problem is arranging for the fine-guidance photomultipliers to be signal quantum noise limited at 4880Å in the presence of scattered light at 6328Å from the neighboring high-power He-Ne laser transmitter.

The magnitude of channel separation needed in the LCSE may be established by considering the signal requirements of the tracking servo detectors as follows. The most difficult case (i.e., when maximum exclusion of transmit light from the receive channel is required) is when, with negligible background light, the amount of incoming beam light is barely sufficient for the tracking function to be carried out. Suppose, for example, that the integration time of the tracking servos is of the order of 10^{-2} seconds. Then, for reasonable servo performance with a bandwidth of ten cycles per second, a minimum of about 10^4 signal photoelectrons are needed per 10^{-2} second period. Given a detector quantum efficiency of 10 percent and an optical efficiency of 33 percent leading to the detectors, it follows that a minimum of 3×10^5 photons per second of signal light (provided by the beacon) are needed by the tracking channel. Therefore the channel separation problem reduces to insuring that the tracking channel detects fewer than 3×10^5 photons per second of the high-power laser light present in the neighboring transmit channel.

As a specific example, let the transmit laser power be 3 milliwatts (9×10^{15}) photons/second. What the tracking channel detects of this must be small compared with 3×10^5 photons per second. Thus, the required channel separation must exceed the ratio of these numbers, which is about 3×10^{10}.

A reduction in receive-channel sensitivity to beacon light may result from the methods used to suppress unwanted transmit beam light. Moreover, the receive channel detectors will in general have different sensitivities at the receive and transmit laser wavelengths.

An appropriate figure of merit, K, for channel separation which takes these considerations into account can be defined as follows:

$$K \text{ (in db)} = 10 \log \frac{P_t}{P_d}$$

where P_t is the power of the transmit laser, and P_d is the response of the receive channel photodetectors to light originating from the transmit laser put in terms of equivalent signal power (i.e., referred to detector sensitivity at the signal wavelength).

If the transmit laser power is P_t then

$$P_d = P_t \frac{\epsilon_t}{\epsilon_r} \frac{\tau_t}{\tau_r}$$

where τ_r and τ_t are the optical transmission at the receive wavelength and transmit wavelength, respectively, ϵ_t is the detector quantum efficiency at the transmit wavelength and ϵ_r is the detector quantum efficiency at the receive wavelength.

It was shown in the Laser/Optics Techniques Project that channel separation in excess of 100 db (10^{10}) can be obtained by dielectric multilayer techniques. The LCSE requirements can therefore be met and comfortably exceeded by:

- applying VLR coatings to lens L_1
- employing the same highly efficient dichroic beamsplitter design used in the Laser/Optics breadboard.
- incorporating a short-wavelength pass filter design into the predetection composite stack filter.

Dielectric Filter Considerations

Scattering from a dielectric multilayer coating on a conventional substrate is partly caused by minute scattering centers in the coating itself and partly by small cracks in the surface of the substrate. These cracks develop during a conventional grinding process. They may be avoided to some degree by following an assiduous grinding and polishing procedure. Evaporating a low-scatter dielectric coating on such a "control ground" substrate helps in obtaining a beamsplitter with the least attainable scattering, and for this reason substrates prepared in this way will be used for the LCSE filters.

A variable field stop is located at the f/70 focal plane to restrict the field of view and act as an aperture for the scattered light. It reduces the solid angle of scattered light rays - emitted from a scattering center of the beamsplitter - which reaches the receiver light detectors, to $\pi/25$ steradian at most. The converging lens system L_2 (Figure 6, page 21) in front of the fine-guidance beam divider has an entrance pupil of 1.4 cm. As it cannot be located too far away from the beamsplitter for mechanical stability, it will not reduce the received bundle of scattered light rays any further than the 2 cm diaphragm in the f/70 focal plane.

The central area of the secondary mirror will ordinarily reflect axial transient light rays back towards the receive light detector. This

area on LCSE will be made nonreflecting, and the absorber will be the surface of the detector used to monitor transmitted light intensity.

Dielectric Multilayer Coatings

Reference is made in this discussion to Figure 6 page 21 which illustrates the location in the system of the following coating designs:

- Dichroic Beamsplitter: This is the central element of the optical system. It has the properties of a color-sensitive mirror. Its requirements are for high transmission at the argon laser wavelengths and high reflectivity at the He-Ne laser wavelength. The current state of development of dielectric multilayers for the dichroic beamsplitter is illustrated in Figure 36. Designed for 45 degree incidence, this beamsplitter is seen to transmit about 80 percent at 4880Å and 5145Å and only 0.1 percent at 6328Å.

- Very-Low-Reflectance Coatings (VLR Coatings): A very-low-reflectance coating design tuned to 6328Å is required for minimizing reflection from the surfaces of the elements of transfer lens L_1. These reflectors consist in general of slightly divergent beams tending to propagate at small angles toward the receive channel photomultiplier. A special design tuned also to the argon wavelength will maximize the amount of argon beacon light reaching the fine-guidance detectors. A reflectance of an uncoated surface can be reduced from about 0.04 to about 5×10^{-4} at 6328Å and to about 5×10^{-3} at the argon wavelengths.

- Short-Wavelength-Pass Filter (SWPF): This kind of filter is located between the beamsplitter and receive channel detectors, and in practice is best located immediately in front of lens L_2. It functions as a final blocking filter to prevent surviving transmit light from entering the receive channel. Its required properties are similar to those of the beamsplitter as it must reject red transmit light by reflection and pass blue beacon light. A special coating design was worked out for the SWPF requirement in the Laser/Optics Techniques

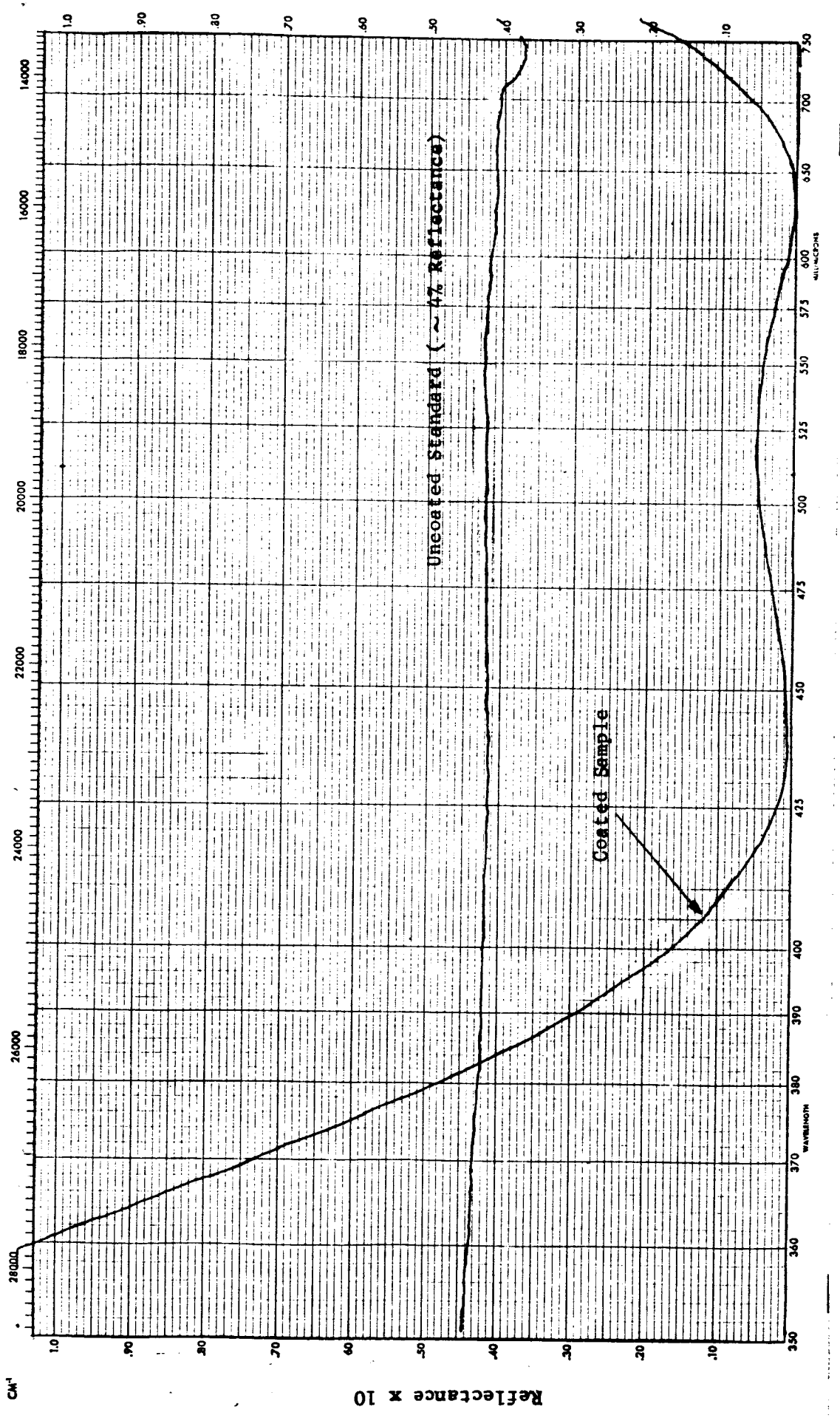

Figure 36. Reflectance vs. Wavelength Plot of Very-Low-Reflectance Coatings Applied to Transfer Lens.

Project; its transmittance characteristics are shown in Figure 37. The transmittance at 6328Å is on the order of 1 part in 10^5. At 4880Å and 5145Å the transmittance is seen to exceed 0.94. These remarkable properties are due to a specific design that enhances the transmittance in the blue without sacrificing attenuation in the red.

The SWPF design is additionally useful as a long-wave blocking filter in conjunction with a Fabry-Perot type spike filter such as may be employed for pre-detection filtering in the LCSE.

- Spike Filter With Enhanced Red Suppression: The receive channel is designed to incorporate a narrowband spike filter centered on one or both of the argon laser lines. This filter may be located immediately in front of the decollimating lens, L_2, and either be a substitute for or be used in conjunction with the SWPF.

  Dielectric spike filters of conventional design employ colored glass elements as blocking filters. As a result of "sandwiching" absorbent filters and dielectric substrates, optical quality and peak transmission tend to suffer.

  The LCSE spike filter will therefore be constructed from purely dielectric stacks. This approach has been successfully worked out and the transmittance plot shown in Figure 38 has been obtained by a design comprising four separate dielectric multi-layer stacks: a Fabry-Perot type multilayer to produce the principal narrow spike, a bandpass filter centered on the spike wavelength blocks the immediate side maxima of the spike and a long-wavelength blocking filter and a short-wavelength blocking filter are used. The remaining leakage of unwanted light in the wings and, in particular, the leakage at 6328Å is determined by the blocking filters. By incorporating the SWPF design for the long-wavelength blocking filter, the transmittance of the compound spike can be reduced to less that 10^{-7} at 6328Å. As shown by Figure 38, the half-width of one such all-dielectric spike filter is about 25Å and the peak transmission at 4880Å is 58 percent.

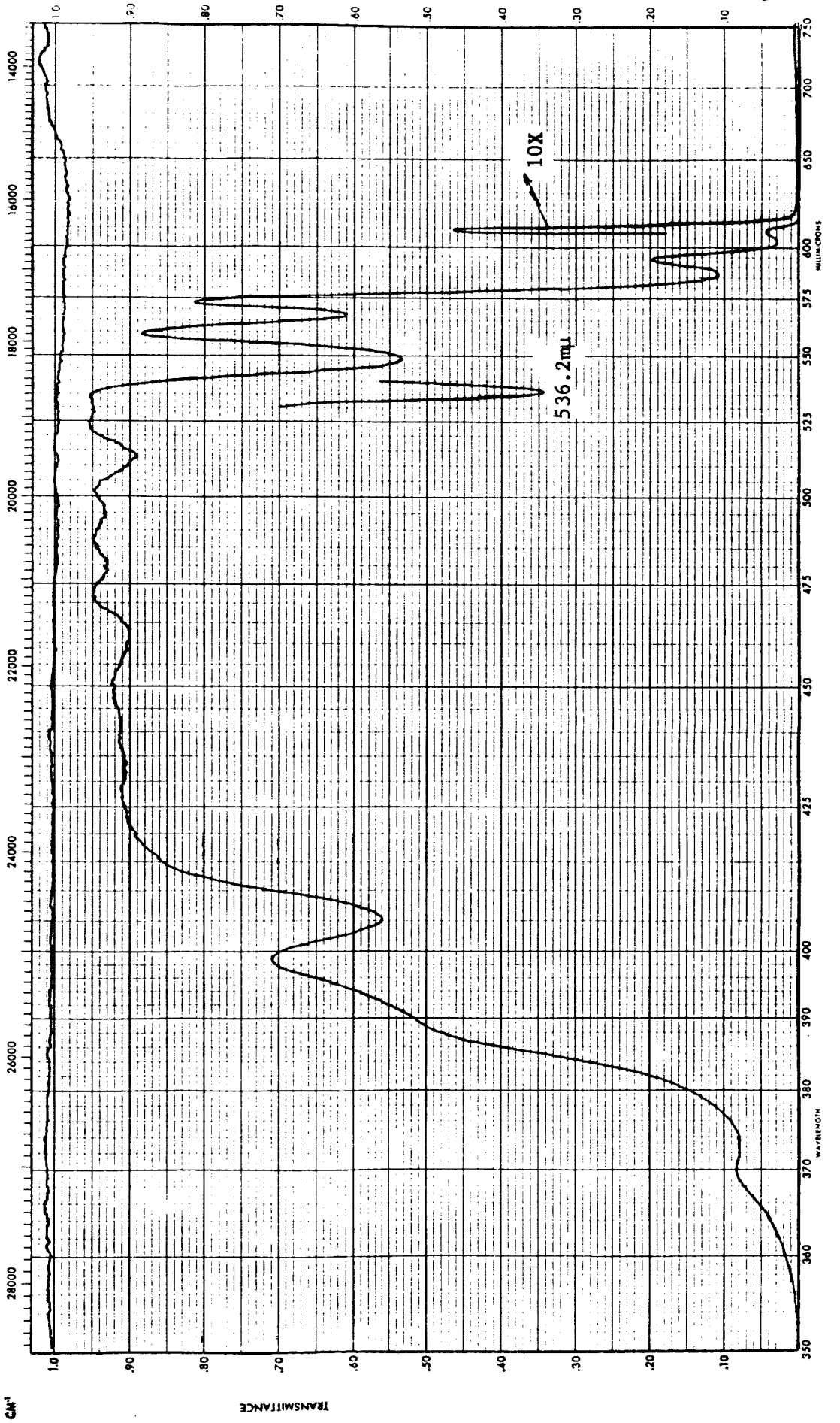

Figure 37. Transmission Spectrum of Short-Wavelength-Pass Filter.

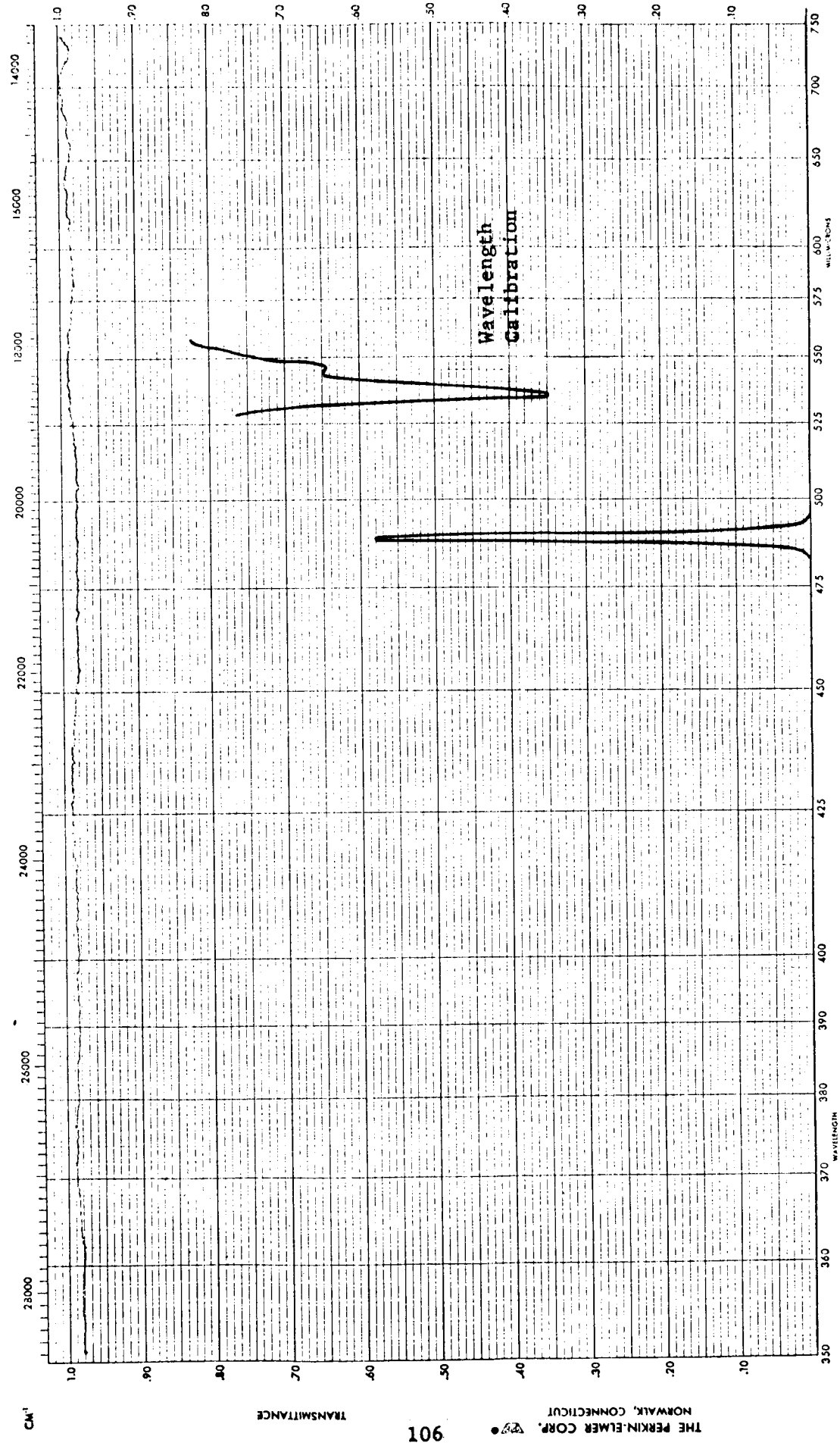

Figure 38.. Transmittance vs. Wavelength Plot of Special Blue Spike Filter.

Predetection Filter

A spike filter of somewhat narrower bandpass characteristics is needed for the LCSE. Its design must be compatible with the ±1.5 degree angle variation encountered in the fine-guidance region of the optical system. This limits the minimum width of Fabry-Perot type spike filter to about 3Å, and a width of 5Å allows for reasonable manufacturing and temperature tolerances. The 5Å width is fully consistent with photometry considerations in the LCSE.

The Fabry-Perot part of the predetection filter will either employ the traditional thin mica spacer or will use a thin fused-silica spacer constructed by the new technique outlined by Harriot.* Bandpass blocking and long and short wavelength blocking will be accomplished by the dielectric, multilayer designs described. Single-substrate construction will be used.

Channel Alignment and Transmit Beam Offset Considerations

It is assumed that system focus has been taken care of by the procedure outlined on page 32. The problem remains as to how alignment of the transmit channel with respect to the receive channel can be simply and accurately determined. Once mutual boresight has been established, it is necessary to provide a mechanism to point the transmit channel away from this reference. In particular the transmit beam must be offset from the receive line of sight by as much as 36 arc-seconds to make up for the transit time and Bradley effects over interplanetary ranges.

The best approach to the problem is the one that uses the least number of components. Consider Figure 39 which illustrates the layout of the two channels and imagine that we are looking into the beamsplitter in the direction shown. The condition of mutual channel alignment is when, from this point of view, an image of the equivalent f/70 laser source appears to be exactly coincident with an imaginary f/70 diffraction image centered on the apex of the image divider. Note that this is completely independent of the rest of the optical system. The telescope and transfer lens merely serve to magnify the diameter of a collimated axial bundle in the region of the beamsplitter 100 times, from about 4mm to 400mm (16 inches), and to demagnify ray angles in that region by the same amount.

There are two possible kinds of misalignment between the two channels; parallel displacement of the optical axes and angular misorientation of the axes. The first of these is illustrated in Figure 40 and results when the axis of the cone of diverging laser light in the transmit channel is not coincident with the axis of the cone of converging light with the receive channel. Since the receive channel axis coincides with the telescope axis, then in the presence of this defect some marginal rays of the transmit laser light are vignetted.

---

*Harriot, D.R., Filters, Wave Plates, and Protected Mirrors, 50th Meeting, Optical Society of America, Washington, D.C.

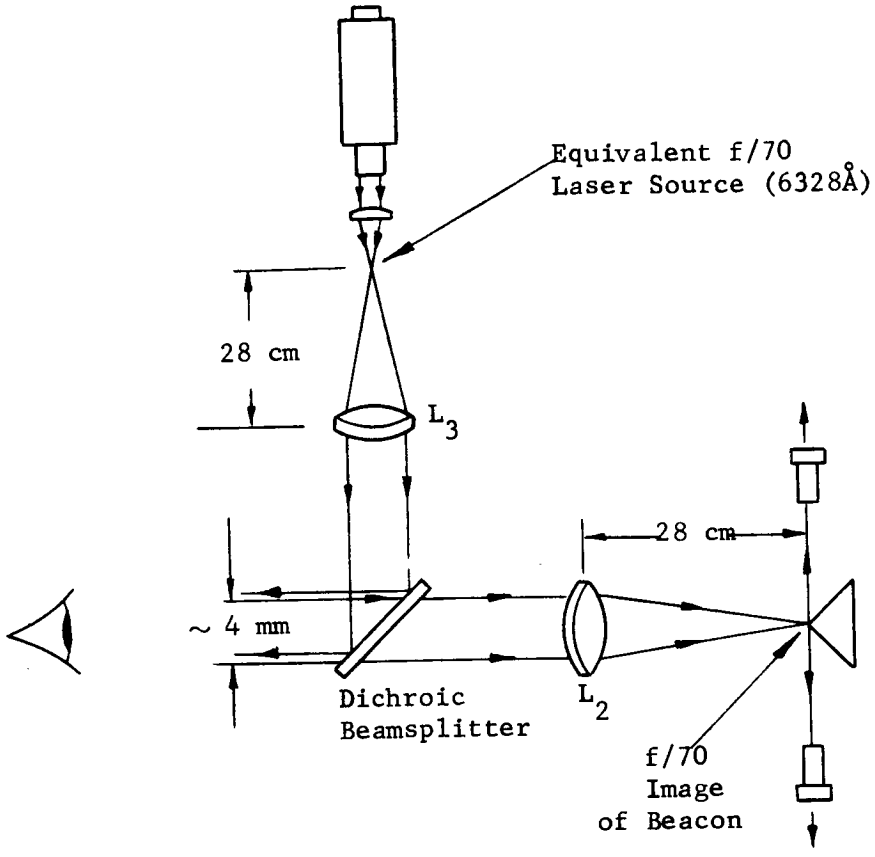

Figure 39. Basic Optical Elements for Channel Alignment Considerations

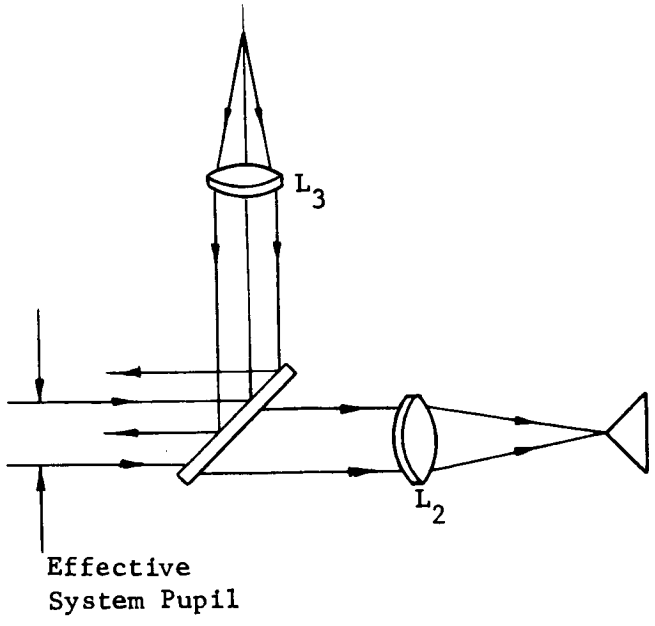

Figure 40. Illustration of Parallel Displacement of Channel Axes.

Since optional mapping of the laser output into the telescope aperture requires some truncation, a nominal amount of vignetting can be tolerated by the system. For example, if when merged by the beamsplitter, the axes of the two channels depart by say 5 percent of the 4mm axial bundle diameter, less than 5 percent of the transmitted light power will be lost through vignetting which is not too serious. Related back to a positioning tolerance on the laser, this means that the axis of the laser must be located to within a suitable fraction, say ±5 percent, of the output beam diameter. Typical He-Ne lasers have an output beam diameter of a few millimeters. Taking 3mm as an example, an appropriate positioning tolerance for the laser axis is ±0.15mm (±0.006 inch). This is a liberal mechanical tolerance and shows there should be no need for post-launch repositioning of the laser axis in a spaceborne optical communications system.

What about angular misalignment of the channels? Assuming the receive channel to be the reference once again, to an observer looking into the beamsplitter as in Figure 39 this defect causes the image of the transmit laser source to form off center with respect to the apex of the fine-guidance image divider. If this relative image displacement equals the diameter of an f/70 diffraction disc, then the transmitted beam will be mispointed by an amount equal to the diffraction cone angle of the primary mirror if the system is diffraction-limited. Back on the earth the center of the beam will miss its mark by one full beam diameter. Smaller misalignments will have correspondingly smaller effects and less important consequences.

As a reasonable tolerance for this form of misalignment, let us demand that the transmitted cone of light shall be pointed with an absolute accuracy of ±10 percent of the cone angle.

To the observer of Figure 39 this means that the center of the equivalent f/70 transmit laser image must lie in a circle that is centered on the apex of the image divider and that has a radius of 10 percent of an f/70 diffraction-limited image. Assuming the image diameter to be equal to the diameter, D, of the first dark ring of the Airy pattern, which is given by the formula

$$D = 2.44 \lambda f$$

where λ is the wavelength of operation and f is the final f-number of the system, the image position tolerance amounts to ±0.011mm (±0.0004 inches). This is also the lateral positioning tolerance of lens L_3 shown in Figure 39 and in Figure 6. An equivalent statement is that the axis of the transmit laser beam must be oriented with an angular accuracy given by the ratio of ±0.011mm to the focal length of L_3, which in our case in 250mm. The angular tolerance is therefore 4.4×10^{-5} radians (9.5 arc-seconds). (Note that this corresponds to about 1/10 arc-second on demagnification by the 16-inch aperture telescope.)

The post-launch alignment tolerance of ±9.5 arc-seconds in the general region of the transmit channel possible can be met by rigorous mechan-

ical design alone. However, fairly long optical pathlengths are involved as are components of substantial mass (such as the laser itself).

These factors may unduly complicate the problem of space qualification of the system and are likely to necessitate some form of backup post-launch alignment equipment. The same equipment is needed in any event to perform the important diagnostic function of measuring, on ground command, whether the channels are aligned correctly.

Technique

An attractively simple technique to measure, and therefore to readjust, the relative angular alignment of the two channels becomes feasible as a fortunate consequence of using the channel separation technique developed in NAS8-20115. Only one additional optical element is required - in this case a cube-corner prism. Advantage is taken of the residual sensitivity of the receive channel to light originating from the transmit channel. This technique is illustrated in Figure 6 and is planned for the LCSE.

The cube-corner prism is located in the unused region behind the dichroic beamsplitter and is ordinarily blocked by a retractable shutter. When the shutter is withdrawn, the small amount of collimated transmit laser light passed by the beamsplitter is reflected directly into the receive channel. This light is further attenuated by the predetection spike and/or SWPF and the remainder converges to a focus at or near the apex of the image divider. If the additional attenuation is only as much as dictated by the channel separation requirements, then the image will be bright enough so that its position can be measured by the fine-guidance photomultiplier. To the extent indicated by such a measurement, the image can then be centered by a lateral translation of lens L_3 or alternatively by means of the Risley prisms.

Methods for Offsetting the Transmit Beam

The same optical or mechanical elements that are used to make the axis of the transmit channel collinear with the receive channel are used to offset the transmit beam and compensate for Bradley and transit time effects. The amount and direction of forward bias can be controlled by either

(1) translating the transmit laser collimating lens, L_3, in its plane or,

(2) manipulating a pair of Risley prisms situated between this lens and the dichroic beamsplitter.

The lateral motion required in the current breadboard system* by (1) is about 0.0004 inches per 1/10 arc-second of post-telescope beam offset. The angular

*NAS8-20115, Loc. Cit.

deflection required by (2) amounts to about 10 arc-seconds at the Risley prisms to offset the beam transmitted by the telescope by 1/10 arc-second. The transmitted beam can be offset 30 arc-seconds by translating L_3 0.12 inch, or by wedging the optical path with the Risley prisms, by 50 arc-minutes.

By either method, the zero bias reference is the lens position or the Risley prism adjustment determined by the initial channel alignment procedure.

Risley Prisms for Point Ahead

The accuracy required for the mechanization of the Risley Prism Point Ahead Subsystem has been developed for LCSE by error analysis. The results of the error analysis indicate that the main roll error contributions are due to gearing between the Risley prism elements and their associated angular position sensors, and due to conversion errors associated with changing digital input commands to shaft rotation form. For the assumed conditions, an algebraic summation of roll error indicates a 0.094 arc-second transmitter line-of-sight error at a maximum point ahead angle of 50 arc-seconds. At smaller point ahead angles, the line-of-sight errors are (not quite proportionately) less. In contrast, the variation of expected transmitter LOS error is nearly independent of offset angles between 15 and 165 degrees. It should be noted that errors, in actual practice, will be less since peak additive errors do not occur simultaneously except for a vanishingly small statistical probability.

The Risley prism servo system is shown in Figure 41. The arrangement features two data conversion units to convert ground commands of point ahead from digital to analog form and a servo to drive each Risley prism element. Also shown is the two-axis, servo driven Sun Tracker whose output error signals control spacecraft pointing during the beacon search roll maneuver, and which tracks the sun during beacon track while providing ATM roll compensation signals to the Risley prism elements. Operation of this subsystem is described below.

During alignment, the zero ground point ahead information is transmitted and the Sun Tracker is used to obtain zero position of the cross offset gimbal axis. This operation removes vehicle roll information inputs to the Risley prism subsystem.

The error signals produced by the tracking photosensor (6328Å reflected from the corner cube in Figure 6) are sent to the ground via radio link. The ground operator then controls the point ahead information commands to obtain an alignment condition as indicated by a reduction of the tracking error signals to zero. The resulting ground commands store the in-flight optical alignment errors for future use. Later in the operation, the point ahead requirement will be modified by this stored information. For acquisition, the sun will be acquired by the Sun Tracker. The Sun Tracker is next offset by slowly introducing the proper ground offset angular command and the roll search maneuver is executed until the telescope 1 degree field acquires the

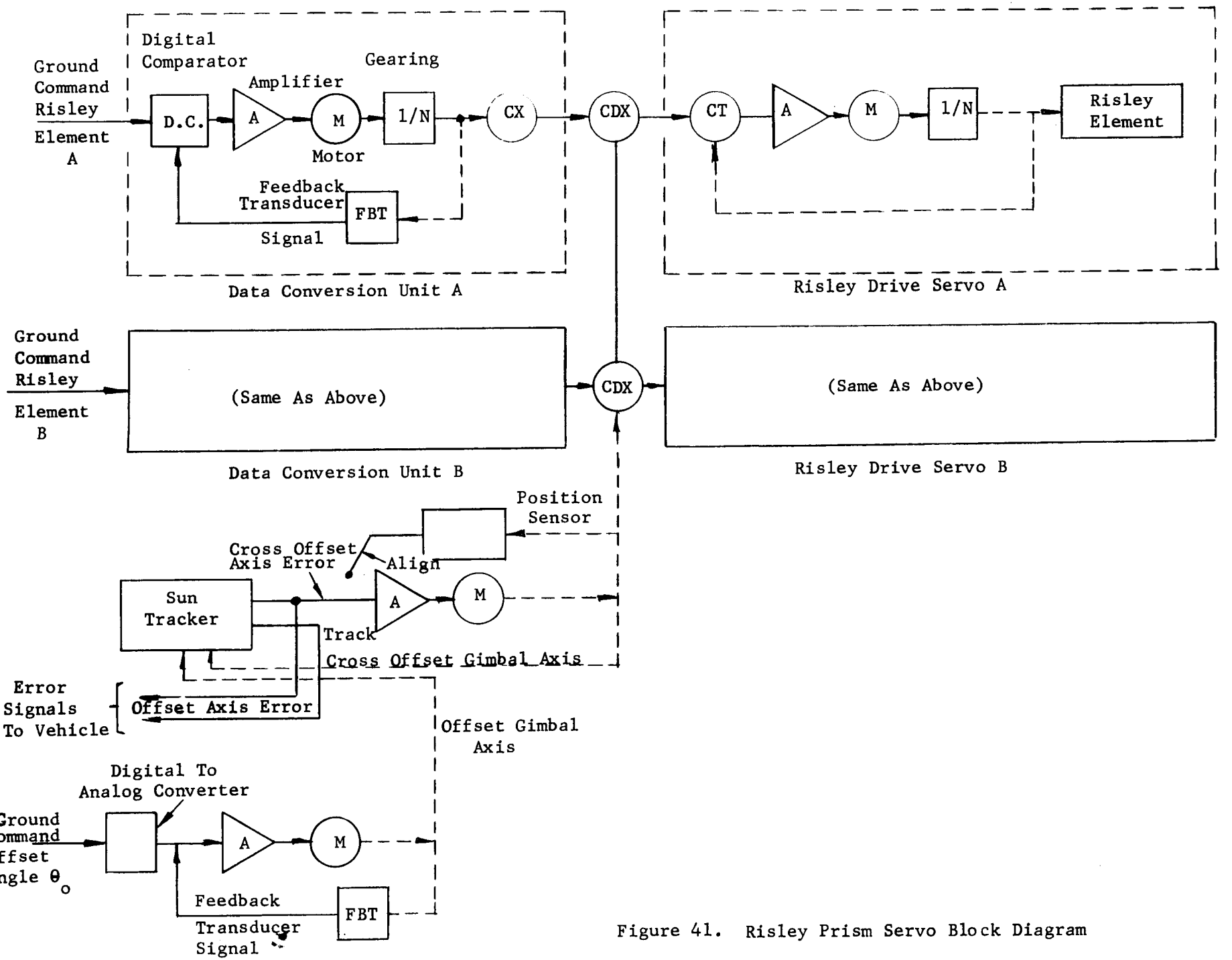

Figure 41. Risley Prism Servo Block Diagram

beacon. During subsequent beacon tracking, the ground commands still control the Sun Tracker offset angle* while the Sun Tracker nulls its cross offset axis error signal by driving this axis. Since the Sun Tracker axis is chosen parallel to the telescope's line of sight, the angular deviations of this axis are equal and opposite to the vehicle roll errors and can be used to correct the Risley prism.

Each Risley prism element is separately driven to an angle corresponding to that required by the control transmitter (CX) in the associated command conversion unit. The vehicle roll angle correction is introduced to both elements via the two control differential transmitters (CDX) whose mechanical input is from the Sun Tracker's cross offset gimbal axis.

The sources of error in this system include the following:

Beacon Tracking Error Effects

Sun Tracking Error Effects

Risley Prism Positioning Errors

Alignment Correction Errors

Point Ahead Scale Factor Errors

Ground Computation Errors

Sun Tracker-Telescope Alignment Errors

Consider the magnitude of the roll error from the first two items listed above. Refer to Figure 42. The roll error due to beacon tracking errors can be expressed** as

$$E_B = \frac{.61\lambda_B}{D_T}\left(\frac{S}{N}\right)^{-1} \cot \phi_o = \Sigma_T \cot \phi_o$$

where λ_B is beacon wavelength

D_T is the telescope aperture diameter

$\frac{S}{N}$ is the signal-to-noise ratio corresponding to the telescope servo equivalent noise bandwidth, and ϕ_o is the angular subtense between the sun and the beacon as seen at the vehicle (i.e., offset angle).

and Σ_T is the beacon tracking error.

*An alternate procedure could have the orientation controlled by nulling the Sun Tracker offset axis error signals.

**This expression is derived in Engineering Report 8387.

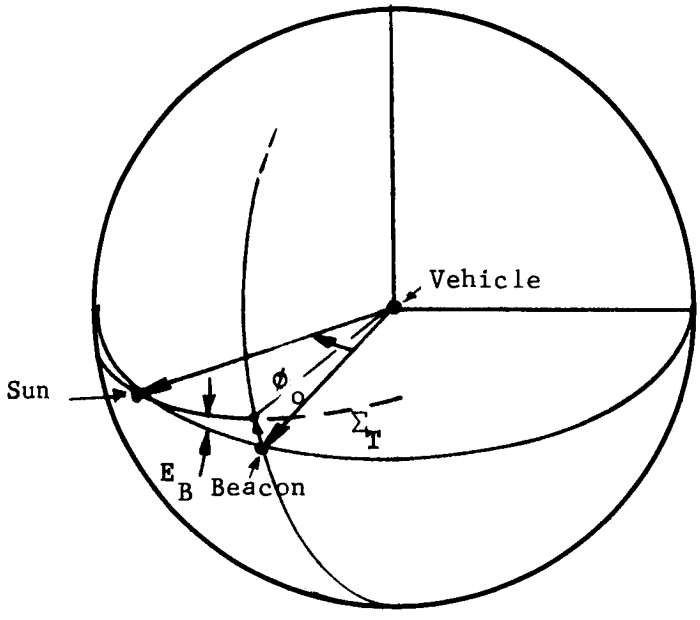

Roll Error E_B is Introduced
by Beacon Tracking Error Σ_T

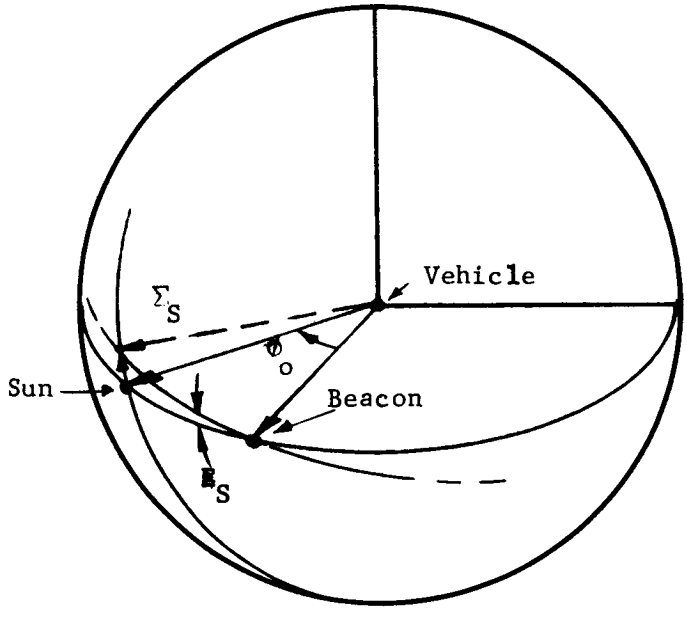

Roll Error E_S is Introduced
by Sun Tracking Error Σ_S

Figure 42. Geometry for Roll Error Caused by Tracking Error

Figure 43 indicates that the roll error induced by a 0.1 arc-second beacon tracking error is very small over a wide range of ϕ_o.

Figure 43 shows the roll error due to a sun tracking error, Σ_S, of 5 arc-seconds (this corresponds to the Sun Tracking accuracy specification of the AOSO vehicle). This curve was developed from the expression*

$$E_S = \Sigma_s \frac{1}{\sin \phi_o}$$

The curves indicate that beacon tracking induced errors are negligible and that solar tracking induced errors, for the assumed conditions, approach 1/2 arc-minute at a 10 degree offset angle. At 15 degrees, which is a conservative estimate of the minimum offset angle, the error will be nearly 1/3 arc-minute.

Risley prism positioning errors are predominately due to data conversion errors, CX-CDX-CT chain error, and gearing errors between the prism elements and the CT sensors. Taking a data conversion error of 1 arc-minute, 40 arc-seconds error for a chain of Kearfott size 15 type CT9-09 units, and 1.5 arc-minutes** of gearing error leads to a maximum prism element positioning error of nearly 3 arc-minutes.

The prism point ahead magnitude errors due to these angular positioning errors can be obtained from the expression (refer to Figure 44).

$$\delta = 2\,\delta_1 \cos\frac{\beta}{2} \triangleq 2\,\delta_1 \cos\gamma$$

where δ is the prism induced angular beam deflection

δ_1 is the deviation of each prism

and β is the angle introduced between the prisms with $\beta = 0$ corresponding to prism alignment to maximum deviation.

Maximum angular deviation errors due to incorrect β inputs can be found by differentiating, i.e.,

$$\frac{d\delta}{d\beta}\Delta\beta\Big|_{max} = -2\,\delta_1 \left(\sin\frac{\beta}{2}\right)\frac{\Delta\beta}{2}\Big|_{max} = -\delta_1 \left(\sin\frac{\beta}{2}\right)\Delta\beta\Big|_{max} = -\delta_1\,\Delta\beta$$

---

* Perkin-Elmer Engineering Report 8387

** Systematic errors can be determined prelaunch and calibrated out.

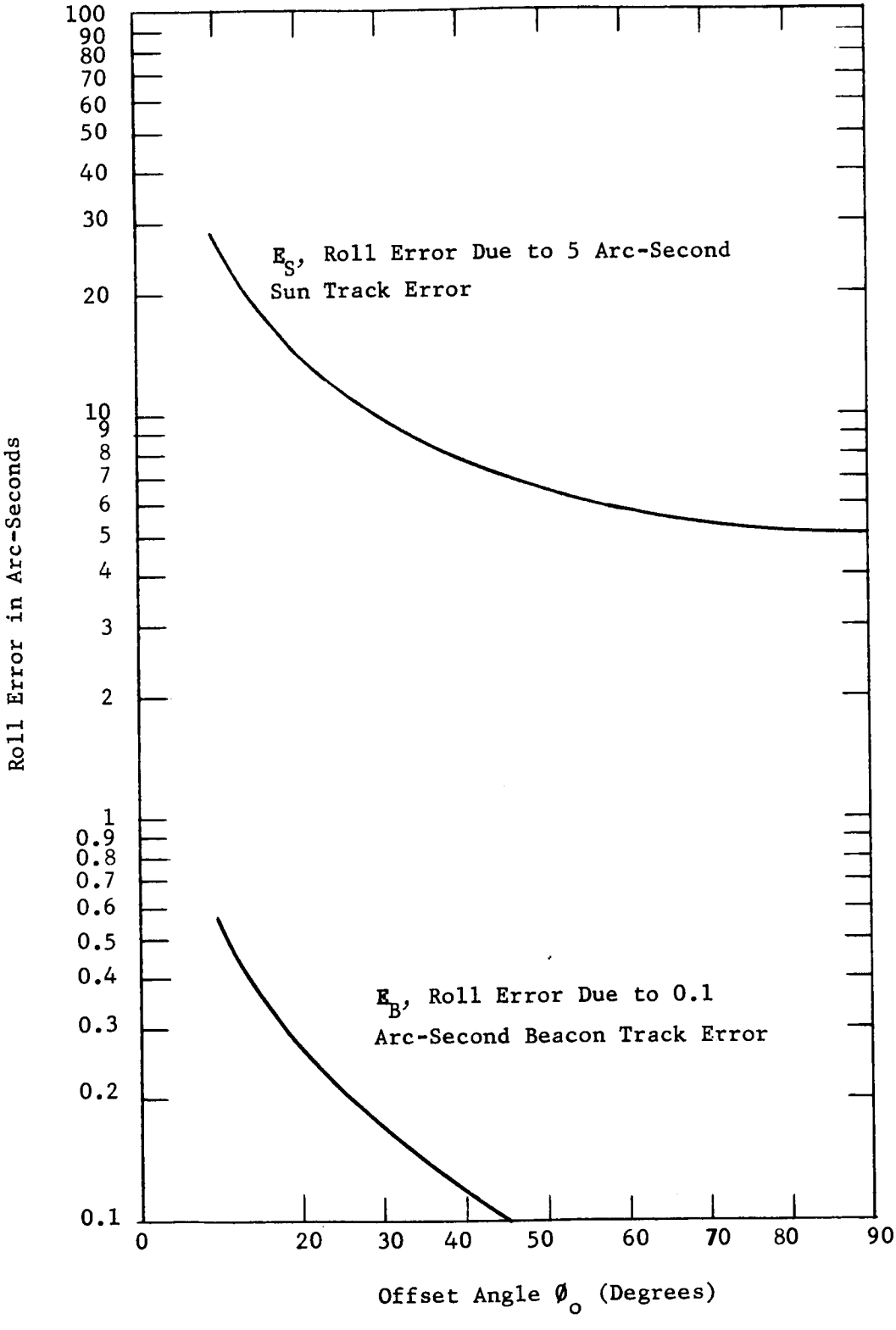

Figure 43. Roll Errors Due to 0.1 Arc-Second Beacon Tracking Error and 5 Arc-Second Sun Tracking Error as Functions of Offset Angular Magnitude

Assuming that the Risley device must have a range of 50 arc-seconds (equivalent LOS angle) then δ_1 must be 25 arc-seconds and, hence, the magnitude of prism deviation error due to β errors is given by the relation

$$\frac{d\delta}{d\beta} = 25.0 \frac{\text{arc-seconds}}{\text{rad}} = .00728 \frac{\text{arc-seconds}}{\text{arc-minutes}}$$

Prism point ahead angular errors due to angular positioning errors, assuming both prisms driven together, will be equal to the angular positioning errors; i.e.,

$$\left(\frac{\text{1 arc-minute point ahead direction error}}{\text{arc-minute error in prism rotational orientation}} \right)$$

Hence, if both elements are in error by 3 arc-minutes in the same direction, the point ahead direction will be in error by 3 arc-minutes. On the other hand if the directions of the error oppose, a point ahead magnitude error of .044 arc-seconds will result. (Refer to Figure 45). A similar analysis can be performed to estimate the errors involved in determining initial alignment errors.

Let it be assumed that a 1-arc-second alignment error exists and requires a setting of

$$\delta \triangleq 1 \text{ arc-second} = 2 \delta_1 \cos \frac{\beta}{2}$$

or

$$\frac{\beta}{2} = \cos^{-1} \frac{1}{50}$$

$$\frac{\beta}{2} = 88.9°$$

The deviation error due to β error is given by

$$\frac{d\delta}{d\beta} \Delta\beta = -\delta_1 \left(\sin \frac{\beta}{2} \right) \Delta\beta \doteq -\delta_1 \Delta\beta$$

Hence magnitude error can be expressed as before by 0.00728 $\frac{\text{arc-second}}{\text{arc-minute}}$ while angular error can be expressed by 1 $\frac{\text{arc-minute}}{\text{arc-minute}}$.

The alignment magnitude correction can be determined within an error of 0.044 arc-seconds with a direction error of zero under one extreme set of circumstances. Under the opposite extreme, the magnitude will be correct but the direction will be in error by 3 arc-minutes. This can result in a roll error under point ahead conditions which varies with θ_p but is equivalent to a 0.044 arc-second transmitted LOS error (see Figure 46).

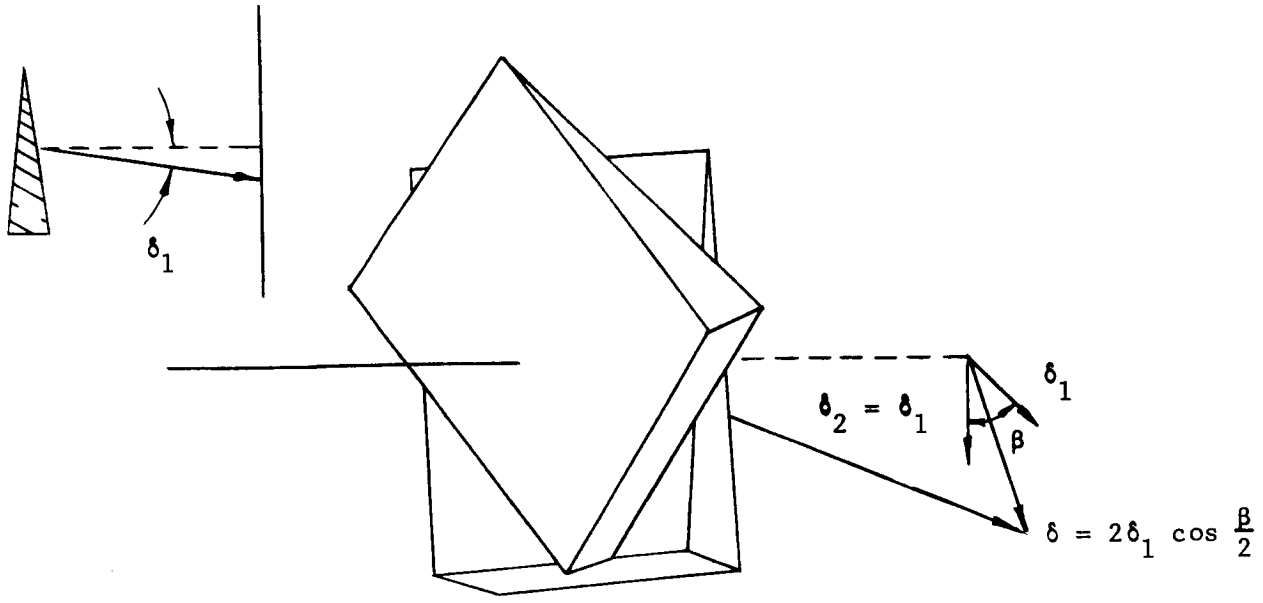

Figure 44. Risley Prism Action

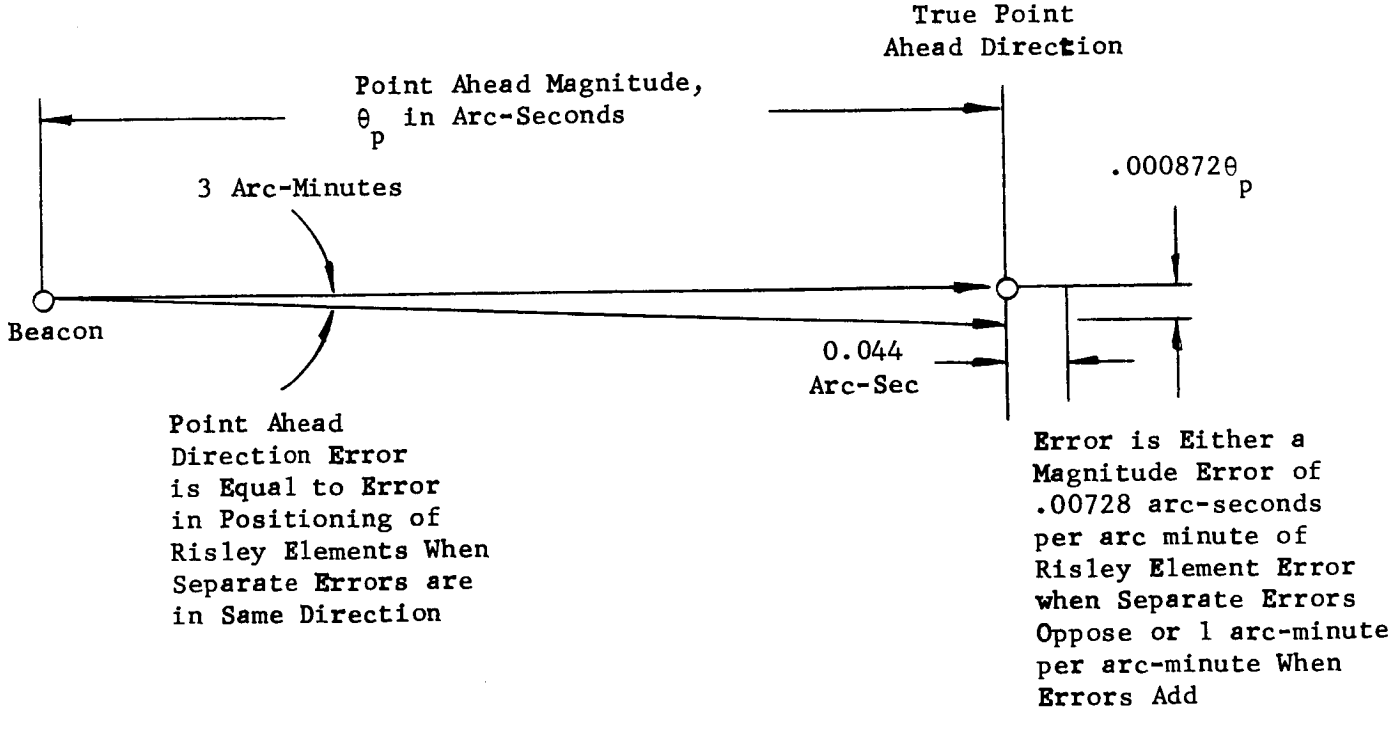

Figure 45. Roll Error Due to Risley Prism Element Angular Positioning Error

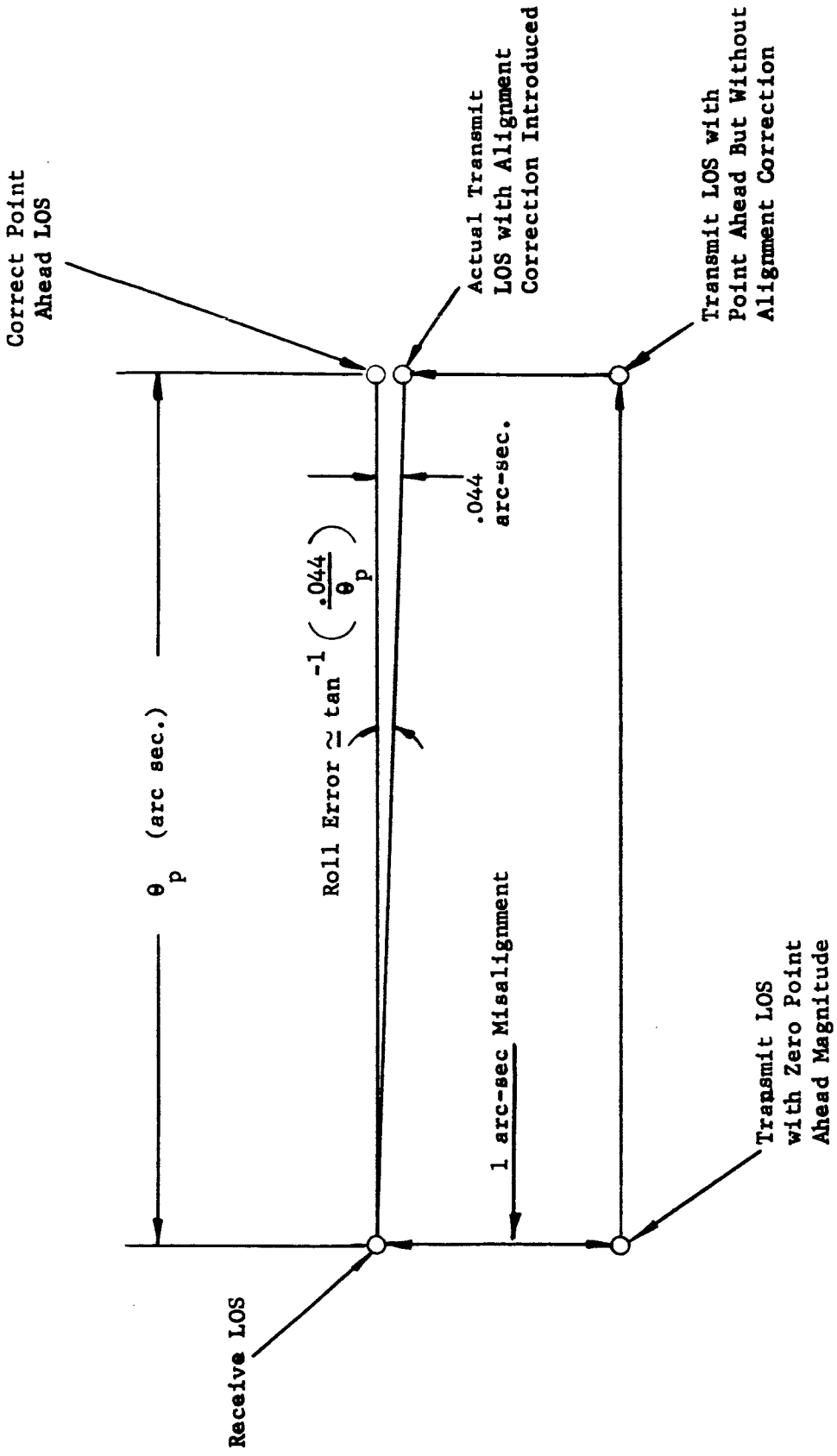

Figure 46. Geometry for Roll Error Due to Misalignment

Point ahead scale factor error arises because the Risley-prism-produced beam deviations do not result in equal line-of-sight deviations; i.e., the transmitted line of sight will be deviated angularly by an amount equal to the Risley prism deviation times the ratio of the transfer lens focal length to the "primary-secondary mirror combination" focal length. While the optical system can be calibrated prelaunch at any given temperature to determine the focal length ratio and therefore the Risley prism scale factor, operation aloft involves temperature differences between optical elements. The amount of scale factor change due to temperature differences is expected to be small. For example, if the primary and secondary mirrors differ by 10°C from the other optical elements, the change in focal length ratio will be in the order of .01%; i.e.,

$$\Delta (fl) = \alpha \Delta T \ (fl)$$

where

α is the temperature coefficient of expansion of the optical elements (assumed as 10ppm corresponding to quartz)

ΔT is temperature difference

and

fl is nominal focal length.

Hence

$$\frac{\Delta fl}{fl} = 10°C \times 10^{-5} \ P/°C = 10^{-4} = 0.01\%$$

This means that a 50 arc-second Risley prism produced point ahead magnitude will be in error by only 0.005 arc-seconds. This value is small enough to introduce negligible roll errors; viz, a 1 arc-second misalignment will be subject to $\pm 10^{-4}$ arc-second scale factor error. Under a 50 arc-second point ahead command, the resulting roll error could be as large as

$$\frac{10^{-4}}{50} \times 57.3 \times 60 = 0.00687 \text{ arc-minutes}$$

Focal length ratio changes associated with removal of "g" loading will be evaluated by calibration procedures performed in the early part of the LCSE flight. No attempt has been made to evaluate ground computation errors since these can be small compared to the errors listed above. Moreover, the Sun-Tracker alignment errors are considered as detectable and correctable during initial operation at short ranges.

Table VIII summarizes the sources of error and indicates the assumed conditions and the resulting roll error contributions.

The total error can be expressed in terms of vehicle transmitted beam pointing error due to roll error; i.e., if θ_p is the point ahead magnitude in arc-seconds, then the transmitted line of sight will have an error of approximately:

$$\leq \left[0.044 + \frac{3.4 \ \theta_p}{57.3 \times 60} \right] \text{ arc-seconds}$$

TABLE VIII

ROLL ERRORS

SOURCE	ASSUMPTION	ROLL ERROR CONTRIBUTION
Beacon Tracking Error	0.1 arc-second* beacon tracking error	0.4 arc-second
Sun Tracking Error	5 arc-seconds sun** tracking error	< 1/3 arc-minute
Risley Prism Element Positioning		
A. Data Conversion	1 arc-minute conversion accuracy	
B. Synchro Chain	40 arc-seconds error in chain	
C. Gearing Between Element and Assoc. Synchro	1.5 arc-minute gearing error	
Sub Total . . .	3 arc-minute/element	3 arc-minutes/both elements
Alignment Determination Error	1 arc-second alignment correction required	$\left[\tan^{-1}\frac{0.044}{\theta_p}\right.$, where θ_p is point ahead magnitude in arc-seconds.$\left.\right]$
Point Ahead Scale Factor Error	Primary and secondary mirrors 10°C different from rest of optics.	Does not introduce significant roll errors
Ground Computation Error	(Assumed negligible)	
Sun-Tracker-Telescope Alignment Error	(Assumed removable)	
	Total Roll Error in arc-minutes	$\simeq\left[3.4 + \left(\tan^{-1}\frac{0.044\sec}{\theta_p}\right)(57.3\text{x}60)\right]_{\text{max.}}$

*At a 15 degree offset angle; errors will be less at greater offset angles.

**Assuming removal of systematic errors.

which is shown in Figure 47 as a function of θ_p. It is seen that alignment determination error (0.044 arc-seconds) predominates when point ahead magnitudes are small, while for large point ahead magnitudes, Risley prism position errors become significant.

Adjustable Field Stop Mechanism

The field of view or the receive channel can be restricted by the variable aperture illustrated in Figure 6. The actual mechanism can consist of a motor-driven iris diaphragm and should be located as close as possible to the f/70 focal plane. The design must be fail-safe in the sense that in case of component malfunction a spring can be triggered to open the diaphragm permanently to its maximum size. The maximum opening is determined by the diameter of the 2-minute field at f/70, which amounts to 0.65 inches. To restrict the FOV to 10 arc-seconds minimum, the corresponding minimum opening is 0.054 inches.

Laser Coupling Optics

It is useful to consider techniques for maximizing the energy in the central portion of the far field pattern. One can map the intensity distribution at the output of the satellite laser assumed radiating in a dominant single transverse TEM_{oo} mode, into a more efficient intensity distribution in the far field. Such a mapping may be accomplished by using aspheric elements*. These elements allow one to transform a given phase and amplitude distribution from a coherent light source into any other phase and amplitude distribution with minimum energy loss as long as the principles of geometric optics can be applied.

It is recommended that further work be done to establish the details of such a mapping implementation. This will consist of first determining the Fraunhofer pattern for a circular Gaussian field restricted by an annular transmitting aperture, and then determining the far field pattern obtained by the optimal energy and phase laser light redistribution technique.

Beam Spoiling Component

The purpose of this subsystem is to widen the transmitted beam from the 0.1 arc-second diffraction limit to a width of several arc-seconds. This operation is necessary as a backup to the point ahead subsystem.

---

* Kreuzer, J., "Laser Light Redistribution in Illuminating Optical Signal Processing Systems", Ch. 22 of "Optical and Electro-Optical Information Processing", M.I.T. Press, 1965.

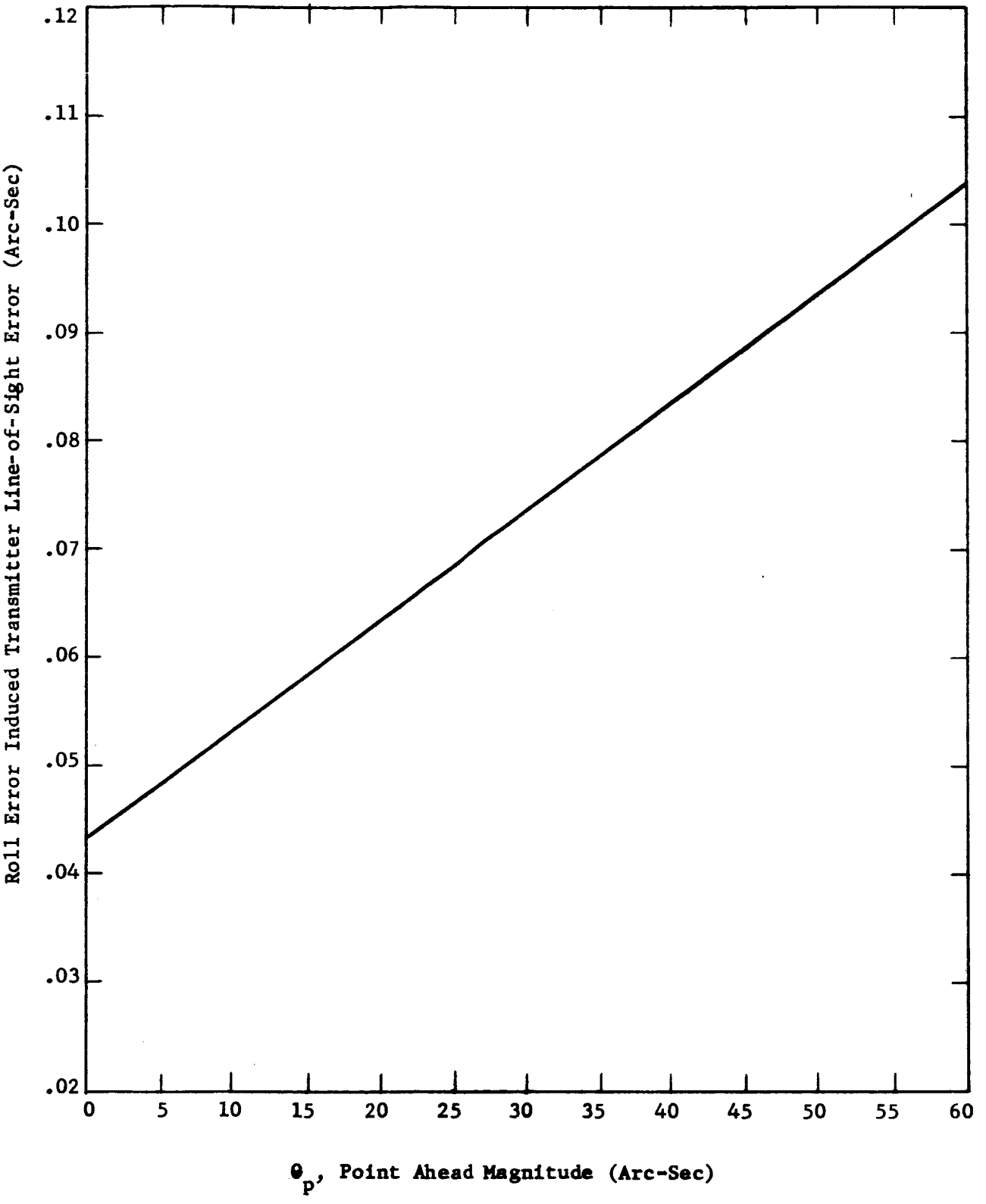

Figure 47. Transmit Laser Pointing Error Due to Roll Error as a Function of Point Ahead Magnitude

The technique chosen is to vary the separation between two similar lenses with coincident focal points. This approach was chosen because of the following reasons:

- The distances to be moved for the focal lengths chosen are of the right magnitude for existing types of position servomechanisms.
- This type of system can readily be made to require zero power for any stationary lens setting.
- Since the component is located in a region of a small pencil of collimated light, the surfaces can be spherical without introducing significant aberrations.

A diagram is shown in Figure 48 along with the equation relating the beam bending, interlens spacing, and the radius of collimated bundle. However, the deviation of the transmitted beam is about a factor of 200 less than this because of the demagnification of the telescope. For the parameters listed in Figure 48 the result is:

$$\text{Beam divergence} = \frac{2\alpha'}{200} = \frac{2\left(1.6 \times 10^{-2}\right)}{200} dt'$$

$$= 1.6 \times 10^{-4}\ dt' \text{ rad}$$

$$\Delta\theta = \frac{1.6 \times 10^{-4}}{0.5 \times 10^{-5}} dt = 32\ dt' \text{ (seconds)}$$

where

dt' = measured in millimeters.

For spoiling to 3 arc-seconds (approximate amount of point ahead) it would require moving the lens about 0.1 mm from the nominal 5 cm spacing.

Wollaston Prism

To achieve redundancy in the transmit laser, two independent systems are incorporated. The only problem with using two lasers is to combine their output beams along the same optical axis. If this were accomplished by partial reflection (i.e., beamsplitter) it would result in a 50 percent power loss since, ideally, only half the power travels in the desired direction. The approach used in the LCSE program is to mount the lasers in the structure so that their beams are incident at the proper angles with orthogonal polarizations on a Wollaston prism. Wollaston prisms are generally used to split

an unpolarized beam into two components with orthogonal polarizations; obviously they can be used for the reverse purpose. The angular separations of the incident beams depend upon the prism design and are typically tens of degrees. Since the prism requires each of the incident beams to have a specific plane polarization, the modulation must take place further along the transmitter channel. This technique is highly efficient and results in a few percent loss which is included in the overall system loss calculations.

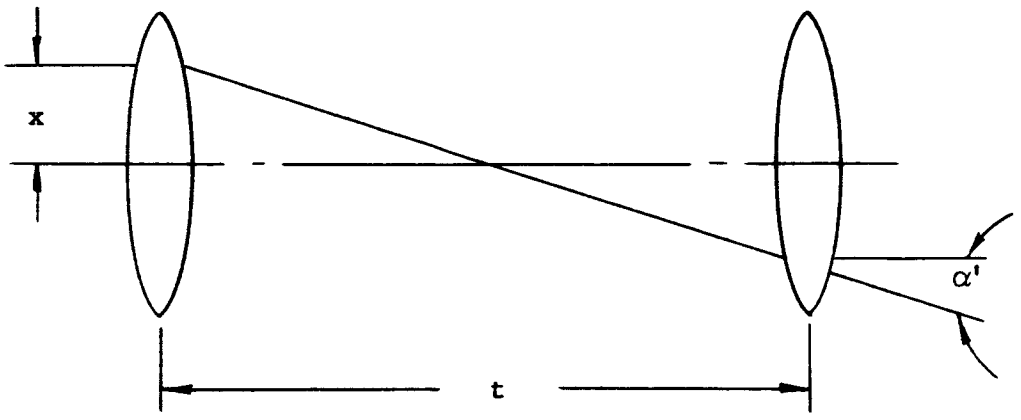

$$\frac{d\alpha'}{dt} = \frac{4x}{t^2}$$

x = Radius of Collimated Beam = 1 mm

t = 5 cm (2.5 cm Focal Length Lenses)

Figure 48. Optical Layout for Beam Spoiler

LCSE LASER SELECTION

The selection of the laser itself is a particularly difficult task because of the rapid change in laser technology. It is almost certain that by the anticipated launch date of 1969 the laser system selected at this time will not be optimum. However, ground rules for choosing the laser system were formulated:

- The LCSE laser must have sufficient power to collect engineering and scientific data for space optical communication from synchronous altitude (23,000 miles).
- The LCSE laser must be within the state of the art of laser technology today (1966).
- The LCSE laser must be suitable for space qualification, and have a two-year operational life in space.
- It must represent an optimum choice in terms of systems requirements including: weight, power, cooling, and detectability (wavelength).

The laser candidates considered for the LCSE are:

Helium-Neon

This laser oscillates in many wavelengths; the principal ones being 6328A, 1.15μ, and 3.39μ. The 1.15μ transition and the 3.39μ transition both have higher gains than the 6328Å. However, S-20 photomultipliers operating with 6328Å offer a relatively high quantum efficiency (8 percent). For an S-1 photomultiplier operating at 1.15μ, the quantum efficiency is lower by a factor of 40 and detectors at 3.39μ are even worse. Power outputs for single frequency systems are typically 0.5 milliwatt and can be 100's of milliwatts for multifrequency, single spatial mode lasers. The output is diffraction-limited, and heterodyning experiments can be done with the laser. Since the active plasma is a low-pressure discharge, these lasers have long and stable operating lifetimes. The cooling and power requirements are modest and the laser lends itself to space qualification. Calculations have shown that this laser has sufficient power for high data rate communication from synchronous altitude, but the laser power becomes the key limitation for deep-space missions using helium-neon laser transmitters.

Argon

The argon laser system operates in many wavelengths also, the principal ones being 4880Å and 5145Å. The advantages of an argon laser are the high output powers (typically 1 to 10 watts) and the high quantum efficiency of detectors in this part of the spectrum (typically 20 percent). The output from this laser is diffraction-limited and operation in single spatial mode is common. The argon laser suffers from several disadvantages for use in space,

which do not preclude its use as a ground-based beacon. First is its poor efficiency (typically 0.1 percent) and high threshold power requirements. Threshold input powers for typical tubes are on the order of a kilowatt. Second, the high current densities in the active region require liquid cooling for CW operation. Associated with the high current discharges are problems of gas clean up and bore erosion which limit the life of a sealed system to below 100 hours.

Carbon-Dioxide

The striking characteristics of these lasers are the very high efficiencies (up to 40 percent), and high output powers available (in excess of 100 watts CW). The radiation is at 10.6μ and there is a severe shortcoming in a 10μ laser communication system. The problem is the lack of a wide bandwidth (megacycle) detector at this wavelength. Megabit modulators at 10μ are also a problem in today's technology. To achieve the high efficiencies reported for CO_2 lasers, they must, at present, operate with gas flow systems (undesirable in a space system).

Gallium-Arsenide

The output frequency of this laser is a function of temperature and varies between 8400Å at 77°K and 9000Å at room temperature. Its efficiency is in excess of 50 percent and solid structure would lend itself to space qualification. There are, however, several disadvantages to the gallium-arsenide laser which make it undesirable for space communication at this time. First, at CW power levels, there is a wavelength variation due to temperature. This prohibits use of extremely narrowband optical filters. Quantum efficiency of detectors at 8400A is only 0.4 percent. Also, the gallium-arsenide laser has a very small rectangular radiating aperture. This would require more complex cylindrical optics for achieving diffraction-limited performance of the radiating aperture. A most attractive feature of the diode laser is the ease of modulation by modulating the diode current. However, until improvement is made in the control of wavelength, this system is not considered a sound choice for this mission.

Ruby

Ruby crystal lasers have been operated CW with water cooling at 6940Å. The efficiency of the laser is about 3 percent and input power levels are on the order of 1 kilowatt. Detector efficiencies at this wavelength are typically 2.5 percent. Ruby requires optical pumping and the laser subsystem would be fairly complex. For these reasons ruby is not considered a good choice for space communications.

Neodymium in YAG

This solid laser has been operated CW with output powers of 200 watts. It has also been operated CW with sun pumping with an output of 1 watt. The output wavelength is 1.06μ and the best detectors at this wavelength have quantum efficiencies of 0.1 percent. The efficiency of this laser is about

5 percent with selective pumping and 0.01 percent when solar pumped. It requires liquid cooling and operates at room temperature. The output wavelength is a function of temperature and the output spectrum is several angstroms wide. Because of these problems, it is not considered a good choice for the LCSE.

LCSE LASER SELECTION SUMMARY

To perform the optical communication experiments from synchronous orbit and utilize techniques applicable for deep-space mission, the helium-neon single frequency laser appears to be the best choice at this time. This choice is based on several factors:

- Helium-neon is the best developed of all laser systems. To build a space qualified laser will require new engineering design, but little fundamental investigation.
- The low-pressure gas discharge has an inherent long life and reliability. The small amount of heat developed (about 5 watts) can easily be dissipated by radiation cooling.
- By employing a phase-locked laser system on the ground it will be possible to perform a heterodyning experiment with no additional components in the spacecraft. This experiment sets the single frequency requirement.
- As new laser systems are invented and existing lasers and detectors are improved, future missions will be able to employ them without changing the basic system. This allows the data and experience of this mission to be applied to the design of future deep-space missions.

THE LASER MODULATOR

The selection of an LCSE modulator to be used with the helium-neon laser represents a compromise between several alternatives each possessing special advantages. The basic ground rules for choosing this component were:

- It must be suited for use in a PCL/PM communication system with a helium-neon laser.
- It must be of sufficient optical quality (both homogeneity and surface finish) so as not to degrade the diffraction-limited performance of the optical system.

- It must be compatible with the entire system and represent an optimum choice in terms of: weight, power requirement, and cooling.
- It must operate in a broadband configuration up to data rates of 10^7 bits per second.

The possibilities considered for the LCSE mission included most of the modulators in use today. Modulators requiring mechanical shutters or liquid-filled cells were disqualified for obvious reasons. Modulators considered for the LCSE include those discussed below.

Linear Electro-Optic Effect (Pockels)

This type of modulator is commonly used in three configurations: the single crystal modulator, the multipass modulator, and the multicrystal modulator. The only strain-free crystal available in reasonable sizes is KDP and only this material was considered. For a typical KDP crystal the half-wave voltage is about 2 kv. The capacitance of these single crystals is on the order of 10 picofarads which requires driving powers on the order of a kilowatt for broadband operation over a 10^7 cps bandwidth.

The efficiency of the modulator can be improved by having the beam make multiple passes through the crystal using an optical system. This results in a reduction of driving power since the effect depends on the path length in the crystal. This technique is not considered suitable for the LCSE mission for two reasons. First is the need for all passes through the modulator to be parallel to the optic axis to reduce the effect of zero field birefringence. The second is the variation of strain induced birefringence across the crystal which tends to cancel the effect of multiple passes.

The third configuration is the multicrystal modulator. The most commonly used is the bi-crystal modulator. This consists of two KDP crystals optically in series and electrically in parallel. The crystals have their axes rotated with respect to each other by 90 degrees, and a half-wave plate is employed between them. This configuration has several advantages--first, by using identical crystals the natural birefringence is cancelled. The second is the elimination of the temperature dependence of the operating point. Two KDP crystals (2x2x25 mm) used this way have a half-wave voltage of 310 volts. The electrical power required for a 10^7 bit rate with the bi-crystal configuration is about 25 watts.

Quadratic Electro-Optics Effect

Several materials such as KTN have been used recently as modulators. The materials, because of their quadratic effect, require very low-driving voltages and powers. For a typical KTN crystal (5x5x5 mm) the half-wave voltage is about 40 volts. In spite of the tremendous modulation efficiencies of these materials they are not suited for use in a diffraction-limited optical

system. It is extremely difficult to grow KTN crystals with high-optical quality; and, to date, no suitable crystals have been reported.

Internal Modulation of the Laser

Any scheme contemplated to internally modulate the laser would be limited by the high Q optical cavity. Typical cavity Q's for gas lasers are on the order of 10^8 and modulation above one or two hundred milocycles are not possible.

Piezoelectric Modulators

These modulators are limited in frequency response to about 5 megacycles when used in thin total reflecting plates. Other configurations such as interferometric piezoelectric modulators* do not lend themselves to PCM/PL as readily as the KDP modulator.

LCSE MODULATOR SUMMARY

The best choice of modulator for the LCSE is the KDP bi-crystal modulator. Several modulators of this type are available commercially** and have been constructed at Perkin-Elmer (NAPS, a laser camera system). Data rates of 10^7 bits per second will be achieved with a power consumption below 50 watts. These modulators will have sufficient optical quality so as not to degrade the diffraction-limited performance of the system. The built-in redundancy in a bi-crystal modulator is appealing for a space vehicle. The failure of a single crystal will only result in partial modulation but not disable the entire system. Since modest amounts of power are required, engineering of cooling provisions will not require exotic solutions. Space qualification of a bi-crystal modulator does not present serious difficulties.

TEST SIGNAL GENERATOR FOR LASER COMMUNICATIONS

A data source with a megabit digital output is required during initial testing of the PCM/PL data link. To have an accurate knowledge both of the number of errors and the distribution of these errors, the earth receiver must have a priori knowledge of the data which is transmitted from the satellite. Because of bandwidth limitations, it is impossible to generate a test bit sequence on the earth, transmit it to the satellite via microwave, and return it to the ground via the optical link. Also, a tape recorder with a continuous tape is a poor choice for the data source because of problems in space qualification.

---

*of the type developed by North American Aviation

**Sylvania

A pseudo-random shift register code generator is easily space qualified and requires little power or volume. This device is basically a series of n registers in series with feedback. By judicious choice of the feedback connections, a bit sequence of 2^n-1 bits is generated. This output sequence is then repeated indefintely. For example, if an eleven-stage pseudo-random shift register were used, a bit sequence of 2^n-1 = 2047 bits with a period of approximately 2 milliseconds will be generated in the megabit system. A larger number of registers will increase the period of the sequence.

An identical shift register will be in use at the ground station. After initial synchronization, the output of the ground shift register will be compared on a bit-by-bit basis. This procedure will yield both the average bit error rate and the time distribution of the errors.

Minimal development is required because both the digital circuitry and the mathematical theory of choosing the correct feedback connections are readily available.

PCM ENCODER

To verify the operation of key components and to gather data required for analyzing the performance of the LCSE system in space, various parameters will be measured and the results sampled, digitized, and multiplexed for telemetry to earth over the microwave link. Some of the diagnostics may require up to 30 analog inputs (e.g., temperature sensors). The total channel capacity for these diagnostics has been estimated to be about 250 bits per second. This channel capacity would accommodate 100 analog inputs. Approximately one third of the channels would be sampled every second and the remainder sampled every 15 to 30 seconds. In addition, the outputs from both the summation (scintillation data) and difference (fine tracking data) circuits following the fine guidance photomultipliers must be telemetered to earth. The scintillation data and tracking data will have analog bandwidths of 100 and 30 cps, respectively. Digitizing these signals and multiplexing them with the 250 bit per second diagnostic bit stream will yield a 1.5 Kcps telemetry requirement for the LCSE.

For the PCM/PL data at 10^6 and 10^7 bits/second, raw video (analog) will feed the PCM encoder and the output of PCM encoder will drive the PCM/PL modulator in the laser transmitter. There are PCM encoders suitable for the LCSE mission available from other space programs.

SUN TRACKER (FOR ACQUISITION AND ROLL REFERENCE FUNCTIONS)

The initial acquisition function of the LCSE requires the sequential use of the Sun Tracker. The Sun Tracker must assist in the orientation of the telescope so that the earth argon beacon will be visible in the 1-degree field of view of the coarse guidance.

The Sun Tracker must also be used to give the rotational reference for the communication link point ahead. In the LCSE simulation of the deep-space point ahead experiment, the rotational angle about the line of sight must be known to a value which varies from 0.056 to 2.26 degrees. The accuracy requirements of the Sun Tracker for point ahead experiments must be better than these numbers. For example, the ITT Federal Laboratories have developed a Canopus star tracker which has a 20 mm f/1 optical system and 15 arc-seconds tracking accuracy. The specification for the LCSE Sun Tracker are within the present state of the art even though the object tracked is the sun and not a point source (star).

The specification (for roll reference) to be met by the LCSE is dependent upon the specific experiment to be performed. The requirements are summarized in Table IX.

TABLE IX
ROLL REFERENCE REQUIREMENTS

Function	Point Ahead Angle	Roll Reference Specification for LCSE Assuming Zero Pointing Error
LCSE Laser Communication Experiment	3.58 arc-seconds maximum	± 2.26°
LCSE Station Transfer Experiment	~ 8 arc-seconds	± 0.45°
LCSE Simulation Experiment of Deep Space Point Ahead Requirement	~ 50 arc-seconds	± 0.16°
LCSE Simulation Experiment of Deep Space Communications	36 arc-seconds	± 0.056°

TELESCOPE STRUCTURAL GROUP

The structural configuration of the proposed instrument is to a large degree influenced by the nature of the various components within the instrument, by their relative sensitivity to dynamic environments, and by the required accuracy of their respective locations.

At the outset, it is evident that the instrument necessarily includes a number of components requiring at least some degree of protection from the dynamic environments imposed by the launch vehicle. The primary mirror, the quartz rods separating the primary and secondary mirrors, the transfer lens assembly, the laser assemblies, and the photomultiplier tubes

are in such a category. A fundamental decision, therefore, is whether to rigidly mount the overall package and provide shock and vibration protection for individual components as required, or, alternatively, to mount the whole instrument on isolators and thereby minimize the need for protection of individual components.

Since the number of components requiring protection is appreciable in this instance, and since there is no requirement for precise alignment of the instrument with respect to the spacecraft, the latter approach proves to be most advantageous. Hence, the structural configuration described in subsequent paragraphs consists in essence of a cylindrical package which is protected by vibration isolators from excessive dynamic inputs and within which most of the individual components are rigidly mounted. This approach has the following advantages:

- By attenuating dynamic inputs external to the package, structural requirements throughout the instrument are materially reduced, with consequent reductions in weight and inertia.
- Hard mounting of most components within the package eliminates most of the mechanical complexity and associated reliability considerations otherwise introduced by caging devices, isolators, and alignment mechanisms.
- Hard mounting of most components on rigid locating structure provides maximum assurance of continued optical alignment.

As will be described, a departure from the concept of hard-mounted components is warranted in the case of the secondary mirror assembly and its positioning elements. In this instance, the optimum operational configuration is not consistent with launch requirements, even with isolation of the entire instrument.

The following paragraphs outline from a structural point of view the important characteristics of the various components of the proposed instrument. Reference is made to Figure 49 for identification of components and illustration of the overall system.

Tube Structure

The major structural component of the proposed instrument is a ring-stiffened aluminum tube designed to support and enclose the internal components and to provide the necessary external attachment points. As shown in Figure 49, the wall of this tube is of sandwich construction or could be of the welded truss-core configuration employed for the telescope tube of the OAO Princeton Experiment Package. As will be described subsequently, however, the optical

alignment in the proposed LCSE package is virtually insensitive to hysteresis effects or thermal distortions of the tube. Consequently, a variety of structural designs and fabrication techniques are available which otherwise would be unacceptable. Final selection of an optimum configuration would represent economic and manufacturing considerations as well as detailed structural analysis.

Included in the basic structural package are two honeycomb sandwich bulkheads in the positions shown. These bulkheads provide mounting surfaces for the instrument package to be described in subsequent paragraphs, and materially reduce the stiffness requirements for the reinforcing rings to which they are attached. They also provide convenient mounting platforms for electronics packages and other ancillary equipment.

The two bulkheads are stiffened in the axial direction by four radially oriented shear webs which divide the space between bulkheads into four identical compartments. The resulting combination of outer tube, bulkheads, and stiffening shear webs results in an efficient and rigid structure which, at the same time, provides convenient equipment bays and is conducive to installation of generous access panels.

The aft end of the tube, already amply stiffened by the aft honeycomb sandwich bulkhead, is closed by a removable, nonstructural, spun or drawn light-alloy cover.

The forward end of the tube includes another honeycomb sandwich panel of annular planform. This panel stiffens the front end of the tube, provides the required aperture for the optical system, and provides mounting points for the hinged sun shade/lens cap, which also is of honeycomb sandwich construction.

Included at appropriate points on the main tube, as shown, are fittings for the gimbal pivots and attachment points for the isolation mounts which support the package in the launch or stowed condition.

PRIMARY MIRROR MOUNT/INSTRUMENTATION HOUSING

The primary mirror and the majority of the rest of the key components of the system are mounted in or on a rigid assembly which in turn fastens directly to the forward and aft sandwich bulkheads described above.

The structural portion of this assembly includes a number of components, the largest of which is a light-alloy casting of essentially cylindrical configuration with a flange permitting direct attachment to the forward bulkhead. This lightweight casting provides the required locating surfaces for the hub-mounted primary mirror, as shown. It encloses and provides attachment points for the coarse acquisition fiber optics bundles and phototubes, as well as for the transfer lens and its driving motor and caging mechanism.

A flanged hole on one side of this casting provides the mounting surface for a separate subassembly which includes the dichroic beamsplitter,

PERKIN-ELMER

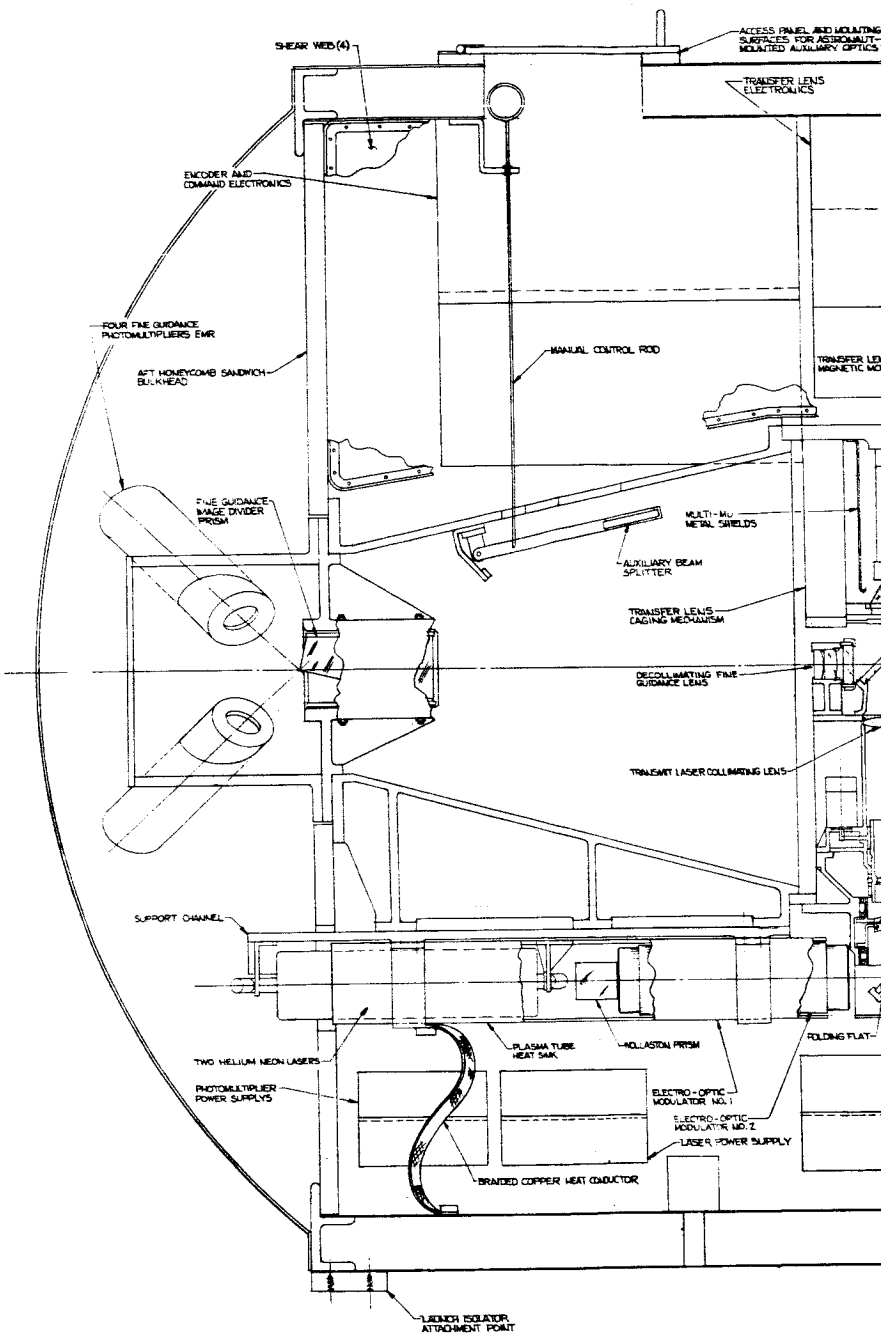

135-1

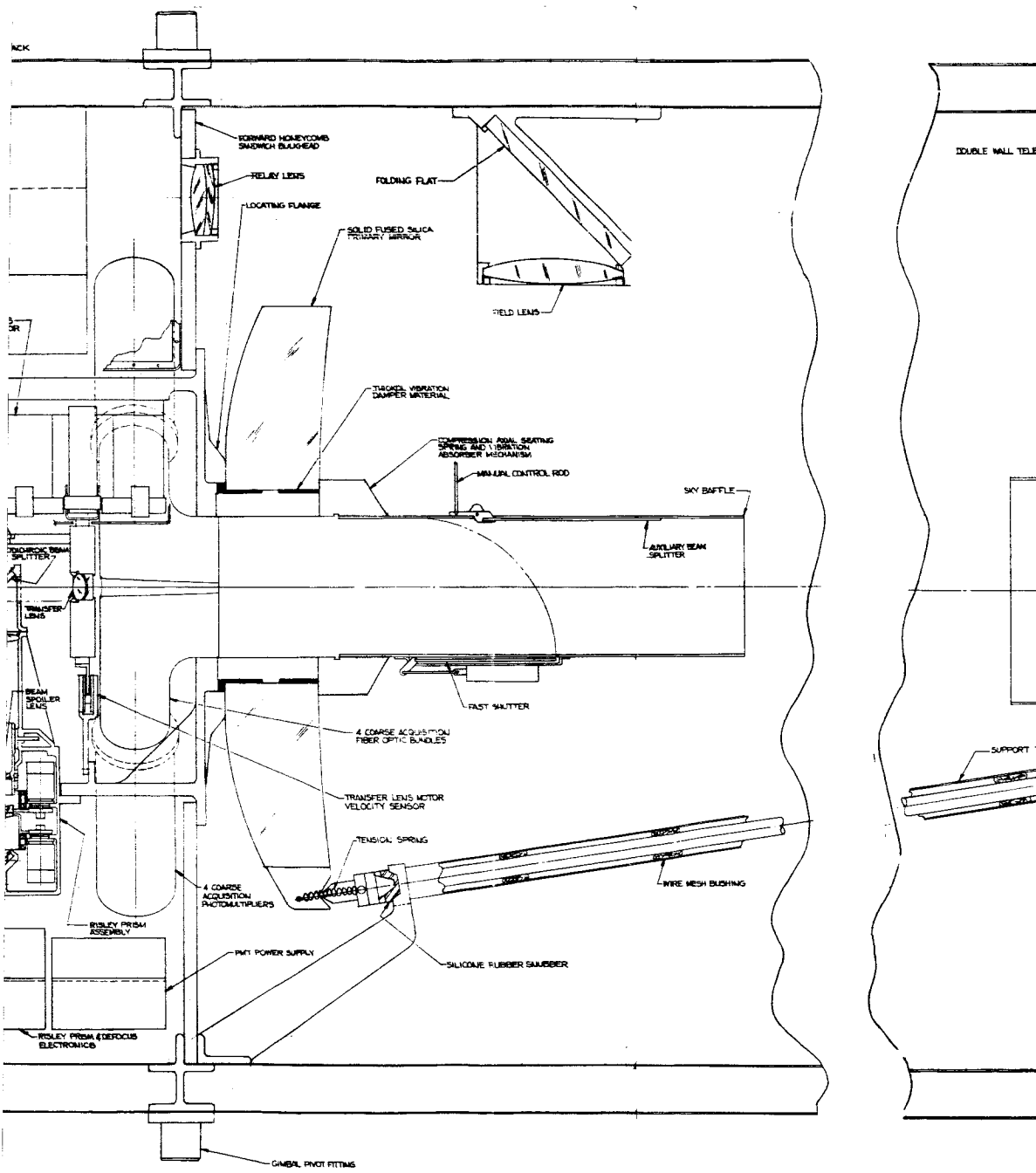
FORWARD HONEYCOMB SANDWICH BULKHEAD
RELAY LENS
LOCATING FLANGE
SOLID FUSED SILICA PRIMARY MIRROR
FOLDING FLAT
FIELD LENS
TRACKER VIBRATION DAMPER MATERIAL
COMPRESSION AXIAL SEATING SPRING AND VIBRATION ABSORBER MECHANISM
MANUAL CONTROL ROD
SKY BAFFLE
AUXILIARY BEAM SPLITTER
DICHROIC BEAM SPLITTER
TRANSFER LENS
BEAM SPOILER LENS
FAST SHUTTER
4 COARSE ACQUISITION FIBER OPTIC BUNDLES
TRANSFER LENS MOTOR VELOCITY SENSOR
TENSICAL SPRING
WIRE MESH BUSHING
4 COARSE ACQUISITION PHOTOMULTIPLIERS
RISLEY PRISM ASSEMBLY
PMT POWER SUPPLY
SILICONE RUBBER SNUBBER
RISLEY PRISM & DEFOCUS ELECTRONICS
GIMBAL PIVOT FITTING
DOUBLE WALL TELE
SUPPORT

137-2

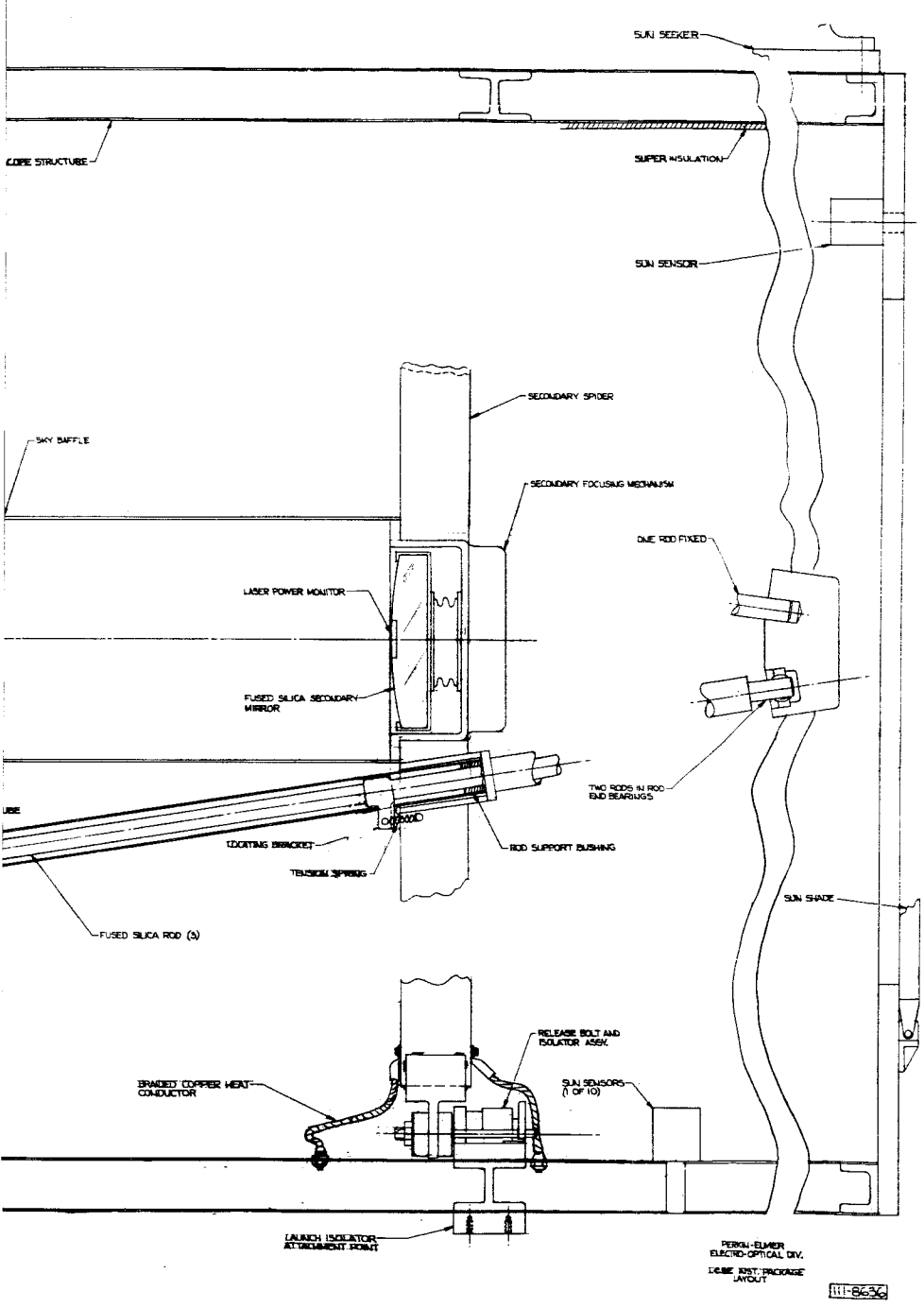

Figure 49. LCSE Laser Telescope Layout

the decollimating fine guidance lens, the transmit laser collimating lens, the beam spoiler lens, the Risley prism assembly, and a small folding flat. This subassembly is appropriately webbed and stiffened to assure continued optical alignment.

Fastened to the aft end of the main cylindrical casting is a conical transition housing which, at its smaller end, attaches to the aft bulkhead and provides a mounting surface for the fine guidance image divider cell and the EMR photomultiplier assembly. Along one side of the conical housing is a webbed and stiffened fin providing support pads for the channel-like support platform bearing the two helium-neon lasers, the Wollaston prism, and the electro-optical modulators.

The system described thus consists of a number of convenient subassemblies which fasten together in a positive and rigid manner to create a structure which precisely defines the optical alignment of the laser sources and the guidance optics to each other and to the primary mirror.

SECONDARY MIRROR SUPPORTS

The most critical optical alignment requirement in the entire system is that governing the location of the secondary mirror with respect to the primary mirror.

Since both mirrors are of fused silica, the optical characteristics of the telescope will be totally insensitive to uniform temperature changes if the spacing elements are also of fused silica. It is similarly evident that the structure establishing the relative positions of the two mirrors should be kinematically correct; i.e., should provide the required number of constraints in a nonredundant manner. Pursuit of this line of thought leads inevitably to the conclusion that, in the absence of significant external loads, the optimum approach to the secondary support problem is a three-legged tripod of fused silica rods. The system shown in Figure 49 and described in the following paragraphs employs exactly this concept, and includes practical means of implementing the basic concept in a manner consistent with the dynamic environments involved and with actual hardware limitations.

As indicated, the primary mirror includes three projecting ears equally spaced around its periphery. The front surface of each of these ears incorporates a conical seat for the rounded end of a fused silica rod which, in turn, forms one leg of a tripod.

The apex of this tripod would ideally consist of a single pivot point about which any leg would be free to rotate in any direction. Although this ideal would be awkward to implement mechanically, it is closely approximated in the proposed system by a fitting in which one of the fused silica rods is rigidly clamped and in which the other two are universally pivoted.

A difficulty is encountered inasmuch as the secondary mirror cannot be located at the vertex of the triangle. This difficulty is circumvented

by mounting the secondary (and its focusing mechanism) in a cell which incorporates three hemispherical "feet," each of which rides in a radial vee-groove on a locating bracket bonded to one of the fused silica rods. The radial vee-grooves permit differential thermal expansion between the fused silica and the metallic secondary mirror cell. Thus, in effect, the secondary mirror is centered and supported on a platform at the proper level of the fused silica tripod.

Light tension springs hold the fused silica rods against the ears on the primary and the secondary package against the locating brackets on the rods. The forces introduced by these springs are localized and are not transmitted into the primary mirror or along the rods.

The components described thus far yield a system which, in the absence of significant accelerations or external loads, locates the secondary mirror in a precise and kinematically correct manner with respect to the primary. This location is completely independent of other structure, being unaffected, for example, by thermal distortions of the main telescope tube.

It is clear, however, that the fused silica tripod is not adequate, by itself, for supporting the secondary during the boost phase of the mission, even though the entire package is vibration isolated. The rods themselves are plainly susceptible to lateral resonance, and it is inadvisable to transmit the inertia loads of the secondary package through the primary mirror.

The first step in providing launch mode capability is to enclose the fused silica rods in stiff metal tubes, with wire mesh bushings providing lateral support and vibration damping at appropriate intervals. The fit between these bushings and the rods would be chosen to provide sufficient frictional force to damp axial resonances of the rod, but not so much that relative thermal expansions would appreciably strain the rods. The rods and the metal tubes are attached in the vicinity of the secondary through a rod support bushing bonded to both members.

The secondary package incorporates a three-legged spider. In the launch configuration, this spider would be pulled forward against isolators by release bolts. The forward motion of the spider:

- Lifts the hemispherical feet on the secondary package out of the vee-grooves in the locating brackets on the fused silica rods.
- Moves the spider legs against collars on the metal support tubes.
- Lifts the lower ends of the fused silica rods away from the ears on the primary mirror.
- Pulls shaped brackets on the lower ends of the support tubes into engagement with silicone rubber snubbers tied to the main structure, thus putting the support tubes into tension.

The resulting launch configuration (which is the one shown by Figure 49) finds the fused silica rods supported and damped in a desirable manner, and all inertia loads associated with the rods and the secondary transmitted directly to the primary structure. In orbit, the release bolts on the spider supports would be actuated, allowing the light tension springs to return the assembly to the operational configuration.

THERMAL INSULATION

Although detailed requirements for thermal insulation must await careful analysis and establishment of an overall concept, it is highly probable that the inside surface of the telescope tube will require a minimal effective emissivity.

The most effective means of attaining this objective is to employ a blanket consisting of multiple layers of aluminized Mylar. The efficiency of this type of insulation depends to a significant degree, however, on proper installation practice. In particular, care must be taken to minimize penetrations or compaction of the blanket, either of which can lead to excessive conduction heat leaks.

A practical means of complying with these requirements when utilizing this type of insulation on the inner wall of a cylindrical structure is that employed on the OAO Princeton Experiment Package. The insulation is held against the wall of the tube by a series of spring-tensioned longitudinal wires attached to short standoffs at either end of the structure. This approach eliminates penetrations and/or compactions of the Mylar layers except at the extreme ends of the insulated space.

A second area in which corrective measures may be required is that of thermal conduction from the tube wall through the bulkheads to the optics and particularly to the primary mirror mount. The structural configuration shown is amendable to inclusion of low conductivity spacing elements or inserts, as required, at the tube-bulkhead and/or bulkhead-instrument housing interfaces.

SUN SHADE/LENS CAP

The combined functions of a sun shade to prevent sunlight from illuminating the secondary mirror or the interior of the telescope tube and a lens cap to close the aperture during periods of inactivity are performed by a pivoted lid or door on the front end of the telescope tube. This unit is similar in function and design to the sun shade on the OAO spacecraft. It consists of a honeycomb sandwich plate hinged on bearings incorporating a fused teflon coating for reliable operation in the space environment. Actuation is by a hermetically sealed geared electric motor driving a nutating arm through a flexible metal bellows.

Actuation is initiated either by remote command or, in the event of inadvertent point towards the sun, by a sun sensor.

FAST SHUTTER

Since it is imperative that the photomultipliers be protected from direct solar radiation, and since it is impractical to provide rapid actuation of the hinged sun shade, a fast shutter is included in the sky baffle in front of the primary mirror. This shutter would close in a small fraction of a second upon signal from the sun sensors that the instrument was pointing dangerously close to the sun.

The shutter would be spring loaded in the open position, and its actuator could be provided with an independent and limited power supply to prevent indefinite closure by a malfunction in sensors or actuator.

LAUNCH MODE ISOLATION

As previously indicated, the system requires shock and vibration isolation of the overall package. Figure 49 indicates tentative attachment points for the required isolators. These isolators would probably be viscoelastic molded mounts designed for optimum damping characteristics and with their line of action passing as nearly as possible through the center of gravity of the instrument.

The instrument would be attached to the isolators with release bolts or pin pullers to permit disengagement following launch.

CAGING MECHANISMS

The only caging requirement not already described is that associated with the transfer lens. To prevent excessive oscillations and/or bearing loads on this component during launch, the lens and the movable armature of its magnetic motor must be securely captured by pin-pullers or by mechanically actuated clamps.

ASTRONAUT SIGHTING OPTICS

Provision is included for visual sighting through the instrument by an astronaut while the system is tracking an earth beacon. The astronaut would open an access panel on the side of the telescope tube, manipulate control linkages to position auxiliary beamsplitters in the system, and attach an auxiliary optics package containing appropriate viewing optics.

For fine guidance and narrow field of view, a beamsplitter in front of the image divider prism directs a light bundle into the auxiliary optics package, which in this instance supplies a relay lens and an appropriate eyepiece.

For coarse guidance and wider field of view, the beamsplitter is positioned in front of the primary, as shown. In this case, a field lens, a folding flat, and a relay lens are incorporated in the system to transfer the image to the auxiliary optics package. The auxiliary optics package includes either a folding mirror and a second eyepiece, or an insertable folding flat to permit use of a single eyepiece.

2.7 GROUND STATION PCM/PL RECEIVER AND TRACKER

The three basic functional operations of the ground station are:

- To acquire the satellite using ephemeris data and to track the helium-neon signal received from the LCSE.
- To provide the argon laser beacon so that the satellite can track the earth station system.
- To receive and decode the PCM/PL signal.

These operations could be accomplished by three independent optical systems. However, problems of synchronization and alignment would be more complex than a common optical system capable of all three operations. To minimize the atmospheric effects occurring close to the ground, a ground telescope with an aperture of approximately 24 inches or larger is required. This 24-inch aperture ground telescope will be used for both the beacon and down-going communication link functions. As in the LCSE, a dichroic mirror with special dielectric layer coatings will be used to duplex the laser beams.

The photoelectron emission rate at the earth PMT photosurface resulting from the down-going PCM/PL signal is approximately 3×10^9 photoelectrons/second. Using 10% of the received energy for tracking and the remaining 90% for the information channel, the tracking loop will have a shot-noise-limited SNR of 10,000 for a tracking loop with a 1 cps bandwidth. The alternative of using the same energy for both tracking and signal demodulation requires a significant increase in ground equipment while the advantages obtained for the experiments are only marginal.

The field of view of the PCM/PL receiver and tracking subsystems will be 20 arc-seconds. Therefore, the feedback from the tracking subsystem (Figure 50) must point the ground telescope to within 5 to 10 arc-seconds of the apparent LOS. Since the angular rates of the earth telescope tracking a synchronous satellite with a 28° inclination are slow (1×10^{-5} radian/second East-West and 4×10^{-5} radian/second North-South), body-pointing of the receiver telescope may be accomplished readily with 5 arc-second accuracy.

TRACKING SUBSYSTEM

A tracking subsystem using an image divider followed by four phototubes is planned.* The tracking subsystem output is used to control the torque motors which correct for pointing errors of the telescope optic axis. The bandwidth of this tracking loop will be low (of the order of one cycle per second).

*Note that this ground station track subsystem is similar in function and equipment to the spaceborne fine tracking system of the LCSE.

The PCM/PL detector spatially separates two linear polarizations and compares the energy contained in each polarization during a given bit interval. Since the PCM output of the satellite optical transmitter is circularly polarized (both right-hand and left-hand), a quarter-wave plate must be inserted to form the orthogonal linear polarizations required by the Wollaston prism. The outputs of the photomultipliers are differenced and amplified. To generate timing information, the difference signal is differentiated. This creates a pulse (alternately plus and minus) when there is a transition between opposite bits. After rectifying, the sequence of pulses (plus differentiation noise) becomes the input to an oscillator with a high Q. The phase of this oscillator is used for the clocking of the integrate and hold circuits of the PCM/PL detector. The zero threshold device is used to "square up" the digital bit stream.

During the initial testing of the PCM/PL link, a pseudo-random digital sequence is transmitted from the satellite. The error detector at the ground receiver compares the output of a synchronized shift register and the PCM/PL signal. The output of this device can provide both the long term and short term bit error data of the communication link. Also, the effect on the bit error rate of changing critical parameters in the satellite and in the receiver optics can be evaluated by examining the error detector output. The effective aperture and field of view are two ground receiver parameters that will be controlled by the stops shown in Figure 50.

A subjective rating will be given the detected video pictures. This rating will help in determining the proper fade margin required for future space-to-earth PCM/PL laser communication links. The effects of quantum noise will be a series of dots in the picture and the atmospheric fading will cause a series of horizontal lines in the video picture.

LCSE EARTH LASER BEACON

The tracking, communication and earth viewing experiments require an argon laser beacon* on the earth. Using tracking information in addition to ephemeris data generated by a computer, the beacon optics will floodlight a one mile by one mile block of space in the vicinity of the satellite. To obtain color separation between the light used for the beacon and the 6328Å PCM/PL signal, the 4880Å line of the argon laser will be used for the earth-to-space beacon link. This emission line was chosen in preference to the 5145Å argon line because the S-20 photosurfaces have a higher quantum efficiency and the isolation requirements are easier at 4880Å.

The parameters required to determine the signal-to-noise ratio (SNR) in the satellite tracking unit are listed in Table X on page 145. Most of the values have been previously defined in Table IV, page 52.

*R.J. Arguello, Downward-Looking Seeing Through the Earth's Atmosphere, Internal Perkin-Elmer Report.

PERKIN-ELMER

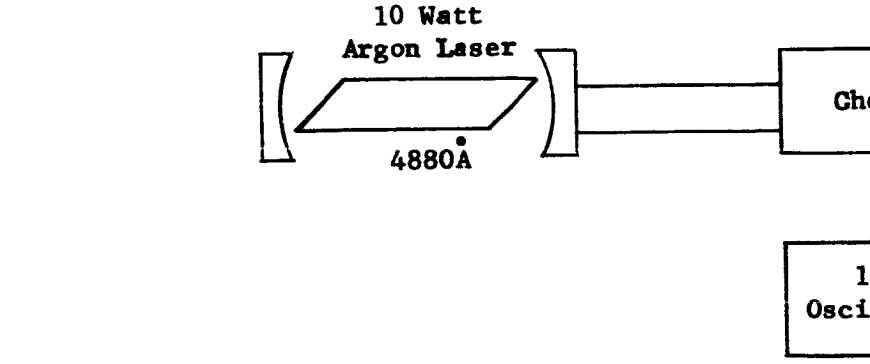

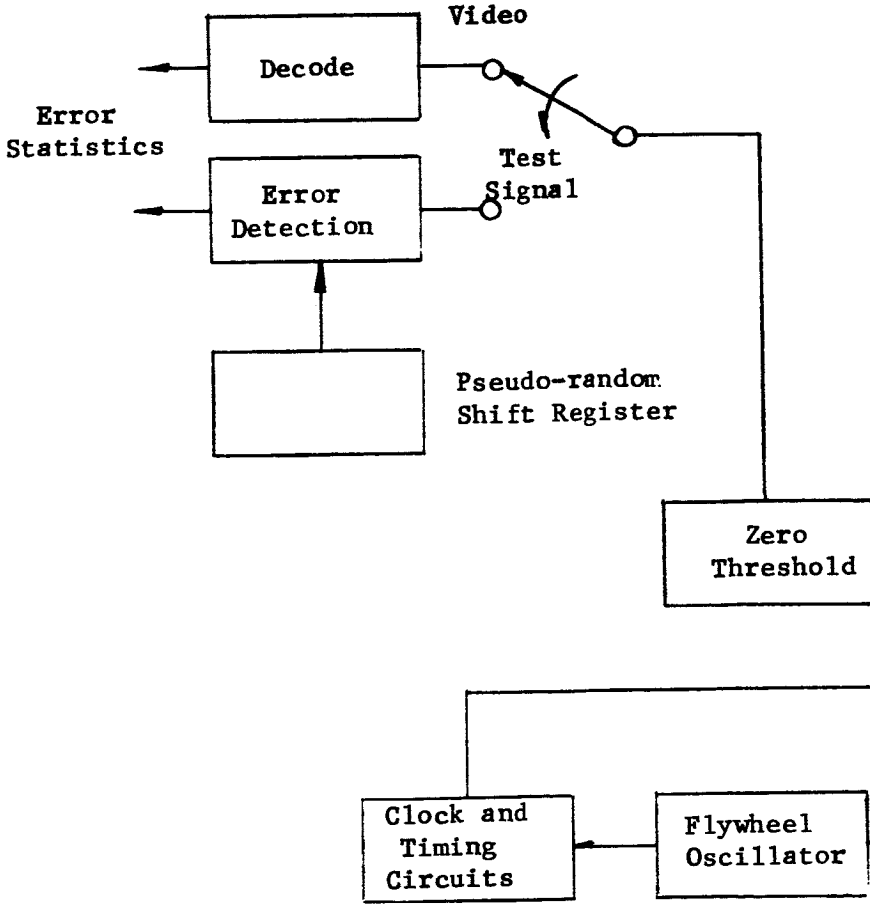

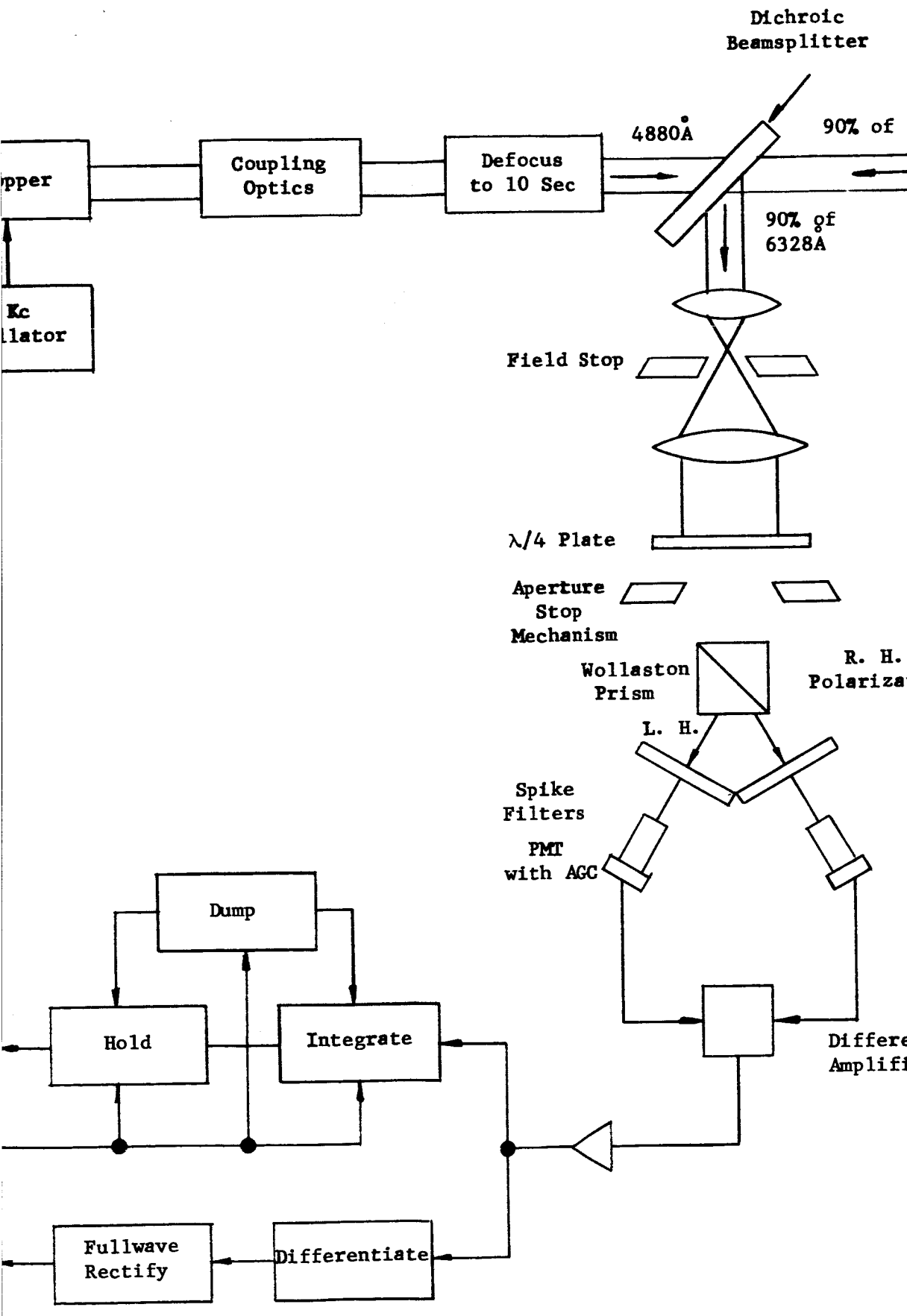
Dichroic
Beamsplitter
4880Å
90% of
pper
Coupling
Optics
Defocus
to 10 Sec
90% of
6328A
Kc
llator
Field Stop
λ/4 Plate
Aperture
Stop
Mechanism
Wollaston
Prism
R. H.
Polariza
L. H.
Spike
Filters
PMT
with AGC
Dump
Hold
Integrate
Differe
Amplifi
Fullwave
Rectify
Differentiate

145-2

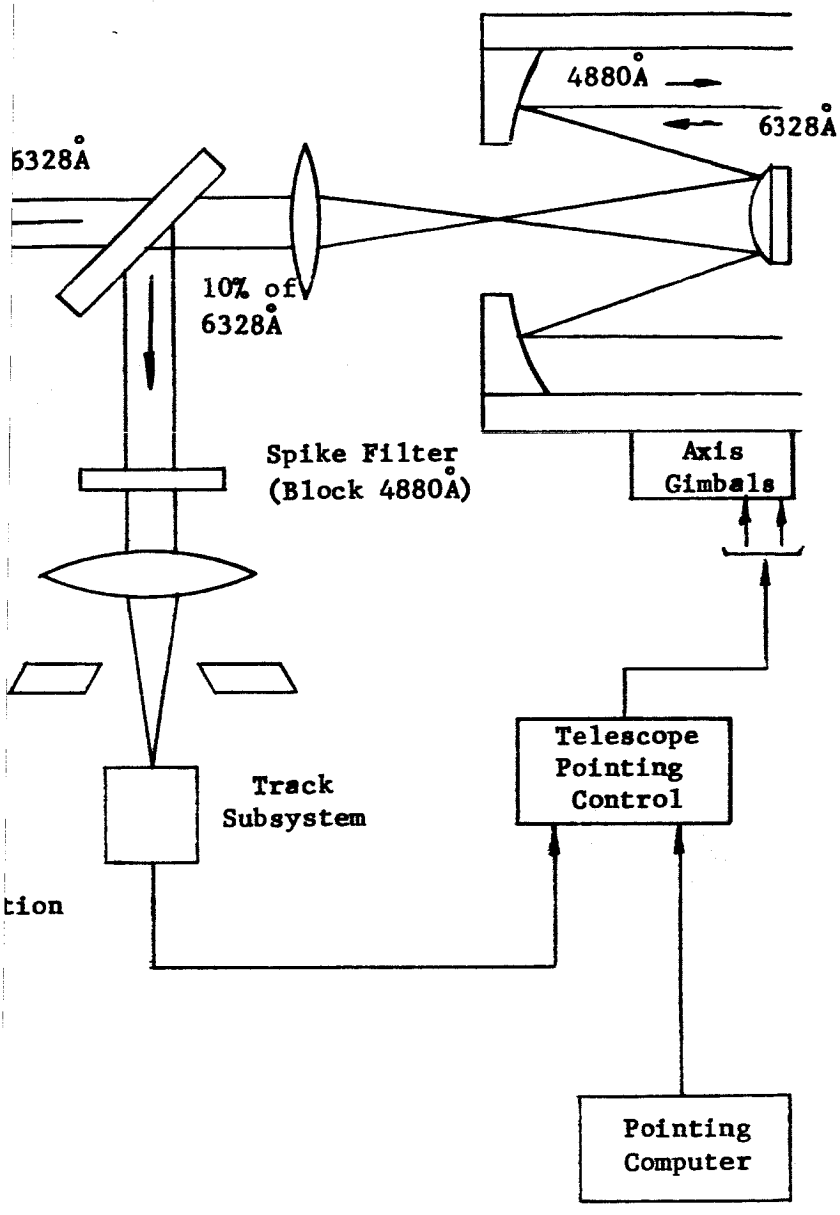

Figure 50. Ground Receiver Block Diagram

TABLE X

EARTH-TO-SPACE BEACON LINK

VARIABLE	SYMBOL	VALUE	UNITS	REFERENCE OR COMMENT
Range	R	34,060	Km	Rx viewing 60° to Zenith
Wavelength	λ	.4880	Microns	
Beacon Power	P_T	10	Watts	Measured at laser output
Beam Divergence of Beacon	α	10 50	Arc-Sec μ-radians	
Satellite Field-of-View	β	2	Arc-Min	
Atmospheric Transmission	τ_A	.6	@60° from Zenith	Table 3-1 NASA CR-252
Beacon Optical System Transmission	τ_{OT}	.33		
Satellite Optical System Transmission	τ_{OR}	.75		
Diffraction Loss	τ_0	.5		
Optical Filter Transmission	τ_F	.40		For filter bandwidth $\Delta B = 2\text{Å}$
Satellite Aperture	d	.40	Meter	
Earthshine	P_E	2×10^{-5}	Watts/m^2-arc-min^2-μ	Derived from Figure 7-6, NASA CR-252
Scintillation	τ_S	?		
Satellite PMT (@ 300°K)	P_P	10^{-14}	Watts	Radiant input power equivalent
PMT Quantum Efficiency	η	.13		S-20
Speed of Light	c	3×10^8	m/sec	

The beacon divergence, α, is 10 arc-seconds. Empirical data on the effect of down-looking scintillation is not available. However, both a theoretical model of the atmosphere* and measurements of star scintillation indicate that fading of the beacon will not be significantly worse than the fading of star light.

The beam steering effect of the atmosphere near the transmitter aperture may be reduced by using a transmitter aperture significantly bigger than 4 to 10 centimeters. Thus, the 24-inch ground receiver aperture will be used for both the transmit and receive channels.

A light ray traveling between earth and a spacecraft will be deflected through a small angle because of atmospheric refraction. At the zenith no refraction takes place, and at 60° from the zenith the refraction is over 1.5 arc-minutes. However, astronomers using single air temperature and pressure measurements made at the observing site, together with semiempirical formulas, can predict the refraction angle to within a second of arc over all zenith angles less 60°. This information is used in the initial acquisition when the ground beacon "flood lights" the area which the ephemeris or radar track predicts as containing the satellite.

The tracking and PCM/PL detector subsystems are sufficiently lightweight and small to be packaged in the volume immediately behind the primary. The argon laser, however, is best mounted externally from the telescope. The transmit and receive channels will be superimposed using a dichroic mirror. One possible method for superimposing these beams is shown in Figure 50.

The coupling optics following the argon laser should be placed at the center of rotation of the telescope mount. Any misalignment between the transmit and receive laser beams will be corrected by this device.

To obtain the required 10 arc-second divergence of the beacon from the 24-inch aperture, defocusing optics must be inserted into the beam of the argon laser output. This device will have the ability to change the divergence of the beacon. The performance data obtained by operating the beacon with several different divergence angles will prove valuable in determining the optimum beacon divergence for future optical communication systems.

RECEIVER POWER BUDGET FOR THE LCSE BEACON LINK

The rate of emission of the unchopped beacon photoelectrons from the detector photosurfaces in the fine tracking subsystem of the LCSE is

*An argon laser was chosen for the earth laser beacon for reasons of high power output and high quantum efficiency of detectors at 4880Å.

$$n_s = \left(\frac{d}{\alpha R}\right)^2 \left(\frac{\lambda P_T \eta}{hc}\right)\left(\tau_D \tau_A \tau_{OT} \tau_{OR} \tau_F \tau_S\right)$$

$$= \left(\begin{matrix}\text{ratio of receiver \&} \\ \text{illuminated areas}\end{matrix}\right)\left(\begin{matrix}\text{Conversion of optical} \\ \text{power to photoelectrons/sec}\end{matrix}\right)\left(\begin{matrix}\text{System Effi-} \\ \text{ciencies}\end{matrix}\right)$$

$$= \left(\frac{.4}{5\text{x}10^{-5}\text{x}3.4\text{x}10^{7}}\right)^2 \left(\frac{.4880\text{x}10^{-6}\text{x}10\text{x}.13}{6.625\text{x}10^{-34}\text{x}3\text{x}10^{8}}\right)\left(.5\text{x}.6\text{x}.33\text{x}.75\text{x}.4\text{x}\ \tau_S\right)$$

$$= 5.3 \times 10^{9}\ \tau_S \text{ photoelectrons per second.}$$

The rate of emission of background (sunlit earth) and phototube photoelectrons is

$$n_n = \frac{\lambda\eta}{hc}\left[4P_P + P_E\left(\frac{\pi D^2}{4}\right)\beta^2\,\Delta\lambda\ \tau_{OR}\,\tau_F\right]$$

$$= \frac{.4880\text{x}10^{-6}\text{x}.13}{6.6\text{x}10^{-34}\text{x}3\text{x}10^{8}}\left[4\text{x}10^{-14}\text{x}2\text{x}10^{-5}\left(\frac{\pi\text{x}.4^2}{4}\right)\frac{\pi 2^2}{4}\ \text{x}2\text{x}10^{-4}\text{x}.75\text{x}.4\right]$$

$$= 2 \times 10^{9} \text{ noise photoelectrons in 2 min field of view}$$

Assuming that the beacon is passed through an on-off rectangular chopper, and the effect of scintillation at low frequencies is small, the average signal rate becomes

$$\bar{n}_s = \frac{n_s}{2} = 2.7 \times 10^{9}$$

For the fine tracking system (FOV = 2 arc minutes), the SNR for shot noise limited operation is

$$\text{SNR} = \frac{\bar{n}_s}{\sqrt{2\Delta f(\bar{n}_S + n_N)}}$$

$$= 5{,}400 = 37 \text{ db when } \Delta f = 25 \text{ cps}$$

$$= 27{,}000 = 44 \text{ db when } \Delta f = 1 \text{ cps}$$

This high SNR will insure proper operation of the tracking loop in the LCSE.

The coarse guidance system has a field of view of approximately one degree. Also, the fibre optics has a transmission of 0.5. Both effects will reduce the signal-to-noise ratio in the coarse tracking subsystem. The modified signal and noise photoelectron count in the coarse guidance photomultipliers is

$$n'_n = 2\times10^9 \left(\frac{60 \text{ min}}{2 \text{ min}}\right)^2 \times .5 = 9 \times 10^{11}$$

$$n'_s = 2.7\times10^9 \times .5 = 1.4 \times 10^9$$

Assuming a bandwidth of 1 cps for the coarse tracking subsystem, the SNR for shot noise limited operation is then

$$SNR = \frac{1.4 \times 10^9}{\sqrt{2 \times 1 \ (1.6\times10^{11} + 9 \times 10^9)}}$$

$$= 2{,}500$$

Thus, sufficient energy is available for proper operation of the coarse guidance subsystem.

Preflight Ground Facilities (Cape Kennedy)

At the launch site (Cape Kennedy) a test facility should be provided to check out nominal operations of the telescope prior to installation in the vehicle. This unit shall provide the electrical and mechanical interfaces normally provided by the vehicle. Vehicle power sources with adjustable voltage levels, input command signals, and output telemetry lines will be simulated to permit console-monitored control of all telescope functions over parameter extremes. The telescope shall be optically coupled to a longer focal length ground station simulator to permit required optical prelaunch checkouts. The optical unit must for example allow transmit-receive line-of-sight alignment, telescope focus, point ahead calibration, and beam spoiler operation checks. Controlled variation of the simulated beacon line of sight and intensity will permit telescope tracking performance evaluations while ability to receive and decode telescope transmitted information through adjustable attenuators will provide nominal checkout of the transmitting laser, modulator, and power monitor.

Either the same console or one of reduced complexity will be required to repeat functional tests after the telescope is installed in the vehicle. However, such checkout would be better performed utilizing the actual command and T.M. channels of the vehicle just prior to launch.

At the actual ground beacon site in Western United States, the test facilities will include a telescope simulating test tower useful for checkout of receiver-transmitter alignment. Transmission of modulated laser light from the tower, over possibly the horizontal air path equivalent of one atmosphere, may be the simplest method of functional checkout via simulation of communication loop-closure with the satellite. Proper boresighting of 5-receiver array is readily checked with input computer commands controlling attitudes toward stars in consecutive fashion while viewing through the separate array optics.

2.8 DATA TO BE DEVELOPED FROM THE LASER COMMUNICATION SATELLITE EXPERIMENTS

In order to gather the data required for analyzing the communication and tracking performance of LCSE system, and to verify the operation of key subsystems and components, (diagnostic data), various parameters will be measured onboard the satellite, and at the ground receiver. The key parameters to be measured at the ground receiver are:

- Measurement of 10^6 and 10^7 bit/sec data rate, and measurement of probability of bit errors, (fade statistics).
- Measurement of 0.1 arc-second pointing by an array of five earth receivers that monitor the position of the satellite transmitter laser beam or by a single earth receiver station.
- Measurement of received signal power and operating SNR. The average signal-to-noise ratio is approximately 30 db for daytime operation at 60 degree zenith angle.
- Evaluation of received video data, i.e., TV picture to establish realistic fade margin requirements.

The above measurements are to be made for several receiver aperture sizes, several fields of view, for daytime and nighttime operation, for various meteorological conditions and slant angles, and various earthshine-to-transmitted-power ratios, and vehicle disturbance inputs.

The key parameters to be measured onboard the satellite are:

- Measurement of performance of fine tracking subsystem.
- Determination of earth laser beacon intensity fluctuations from phototube outputs of the fine tracking subsystem.
- Determination of time for satellite to acquire earth laser beam.

In addition, there will be diagnostic measurements of the following parameters. These measurements are to be made post launch and after a quiescent three month period.

- Monitoring of the axial spacing of the secondary mirror to the primary as this parameter affects system focus. The data on monitoring best focus can be obtained from velocity pickoff sensors in the transfer lens servo subsystem.

- Determining the alignment of the transmit channel with respect to the receive channel behind the mirror optics. This consists of monitoring any angular misorientation of the optical axes. The post launch angular alignment tolerance is 9.5 arc-seconds. The measurement of angular misorientation of the axes to determine channel alignment is to be made post launch and after a quiescent three month period upon ground command.

ATMOSPHERIC SCINTILLATION AND IMAGE JITTER EXPERIMENT DATA (SPACE-TO-EARTH TRANSMISSION)

Refer to Table XI for a summary of the satellite transmitter and earth receiver data for the uplooking atmospheric scintillation and image jitter experiment. The required sensor groups for the meteorological data collection system are identified, and the data reduction and processing operations which would follow the experiment are indicated.

As described in Table XI, the experiment objective is the measurement of fluctuations of light intensity and image jitter from a coherent source, (after passage through the entire atmosphere). This experiment is to be conducted for downward transmission of coherent light from the satellite to earth. These intensity and image fluctuations should be correlated with measurements of intensity and image fluctuations of starlight. This should be done for several small receiver aperture sizes, for day and night operation, for several zenith angles, and for various meteorological conditions. In addition, there should be determination of the auto- and cross-correlations and power spectral densities of the intensity and image jitter fluctuations, as well as correlation with received television picture quality. This information should be correlated with the outputs of a meteorological data collection system.

TABLE XI

ATMOSPHERIC SCINTILLATION AND IMAGE JITTER EXPERIMENTS

SATELLITE AND STARS TO EARTH

Satellite Transmitter Data	
Optical:	He-Ne 6328Å - with relatively low-frequency, modulated tracking signature.
Microwave Telemetry:	Laser power level monitor Output of fine track subsystem.
Earth Receiver Data	
Optical:	Detection of laser beacon intensity fluctuation. Image motion frequency components for beacon and stellar channel provided by separate telescope tracker on earth.
Electrical:	Detection of relatively low-frequency tracking signature. Monitor of television picture.
Meteorological Data Collection System	
Sensor Groups for:	Temperature (air, ground), Pressure, Humidity, Temperature Gradients, and Wind Velocity.
Data Recording and Processing	
Oscilloscope and Camera Recording of Scintillation Waveforms, Intensity Fluctuations, and Image Jitter	Auto- and cross-correlations Power spectral densities Correlation with meteorological data collection system Correlation of television picture quality with scintillation data

It is clear that this phase of the experiment will provide quantitative data on the susceptibility of a space optical communication system to fading caused by atmospheric turbulence. The resulting data can be used to verify theoretical models describing the interaction between coherent light and atmospheric turbulence.

One useful measure of the effect of atmospheric turbulence, i.e., index of the severity of the interference caused by turbulence, is the ratio of mean square value of the fluctuations about an average to the square of the average value. This measure has the useful property of being independent of the type of encoding or modulation of information contained in the optical signal. It is of the form that will describe the random, noise-like behavior of the interference. The conventional percent-type modulation, although useful for instantaneous measurements, depends upon the instant that the measurement is made and does not average over a time sufficiently long enough to describe average effects.

The index proposed should be relatively easy to measure, which enhances its utility for the envisioned experiment.

The radiant power from a laser beacon which impinges on a detector and is converted into an electrical signal is given by I(t). Then the average of I(t) is:

$$\overline{I(t)} = \lim_{T\to\infty} \frac{1}{2T} \int_{-T}^{T} I(t)\, dt$$

and the rms value of the fluctuations about this average is:

$$\overline{I^2(t)} = \lim_{T\to\infty} \frac{1}{2T} \int_{-T}^{T} \left[I(t) - \overline{I}(t) \right]^2 dt$$

the modulation index M is then given by:

$$M_i = \overline{I^2(t)} \,/\, \overline{I(t)}^2 = V^2(t) \,/\, \overline{V(t)}^2$$

since the output voltage V(t) of a photodetector is proportional to the radiant power.

To facilitate the measurements of any index of turbulence against a fluctuating background, it is desirable to have the laser transmitter system provide a constant average power level during scintillation measurements. This will allow the fluctuation values to be referenced against a relatively steady level. The pulse code modulation satellite transmitter configuration utilizing polarization modulation (PCM-PL) can be used for this experiment. An adequate relatively low-frequency tracking signature can be obtained from the satellite

PCM-PL system by sending a few hundred bits of all right-circular polarization followed by a few hundred bits of all left-circular polarization (constant signal level). The satellite laser transmitter power level should also be monitored during this experiment, and sent via the microwave telemetry link to the earth terminal.

EARTH RECEIVER DATA

The earth receiver configuration consists of the basic PCM-PL receiving system for detecting laser beacon intensity fluctuation, and a separate telescope tracker arrangement for detecting an adjacent star's intensity fluctuations, and determining image motion frequency components for both the satellite beacon and starlight. A synchronized aperture control for the ground receiver and separate tracker will allow simultaneous scintillation measurement at several aperture diameters. The scintillating light with its tracking signature will pass through the light collector, aperture control unit, predetection filter, variable field stop, and then on through the polarization resolving optics, photomultipliers, amplifiers and difference circuits. At this point, the tracking signature can be extracted through a narrow bandpass filter, and the scintillation data can be extracted through a low-pass filter amplifier combination.

The power spectral density of the intensity fluctuations measured by a wave analyzer will provide an indication of the frequency content of the scintillation. The power spectral density measurements can be made with various aperture diameters and under different meteorological conditions. The index of turbulence, M, can be determined from plots of the power spectrum. The index, M_i, can be related to aperture diameter and also to the corner breakpoint frequencies of the spectrum. Oscilloscope and camera recording of the scintillation waveform will also be provided, as well as recording with other apparatus. The scintillation data will be correlated with various outputs of the meteorological data-collection system.

Statistical measurements of the thermal microstructure at the earth terminal should also be recorded. Various Rawinsonde systems employing balloons to measure temperature and humidity at various altitudes could be employed at the ground terminal where the experiment is to be conducted. The altitude information can be used together with humidity and temperature data to obtain pressure. Slant range of the balloon can be employed to obtain wind zone velocity.

There will be simultaneous ground recording of the scintillation of a star and satellite laser beacon. The star will be chosen to be close in elevation angle to the satellite laser beacon to allow a comparison of the effects of the atmospheric fluctuations over approximately equal zenith distances. An optical pickoff should also be provided for visual acquisition of the star.

ATMOSPHERIC SCINTILLATION (EARTH-TO-SATELLITE TRANSMISSION) EXPERIMENT DATA

Refer to Table XII for a summary of the earth transmitter and satellite receiver data for the downlooking atmospheric scintillation experiment. As described in Table XII the objective of the experiment is the measurement of fluctuation of light intensity from a coherent source after passage through the entire atmosphere. The experiment should be conducted for upward transmission of coherent light from the earth to the satellite. An argon laser at 4880Å, which is used for beacon guidance will be required to obtain scintillation data. Ground laser power will be monitored to insure the constant average power level required for the scintillation-modulation index determination. Also, a low-frequency tracking signature will be provided.

The satellite receiver system will detect the ground laser beacon signal and modulated ground tracking signature. The received laser signal will pass through a transfer lens, aperture control system, and then into the predetection filters at 4880Å. After passing through the predetection filter, the scintillation signal will pass through a low-pass filter and then be encoded for real-time microwave return transmission to earth.

SIGNAL-TO-NOISE RATIO AND SKY BACKGROUND EXPERIMENT DATA

In the visible region during daytime operation, it is clear that we must utilize a narrow spectrum and narrow field of view or else we can easily become sky background limited. It is useful to measure communication performance under different conditions of both day and night sky background. Measurement of signal-to-noise ratio for different background conditions with various combinations of predetection optical filters and fields of view will allow a quantitative determination of the background immunity of the communication system.

SIGNAL TRANSMISSION THROUGH THE ATMOSPHERE, CLOUDS, PARTICLES EXPERIMENT DATA

In general, atmospheric transmittance is subject to wide variation, depending on meteorological conditions and zenith angle. Relative transmittance drops sharply as the path approaches the horizontal.

The atmosphere is generally composed of a mixture of gases in which are suspended a wide variety of particles which differ considerably in size and chemical composition. These gases cause radiation to be absorbed, and the suspended particles scatter the radiation. As a result, the radiation from a source is attenuated, decreasing the received SNR. The loss in signal caused by atmospheric effects arises from: absorption by gases in path of source of radiation, deflection or scattering of source radiation by particles suspended

TABLE XII

ATMOSPHERIC SCINTILLATION EXPERIMENT

EARTH TO SATELLITE

Earth Transmitter Data	
Optical:	Argon 4880Å with relatively low frequency, modulated tracking signature.
Satellite Receiver Data	
Optical:	Detection of laser beacon intensity fluctuation.
Microwave Telemetry:	Scintillation data encoded for real-time return transmission to earth.
Ground Data Recording and Processing	
Oscilloscope and camera recording of scintillation waveforms	
Intensity Fluctuation	Auto and cross-correlations Power spectral densities

in path. In addition, particles or gases suspended in path may radiate causing an increase in the background; i.e., scattering agents in the path may deflect or scatter radiation from other sources toward the receiver, thus increasing the background.

The presence of clouds can obviously impair laser communication performance as is suggested by the damaging effect of cloud cover on visibility shown in pictures obtained by Tiros weather satellites. One must be extremely cautious in interpreting cloud cover statistics. It is difficult to determine cloud cover hinderance for nighttime operation from cloud cover data taken during the day. The global cloud cover pictures taken by the Nimbus satellite will certainly be a useful source of information. It is interesting to note that a lower limit to the actual cloud cover hinderance for satellite photography is usually established for high thin or broken clouds, since satellite photographs are occasionally attempted under these conditions.

EXPERIMENT DATA ANALYSIS AND PROCEDURES

Measurement of 0.1 arc-second pointing by an array of five earth receivers that monitor position of the satellite transmitter laser beam will provide quantitative data that will allow a separation of several sources of error. There is a separate determination of measurement effects due to torque disturbances, atmospheric refraction, and scintillation at the earth detector array. These errors can be recorded as a function of time and analyzed to obtain the spectral distribution of measured errors as well as error probability density functions.

Megabit communication performance may be assessed by measurement of received signal power level, instantaneous signal-to-noise ratio, and probability distribution of bit errors, (fading statistics caused by atmospheric turbulence, satellite perturbations, etc). It is useful to determine the probability distribution function for the bit error probability for several averaging intervals.

The telescope data will fall into several categories: diagnostic (temperature, voltages); proper operational control (effective receiver aperture, beam spoiler position); and performance evaluations (received signal level, transmitter laser power output, time). Conventional time sharing techniques, wherein slowly varying data is transmitted occasionally while rapidly varying data is made available more often and only when required, can be used to conserve telemetry channel capacity. Upon ground reception, the data will be stored on multichannel magnetic tape. Those signals required for operational control can also be demultiplexed and used to actuate readout devices on the operators console. Data originating on the ground can also be tape recorded along with a time signal which will facilitate subsequent tape playback synchronization. This data, however, need not be either sampled or quantitized but can be stored in any form most convenient for later data processing, at possibly other than real time rates. Meteorological data, cloud cover observations, zenith angle, earthshine conditions, transmitted and received laser light attenuator setting,

beacon pulse duty cycle, receiver aperture and field of view settings, transmitted beam spoiler position, telescope attitude information, and other slowly varying information can be multiplexed onto one tape channel or even logged in manually. Angle of arrival fluctuations, received signal magnitude and background level, received intensity fluctuations, point ahead and sun offset angles, communication error rates, and other more rapidly varying data can be stored in parallel on other channels of the same tape or on a separate tape to preserve time coincidence and high frequency information. A recording delay, moreover, could be introduced so that the record could also hold orbiting telescope data in close time synchronism where important; i.e., laser power, tracking error signals, transfer lens position, received signal and background levels. Other received signals (temperature, voltages, currents, transmitter beam spoil setting, effective receiver aperture adjustment, etc.) might be stored along with the slowly varying ground signals on a separate tape. The video picture transmission data will be on film to avoid otherwise large data storage facilities.

2.9 ASTRONAUT TIME REQUIREMENTS

PREFLIGHT TIME

The preflight time of 4 weeks per astronaut would be required. One week would be allocated to principles and practice of optics, optomechanical mechanisms and laser elements. The second week would be devoted to mission-peculiar class room and (Laser/Telescope hardware) subassembly training. The latter two weeks of the four week period would be in training the astronauts to perform the duties required during the flight. The work would involve operation of the Experiments Monitor Console, viewing through the telescope at earth type targets, and the EVA astronaut would be suited up and trained to work with the telescope controls and attachments. Also, the EVA astronaut would observe and participate in the deployment operations.

IN-FLIGHT TIME

22 hours of in-flight time would be required for the LCSE. This would be distributed between the EVA astronaut and the Experiments Monitor Console operator. The EVA astronaut would spend about 1 hour observing the deployment operations of the Laser/Telescope from the launch mounts. The LCSE equipment is to be carried into space on the launch mounts which are located inside the LEM descent stage structure. The location of the astronaut is illustrated in one of the concepts for the experiment (Figure 2 on page 13). The experiments monitor astronaut is illustrated at his control station in this same sketch. He would control the deployment operations using voice cues from the EVA astronaut. After the one hour of deployment operations, the EVA astronaut returns to the Command Module.

The experiments monitor astronaut can address himself to other duties in the LEM Life Cell or he too can return to the Command Module. There would be no demand on the astronauts during the next two days while the LCSE equipment outgasses. The Laser Communications Experiments would be conducted by the astronaut in the LEM Life Cell at the end of day 2 or the beginning of day 3 in orbit. The earth station should be in shadow (nighttime) while the spacecraft will be in sunlight (the synchronous orbit and 28.3 degree inclination will permit the spacecraft to remain in sunlight continuously for the entire two week period that the astronauts are present). Acquisition operations must take place with the sun present (spacecraft in the sun).

It is planned to have the Laser Communications Experiments proceed for eight days (continuously) during day 3 to day 11 of the flight. During this time, the astronaut in the LEM Life Cell will be needed for 2 hours per day for a total of 16 hours of experiment time. At the conclusion of eight days of Laser Communication Experiments, the EVA astronaut will proceed to the Laser/Telescope and conduct several earth viewing experiments. During the earth viewing operations, the experiments monitor astronaut is at his station in the LEM. It is anticipated that the earth viewing experiments would take place for 1/2 hour per day from day 11 to day 14. The total in-flight time adds up to:

	EVA TIME	LEM TIME
Laser/Telescope Deployment	1 hour	1 hour
Laser Communications Experiments		16 hours
Earth Viewing Experiments	2 hours	2 hours
Subtotals	3 hours	19 hours
		Total 22 hours

POST-FLIGHT TIME

Following the flight, the EVA astronaut and the experiments monitor astronaut will require about 4 hours each of debriefing. The Laser Communication Experiments were conducted over 8 days with the experiments monitor astronaut in attendance for 2 hours per day. It should be possible to debrief this astronaut in 1 day. The EVA astronaut who conducted the earth viewing experiment sould be capable of being debriefed in 3 days by "photo interpreters" and NASA project planners. An additional week should be allocated for this astronaut with optical equipment engineers and designers. The optical equipment engineers and designers should be allowed three months to make modifications to the equipment in accordance with suggestions of the astronaut and test data. Then, this same EVA astronaut should spend two weeks testing the modified equipment when suited up. The total post-flight time requirements are:

	EVA Astronaut	LEM Astronaut
Laser/Telescope Deployment	4 hours	4 hours
Laser Communications Experiments		8 hours
Earth Viewing Experiments (Earth Feature Recognition, Photo Interpretation, TV)	24 hours	8 hours
Debriefing with Optical Equipment Designers	40 hours	
Testing with Modified Telescope while Suited	80 hours	
Subtotals	148 hours	20 hours

Totals 21 days

2.10 LCSE COST AND SCHEDULE SUMMARY

DESIGN, DEVELOPMENT, FABRICATION, TEST AND GENERAL SUPPORT OF EXPERIMENT

(Basic AAP Concept Without Boom/Gimbals)

Item		Amount
Direct Labor, Estimate		$1,610,000
Materials		1,510,000
Subcontracts		345,000
Special Equipment		800,000
Travel		35,000
	Total Costs	$4,300,000
General and Administrative	Rate (20%)	860,000
	Total Estimated Cost	$5,160,000
	Fee	516,000
	Total	$5,666,000

DATA ANALYSIS AND PUBLICATION COST BREAKDOWN

Item		Amount
Direct Labor		$ 290,000
Materials		1,000
Subcontracts (Consultants)		5,000
Special Equipment (Lab Gear)		30,000
Computer Time		20,000
	Total Costs	$ 350,000
General and Administrative	Rate (20%)	$ 70,000
	Total Estimated Cost	$ 420,000
	Fee	$ 42,000
	Total	$ 462,000

FABRICATION, TEST AND DELIVERY OF FLIGHT UNIT

(Basic AAP Concept Without Boom/Gimbals)

Item		Amount
Direct Labor		$ 550,000
Materials		270,000
Subcontracts		120,000
Special Equipment		100,000
Travel		10,000
	Total Costs	$1,100,000
General and Administrative	Rate (20%)	$ 220,000
	Total Estimated Cost	$1,320,000
	Fee	$ 132,000
	Total	$1,452,000

QUARTERLY FUNDING REQUIREMENTS (Dollars in Thousands)
(Basic AAP Concept without Boom/Gimbals)

Quarter Number	Design, Development Fabrication, Test (Mock-Ups and Prototypes and General Support of Experiment Without Fee	Fabrication, Test and Delivery of Flight Units Without Fee	Data Analysis and Publication
1	300,000		
2	400,000		
3	700,000		
4	700,000		
5	800,000		
6	900,000		
7	700,000	500,000	
8	400,000	250,000	
9	100,000	300,000	
10	60,000	200,000	
11		35,000	
12		35,000	
13			
14			210,000
15			210,000
	$5,160,000	$1,320,000	$ 420,000
	Fee $ 516,000	Fee 132,000	Fee 42,000
	Total $5,660,000	Total $1,452,000	Total 462,000
		GRAND TOTAL	$7,480,000

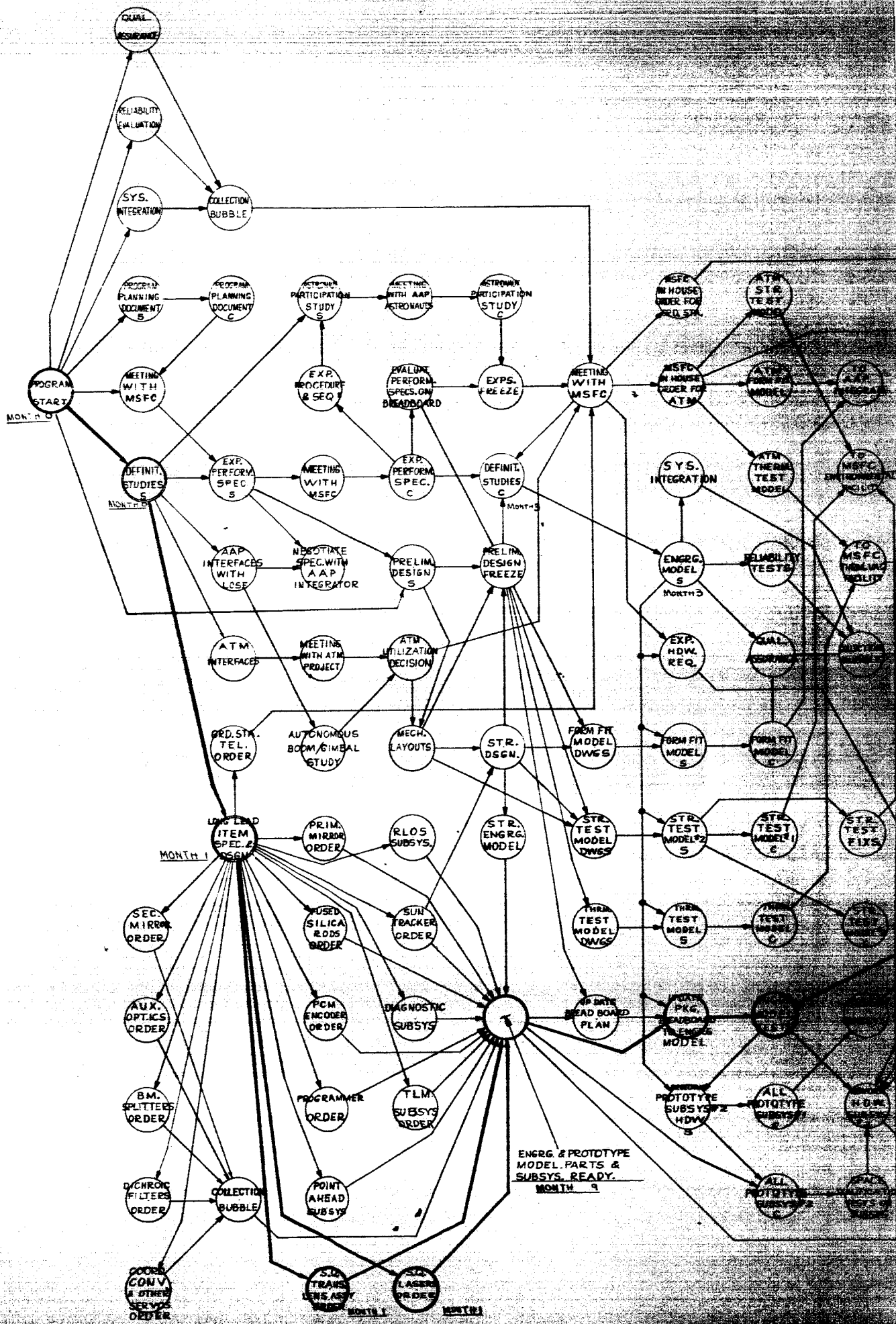
QUAL. ASSURANCE
RELIABILITY EVALUATION
SYS. INTEGRATION
COLLECTION BUBBLE
PROGRAM PLANNING DOCUMENTS
PROGRAM PLANNING DOCUMENT C
ASTRONAUT PARTICIPATION STUDY S
MEETING WITH AAP ASTRONAUTS
ASTRONAUT PARTICIPATION STUDY C
MSFC IN HOUSE ORDER FOR ATM STR.
ATM STR. TEST MODEL
PROGRAM START
MONTH 0
MEETING WITH MSFC
EXP. PROCEDURE & SEQ
EVALUAT. PERFORM. SPECS. ON BREADBOARD
EXPS. FREEZE
MEETINGS WITH MSFC
MSFC IN HOUSE ORDER FOR ATM
ATM THERM. TEST MODEL
DEFINIT. STUDIES S
MONTH 0
EXP. PERFORM. SPECS
MEETING WITH MSFC
EXP. PERFORM. SPEC. C
DEFINIT. STUDIES C
MONTH 3
SYS. INTEGRATION
ATM THERM. TEST MODEL
AAP INTERFACES WITH LOSF
NEGOTIATE SPEC. WITH AAP INTEGRATOR
PRELIM. DESIGN S
PRELIM. DESIGN FREEZE
ENGRG. MODELS
MONTH 3
RELIABILITY TESTS
ATM INTERFACES
MEETING WITH ATM PROJECT
ATM UTILIZATION DECISION
EXP. HDW. REQ.
QUAL. ASSURANCE
GRD. STR. TEL. ORDER
AUTONOMOUS BOOM/GIMBAL STUDY
MECH. LAYOUTS
STR. DSGN.
FORM FIT MODEL DWGS
FORM FIT MODELS
FORM FIT MODEL C
LONG LEAD ITEM SPEC. & DSGN.
MONTH 1
PRIM. MIRROR ORDER
RLOS SUBSYS.
STR. ENGRG. MODEL
STR. TEST MODEL DWGS
STR. TEST MODEL #2 S
STR. TEST MODEL #1 C
STR. TEST FIXS.
SEC. MIRROR ORDER
FUSED SILICA RODS ORDER
SUN TRACKER ORDER
THRM. TEST MODEL DWGS
THRM. TEST MODEL S
THRM. TEST MODEL C
AUX. OPTICS ORDER
PCM ENCODER ORDER
DIAGNOSTIC SUBSYS
UP DATE BREAD BOARD PLAN
FLIGHT PKG. BREADBOARD & ENGRG MODEL
BM. SPLITTERS ORDER
PROGRAMMER ORDER
TLM. SUBSYS ORDER
PROTOTYPE SUBSYS #2 HDWS
ALL PROTOTYPE SUBSYS #2 C
DICHROIC FILTERS ORDER
COLLECTION BUBBLE
POINT AHEAD SUBSYS
ENGRG. & PROTOTYPE MODEL PARTS & SUBSYS. READY.
MONTH 9
COORD. CONV & OTHER SERVOS ORDER
S.C. TRANS. LENS ASSY ORDER
MONTH 1
S.C. LASER ORDER
MONTH 1

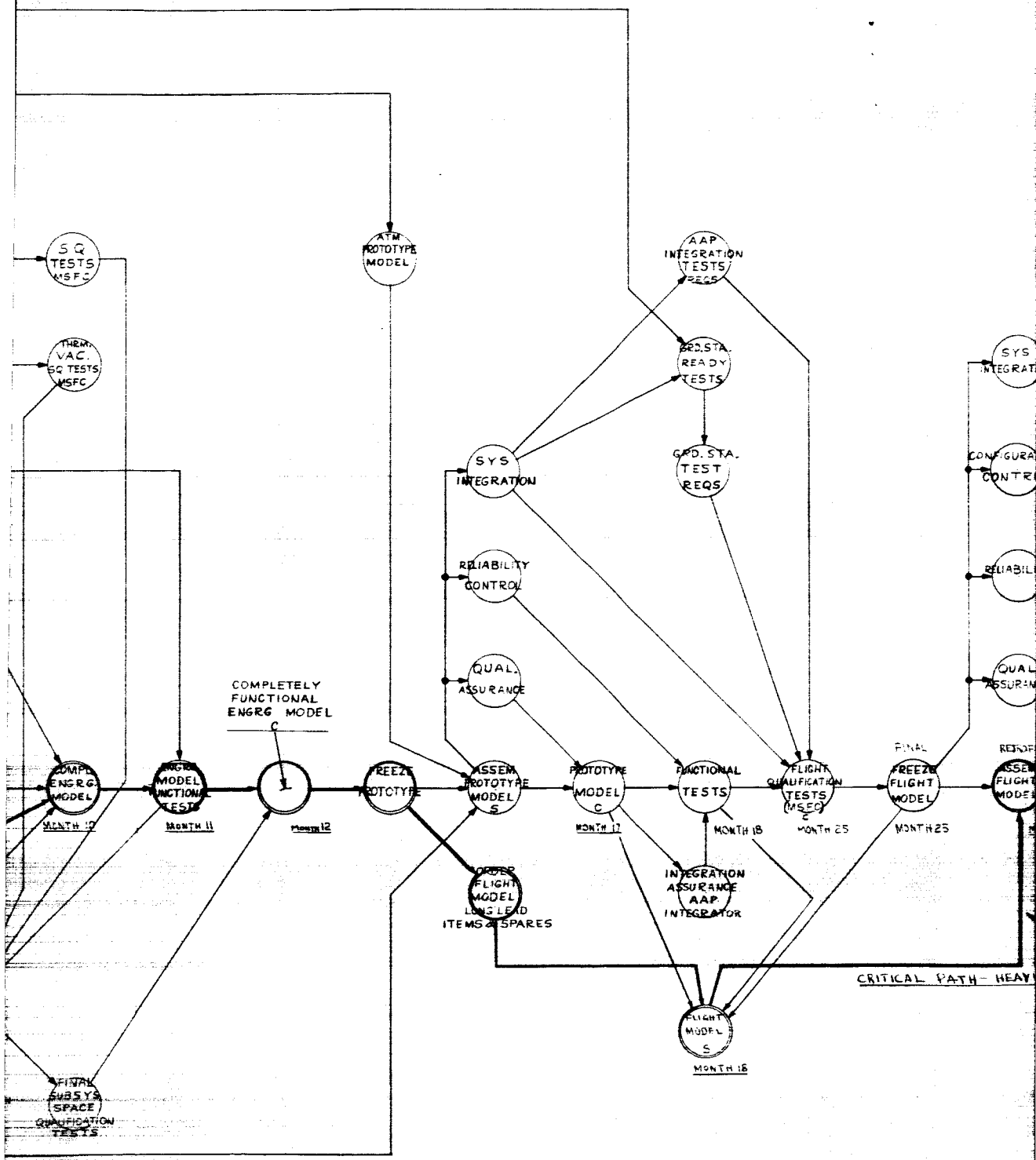
SQ TESTS MSFC
THERM. VAC. SQ TESTS MSFC
ATM PROTOTYPE MODEL
AAP INTEGRATION TESTS REQS
GRD. STA. READY TESTS
GRD. STA. TEST REQS
SYS INTEGRATION
RELIABILITY CONTROL
QUAL. ASSURANCE
SYS INTEGRAT
CONFIGURA CONTR
RELIABIL
QUAL ASSURAN
COMPLETELY FUNCTIONAL ENGRG MODEL C
COMPL ENGRG MODEL
MONTH 10
ENGRG MODEL FUNCTIONAL TESTS
MONTH 11
MONTH 12
FREEZE PROTOTYPE
ASSEM PROTOTYPE MODEL S
PROTOTYPE MODEL C
MONTH 17
FUNCTIONAL TESTS
MONTH 18
FLIGHT QUALIFICATION TESTS (MSFC) C
MONTH 25
FINAL FREEZE FLIGHT MODEL
MONTH 25
RETROFI ASSEM FLIGHT MODEL
ORDER FLIGHT MODEL LONG LEAD ITEMS & SPARES
INTEGRATION ASSURANCE AAP INTEGRATOR
CRITICAL PATH - HEAV
FLIGHT MODEL S
MONTH 18
FINAL SUBSYS SPACE QUALIFICATION TESTS

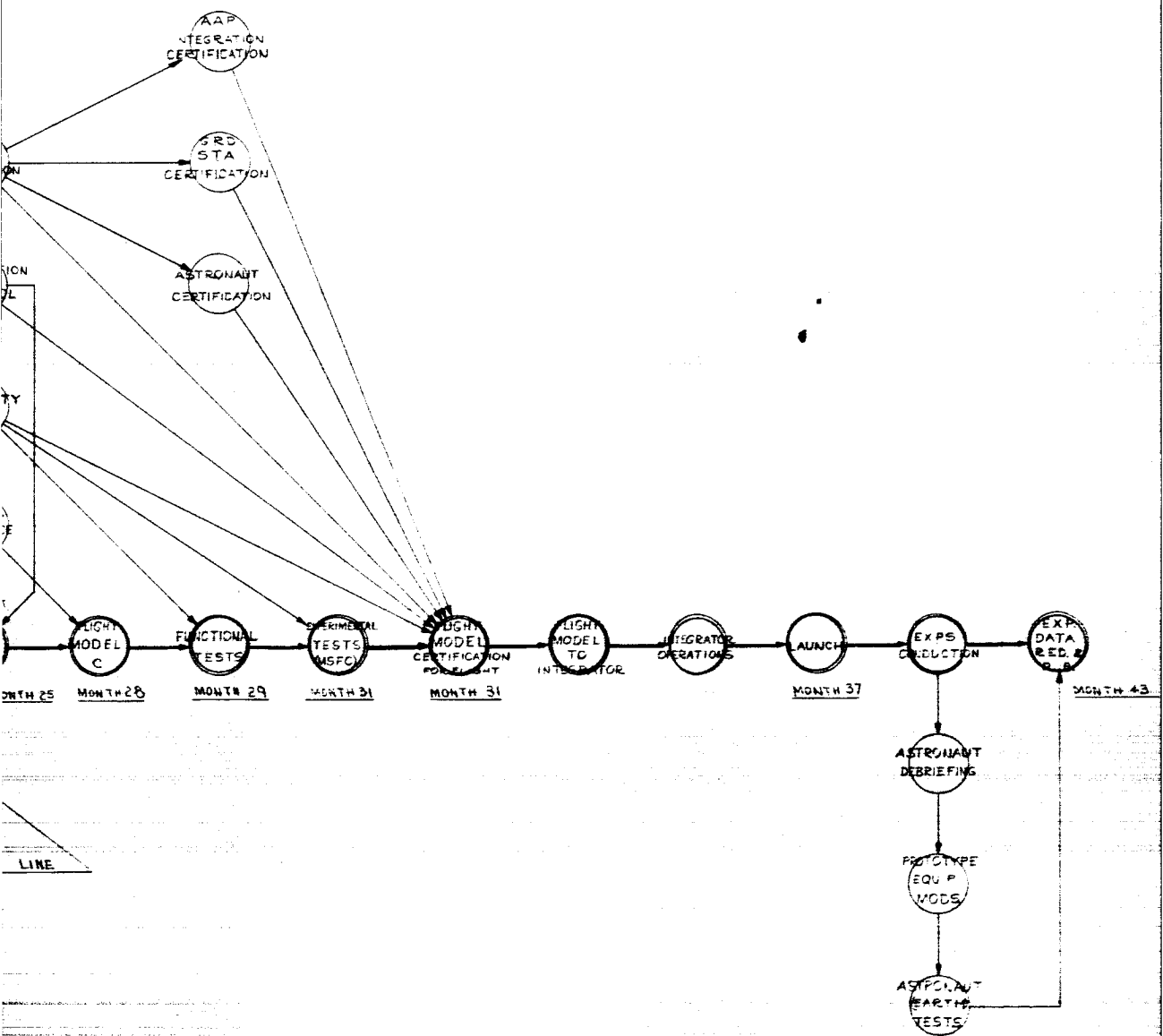

Figure 61 LCSE Schedule